Theoretical and Experimental Investigations Into Umbilical Cables for Communications Under the Sea

Thesis

Author: Andrew George Cairncross Mitchell

BSc. (Hons.) Electronics and Microprocessor Engineering, University of Strathclyde, 1984

Thesis: Theoretical and Experimental Investigations Into Umbilical Cables for Communications Under the Sea

Submitted for PhD, 30th September 2012

The Open University

Faculty of Mathematics, Computing and Technology

Thesis: Theoretical and Experimental Investigations Into Umbilical Cables for Communications Under the Sea

Abstract

Continual advances are being made in the control and monitoring of subsea oil wells by the application of new technology for sensors, subsea processing and communications devices. With these advances, the demands on the subsea umbilical are constantly increasing with deployment lengths and depths growing and the quantity of controlled functions now greater than ever. The need for a good understanding of the effects of deployment subsea is essential, as communications frequencies and data throughput constantly increase. This research aims to address some of the issues regarding umbilical modelling and sets up a series of tests to measure the effects of pressure and cable flooding within the umbilical and assesses the effect of steel tubes, hydraulic hoses and cable armouring on the operating parameters of the cables. In addition, the cables are modelled using electromagnetic field solver tools and the results compared with those measured. Once prediction losses have been established, these are compared with measurements taken on the full lengths of umbilical and the reasons for any discrepancies examined.

It is shown that, in a typical subsea umbilical, the proximity of conducting cores to adjacent components, such as hydraulic hoses or steel wire armour, the flooding with sea water and the pressure due to the depth of deployment all have a significant impact on the impedance parameters of the cables.

The effect of cable screening on attenuation is also examined and it is shown that, as well as affecting capacitance and conductance, the screen has a significant impact on the cable resistance and inductance, with the resistance rising to a maximum at a certain screen thickness before a subsequent reduction. This effect was investigated further by modelling with an electromagnetic field solver and a possible explanation for this effect is proposed. Comparison of the modelled data and measurement of cables under the various operating conditions investigated show good correlation with the

results, allowing very accurate prediction of the effects on electrical performance of cables when deployed subsea in Subsea Control System umbilicals.

1 Contents

List of Figures

List of Tables

List of Symbols used

Greek Symbols

μ	magnetic permeability of the signal conductor, typically $4.\pi.10^{-7}$ H/m and is also generically used for 'micro', i.e.10^{-6}. Meaning is clear by the context of use.
ε_r	relative permittivity (or dielectric constant) typically around 2.25 for polyethylene
ε_0	absolute permittivity in free space. This is $8.854x10^{-12}$ F/m
ε_{DLF}	the dielectric loss factor
δ	delta, used in the context of 'tanδ' representing the loss tangent of a dielectric material
γ_0	the propagation constant
π	pi
σ	conductivity of copper, $5.435x10^{7}$S/m
Ω	ohms, standard for electrical resistance measurement
ω	angular frequency in radians per second

English characters

°C	degrees centigrade
C	capacitance
d	conductor separation
F	unit of capacitance, Farads

G conductance

H unit of Inductance, Henries

i current

Hz unit of frequency, Hertz

j complex operator, $\sqrt{-1}$

J_1 first-order Bessel function of the first kind

J_0 zeroth order Bessel function of the first kind.

k 'kilo' i.e.10^3

L inductance

l length

M 'mega' i.e.10^6

m metres and also 'milli' or 10^{-3}. Use will be clear by the context.

mm millimetres

n 'nano' i.e.10^{-9}

r radius

R Resistance

S Siemens

s Laplace operator, σ+jω

T Tesla

V	Volts
Z_o	Characteristic Impedance

Abbreviations

AC	Alternating Current
DC	Direct Current
FPSOs	Floating Production Storage and Offloading
Hz	Hertz
IEEE	Institute of Electronic and Electrical Engineering
km	Kilometres
kHz	Kilohertz
kV	Kilovolts
mm	millimetres
R, G, L, C	Generally used together to represent Resistance, Conductance, Inductance and Capacitance
SCM	Subsea Control Module
SEM	Subsea Electronics Module
SUTU	Subsea Umbilical Termination Unit
VAC	Voltage, Alternating Current
XLPE	Cross linked polyethylene

Chapter 1. Introduction

Electrical communications cables were used in subsea applications as far back as the early 1850s when the rise of the telegraph created a significant worldwide demand for a communications network that would link all the major cities of the world. Within a few years, telegraph cables crossed the English Channel, Irish Sea and even the Atlantic Ocean. So that loss predictions and compensation systems could be developed to improve signal quality, the demand for a good mathematical model was clear and this was exactly what was provided by Oliver Heaviside in his telegrapher's equation in the late 19th Century, IEEE GHN (2012). This equation is still the primary basis for modern communications modelling today and gives an excellent model of the propagation and loss effects in a cable, dependent on the four fundamental impedance parameters of resistance, inductance, conductance and capacitance.

Over the subsequent years, much work has been done, e.g. as explored by Dwight(1921), Arnold(1941), Ramo, Whinnery, Van Duzer (1994) and others described in Chapter 2, to establish methods of prediction of these four fundamental cable parameters from cable dimensions and materials. More recently, with modern electromagnetic modelling techniques outlined in Section 2.3, work such as that done by Gustavsen B et al. (2009), Salles M B C et al. (2010), Chien C H (2009), Yazdani J et al. (2005) and Rocha P(2007), has gone some way to enabling the effects on the conductors of the surrounding umbilical materials to be assessed, however the impact on these umbilical parameters from submersion in sea water and under pressure at depth is an area where still little has been done. Within the oil industry, due to the very large value of equipment produced, there is a great deal of competition and any measurement data recorded is considered highly confidential. So the opportunity to

obtain sufficient data for an in depth study into the operating effects is extremely rare and the work done in this research brings together many measurements and models of the effects of deployment of umbilicals which are rarely available together on the one project.

Traditionally, umbilical electrical cores have been used interchangeably as power or communications conductors and are therefore of substantial cross sectional area. Core sizes of 2.5mm^2 are about the smallest normally seen with 10mm^2 or 16mm^2 commonly used to carry power or communication signals. Since up to the tail end of the 20th Century, as data rates did not have to be high for control of the sensors and valves deployed at that time, communication frequencies employed by equipment were generally less than 10KHz, like in the system employed by Aker Solutions which used carrier frequencies of 1 or 2kHz as defined in the Bell 202 standard, and communications equipment has generally served its purpose well. Models were sufficiently accurate for the requirements of such low data rate systems and, in the main, allowed successful deployment of the well control equipment at that time. Since around the turn of the millennium however, and as oil prices have continued to rise steadily since the 1990s, this is rapidly changing. The ability to recover oil from remote fields is becoming increasingly cost effective as technology, sensor and subsea processing capability improve and, as a result, the increase in data throughput is significant. In addition, the need to control wells at distances in excess of 100km is now not unusual and the number of devices under control remotely is also significantly greater. A modern umbilical, shown in Figure 1, is an extremely complex piece of equipment and is by far the most expensive part of any subsea control system, with costs upwards of tens of millions of pounds, not uncommon. Communications systems utilising frequencies at several hundred kilohertz are now not uncommon, as outlined in Section 1.1, and as umbilical complexity increases, with steel tubes for hydraulics, steel

wire armouring for mechanical strength and even the inclusion of oil production cores, the impact on the cable impedances must be carefully assessed. Figure 1.1 shows a typical subsea umbilical. In this case the electrical quad cables would typically carry power, possibly up to 1kV on one diagonal pair and communications signals on the other.

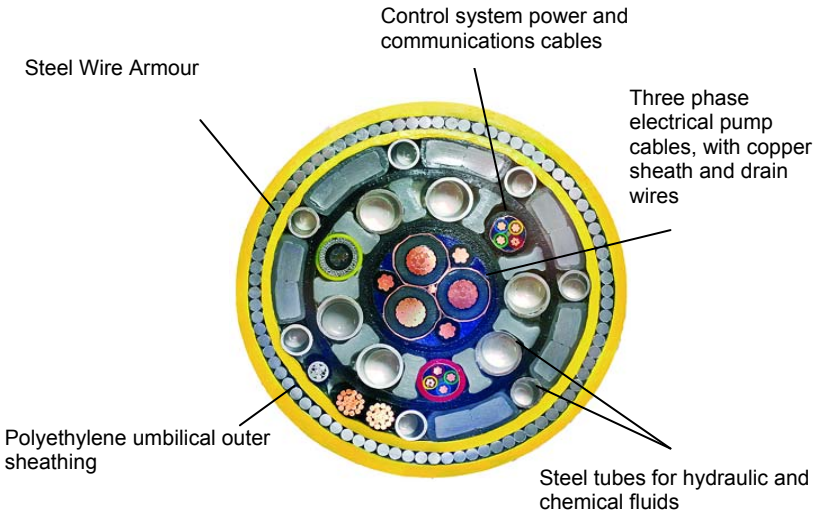

Figure 1-1 Typical subsea umbilical (Parker)

As the demand is constantly growing for new umbilical systems to operate under extreme pressure conditions in excess of 300 bar as seen in the Gulf of Mexico, and in sub-zero temperatures as seen in areas such as the Barents Sea to the north of Russia and Norway, communications failures seen during the installation phase of systems such as Shell Penguins by Aker Solutions in 2002/3 and BP Devenick in 2011 by GE Vetco make it clear that the methods of modelling the cables for use at the higher communications frequencies are no longer sufficiently accurate and it is now crucial that better models are derived. This thesis examines these effects, considers the impact of the surrounding materials on the impedance of the electrical cores and establishes the models necessary to ensure accurate prediction of losses.

1.1 Well Control Equipment

Although technology has played a large part in the oil industry since its early years at the turn of the 20th century, allowing more efficient and therefore more cost effective recovery, it is the subsea oil and gas industry that has really pushed the advances in subsea technology. To a large degree, the exploration of seas has required a continual improvement in the technology of production efficiency and feasibility and, as a result, subsea control technology has been making continual advances in sensing, monitoring and control technologies. The control of a subsea system is no longer a case of operating a few valves via a bundle of hydraulic hoses to control and balance oil flow. The demand for sensors for flow rates, valve positions, temperature, hydraulic pressure, oil/gas pressures, voltages and currents as well as providing communications with devices such as subsea control computers, pipeline protection equipment and subsea pumps have meant a complex network of communication and power cables as well as high pressure hydraulic hoses and chemical flowlines are all interconnected to form very sophisticated command and control systems. As a result, the communications systems are increasingly required to reach distances in excess of 100km, such as in fields like Statoil Snohvit at 145km, Douglas N (n.d.), and Ormen Lange at 120km, Bertmand T. (2003), and electrical data rates of hundreds of Kbits/sec are now being offered by all the major control system vendors, such as Proserv (2013) and GE Vetco (n.d.). Accurate models of the communication systems are more crucial than ever.

The Subsea Control Module (SCM),such as described by Proserv(2013) is the heart of the subsea Oil Well control system and sits on a structure known as a Christmas tree, Aker Solutions (2013), due to the tree-shaped arrangement of the early land base structures with many valves and sensors hanging off, like baubles. The Christmas Tree

shown in Figure 1.2, contains the well pressure and provides valves, sensors and oil flow lines to direct the flow as commanded by the SCM, shown in Figure 1.3.

Figure 1-2 A typical Subsea Christmas Tree (Aker Solutions)

Figure 1-3 A Subsea Control Module (Proserv)

Within the SCM is a Subsea Electronics Module (SEM), the 'brain' of the subsea system, controlling valves, sensors and generally monitoring the performance of the subsea tree. The SEM is in constant communication with the surface via the controls umbilical, and this umbilical is the object for study in this thesis.

1.2 Umbilicals

Subsea umbilicals take many forms and are constructed in many different ways according to their installed environment, function and required cores.

1.2.1 Controls Umbilical construction

Typically, a dynamic umbilical, designed to take constant flexing and with a specific buoyancy depending on the installation conditions, connects the control vessel or rig to a Subsea Umbilical Termination Unit (SUTU). This umbilical will normally contain all the cores required for the distribution network subsea and will have a significant steel wire armouring outer skin to provide the required robustness and buoyancy as well as ensuring the specified flexing requirement is met. This would typically be in the order of a few hundred metres, depending on the water depth but up to a few kilometres is not unusual as in the Tobago field at 2.934km (9627 feet) and the Silvertip field at 2.843km (9326 feet) as described by Dutch Daily News (2011)

A static umbilical will then connect the SUTU to the Christmas Trees and although this is, as the name suggests, not expected to see any movement over its lifetime, the length can in some cases, as highlighted in section 1.1, be greater than 100km.

The controls umbilical typically provides power, communications, hydraulic pressure and fluids, scale inhibitor, methanol and corrosion inhibitor to control the subsea control system. As this is the lifeline to the control system, this is normally configured with spare electrical conductors and spare hydraulic hoses and chemical tubing to allow for long term management of failures. A failure in the umbilical can have huge cost implications running to millions of pounds for repair and hundreds of millions in lost revenue if oil production is affected and for this reason is subject to several industrial standards such as ISO 13628-5 (2009) and the NORSOK Standard(1995).

The outer jacket of the umbilical is typically a solid polyethylene sheath, however it is designed such that the umbilical will flood with sea water once deployed. In some cases the umbilical jacket is made of a woven Kevlar material and will flood as soon as entering the water. There is a consequent effect on the electrical parameters of the conductors within the umbilical and this is examined in this thesis.

As outlined later in Section 3.2.5, much work has been done throughout many industries, on studying the effects of water treeing in polyethylene cable insulation and it is generally recognised that over time, all polyethylene will pass water albeit to differing degrees and at different rates depending on the chemical structure and applied voltage and temperature, as the water permeates between the molecules in the structure. This is examined later in Chapter 3 although, in the power and communications cables in oil field subsea control systems, this has not been seen as a problem to date, as the high voltage dependency of water trees and long term growth effects mean there is little impact on the electrical cables of the typical subsea control systems of the present time.

1.2.2 Hydraulics

The carrying of hydraulic fluids and pressure to the subsea equipment needs careful design and the analysis of the hydraulic performance of valves and tubing is an area of considerable effort before each system is deployed. It is essential that subsea hydraulic charge up times and vent down times are kept within defined limits to ensure the system dynamic performance is adequately responsive but also that safe shutdown can be achieved quickly, should this be required. The operation of valves subsea will cause a local drop in pressure in the hydraulic connections so this must be maintained within adequate limits to ensure that, since subsea valves are typically hydraulically

latched and low pressure could cause valves to close, an unwanted system shut down does not occur. Hydraulic tubing typically takes two forms:

Steel tube: These have no elasticity and therefore no reservoir effect or accumulation to 'dampen' the pressure change when valves are operated. Due to the impervious nature of the steel tube and the very high withstand pressure to greater than 30000psi, AB Sandvik Materials Technology (2010), the steel tube is preferred for long step-out and deep water systems as it provides an enhanced response time over the thermoplastic hose and has a much better fatigue life and corrosion resistance, Chai G et al. (2009).

Thermo plastic cores: These have good elasticity and therefore provide a degree of accumulation helping to prevent a large pressure drop with valve operation. For shallow water systems the benefits provided in the inherent accumulation and lower cost of construction are significant.

The effect of these hydraulic tubes and hoses on the electrical parameters of the adjacent cables in the umbilical is an area of great concern within the oil industry as there is evidence that communications systems have failed due to the proximity of cables to hydraulic steel tubes.

1.2.3 Electrical cores

The electrical conductors within the typical subsea controls umbilicals are of quad or twin arrangement, sometimes screened and sometimes armoured depending on the perceived noise sensitivity and dynamic requirements of the umbilical. In general cables are rated to 1000V as the majority of systems are designed to operate below this and lower cost of manufacture can be achieved in the umbilical. For example, Aker Solutions (n.d.) offer systems to 500VAC as standard and Weatherford (2008) operate to 480VAC. Generally SCMs are of relatively low power, typically less than a couple of

hundred watts each, with modems normally designed to match approximately the cable characteristic impedances of around 100Ω. None of these elements in themselves represent any engineering challenge but when combined together into distributed field layouts with multiple loads at remote distances, it can be extremely challenging to ensure stable and reliable performance of the communications and power distribution. Cables employed will generally have 2.5mm^2, 4mm^2, 10mm^2 or 16mm^2 cross sectional areas with these cores operating as power and communications conductors.

As subsea power loadings increase, with the increasing addition of subsea monitoring equipment, the control system vendors are working on the development of higher voltage systems, up to 3KV and beyond as well as operation at DC rather than the conventional 50Hz or 60Hz AC systems. Communications companies, such as Alcatel, are starting to make inroads into supplying systems to the oil industry operating to 10KV with their own specifically designed optical/power umbilical, making use of the seawater for the electrical return path.

It is expected that the next decade will see significant changes in the power delivery of the new, extended step out high performance subsea control systems.

1.2.4 Optical fibres

As data rate requirements increase, so optical communications systems are becoming more common place with the fibres bundled into gel filled steel tubes to prevent water ingress. Despite the major advantages in communications speed and significant reduction in the required cross section of the communications cores, a major factor in reducing umbilical manufacture and deployment cost, the cost of wet mate optical connectors and the fact that copper conductors are still essential for power distribution with a couple of additional electrical cores for communications purposes often not

being a great overhead, means that optical communications systems are still not employed for the majority of subsea control systems at this time.

1.2.5 Umbilical manufacturers

Some of the major umbilical suppliers within the oil industry are Aker Solutions, Nexans, Oceaneering, Duco, Cortland, JDR and Prysmian. The subsea umbilical is probably the one single biggest cost of a subsea control system; where the control system components Christmas tree (SEMs, valves, manifolds and umbilical termination assemblies) maybe total a few million pounds, the umbilical itself is easily upwards of £10 million. A large amount of engineering time and money is allocated in the project bid stage and throughout the engineering phase to make sure umbilical costs are optimised.

Oil platforms (rigs) and FPSO (Floating Production Storage and Offloading) vessels are expensive to design, man and maintain, so as oil companies reach fields further out to sea and in more remote and inhospitable areas of the world, control from the land becomes increasingly attractive.

These requirements taken together: subsea control systems at greater distances, increased sensor and monitoring equipment and in more extreme environments in the world means an increased reliance on umbilical performance and accuracy of models.

1.3 Current modelling and commercial issues

Since, as outlined earlier in this chapter, there is a high level of company investment and confidentiality within the subsea industry, and while the focus of these companies is primarily on the deployment of systems to enable the control of oil wells and the need for high speed communications has not before been a high priority, there is very little published research data on the issue of modelling subsea umbilicals for high

speed communications networks. It has now become crucial however, as seen by the communications problems encountered in recent years in several subsea systems described at the beginning of Chapter 1, that a precise understanding of the effects of deployment on the cables is essential if accurate models and reliable communication systems are to be available for the designers of future systems.

1.4 Aims and Objectives

As a result of such problems, this research undertakes to establish an accurate understanding of the effect of subsea deployment of an umbilical on its electrical characteristics in order to enable the future design of subsea systems to be based upon reliable and repeatable scientific principles.

The overarching research aim is to model and understand the issues affecting subsea umbilicals in their use for electrical communications, and how construction and deployment affect performance.

As will become apparent, establishing an accurate model of the subsea umbilical is a complex task. Clearly, the construction and operating environment will both have a significant impact on the impedance. The effect of umbilical deployment will require an examination of the effect of sea water on the impedance but clearly the very high pressures seen at depth may well also affect the results. The physical construction, too, must be examined for a full understanding, so the effect of hydraulic tubes, armouring and screens are also essential considerations. For these reasons, to understand the complex operating environment, this research has been broken down into a number of subsidiary goals:

- **To model and elucidate the effect on the cable distributed electrical impedance of adjacent conductors, screens and umbilical steel wire armouring.**

  In order to address this issue, measurements are made of electrical quad cables in proximity to steel surfaces in Section 5.2, and are compared, in Sections 5.2 and 6.2, with the results of detailed models described in Section 5.1, to establish the impact of surrounding conductors on the cable impedance. Also examined are the effects on cables installed in a subsea umbilical, Section 6.5, and these measurements are again compared with the results of detailed models. The effect on cable impedance of the physical properties of a cable screen, are also investigated, in Section 6.6.

- **To understand the effect on the cable distributed electrical impedance when the umbilical is flooded with sea water.**

  To examine the effect of seawater deployment, measurements of electrical quad cables in a variety of conditions are examined in Sections 5.2 and 5.3. Sea water and fresh water effects are measured, and these are compared in Sections 5.3 and 6.3 with the results of models carried out in Section 5.1.

- **To understand the effect on the cable distributed electrical impedance when the umbilical is deployed subsea and under pressure.**

  Establishing the effect of pressure on the electrical impedance required a series of electrical measurements to be made on a cable installed in a water filled pressure chamber, as defined in Section 5.2, with results examined in Section 6.4.

Prior to this research none of these effects had been thoroughly analysed or understood. The conclusions of this research project are therefore a considerable addition to knowledge as well as a practical aid to future designers and users.

1.5 Organisation of Thesis

In Chapter 2, the background theory applicable to calculation of cable impedance parameters, the methods adopted for cable modelling and the means by which these may be applied in mathematical tools for prediction of signal attenuation and cable loss will be outlined.

Chapter 3 will describe some of the known theory with regards subsea deployment of cables and the main issues to be investigated by this research with Chapter 4 detailing the experimental testing and modelling to be carried out.

Chapter 5 will then go on to present the results of the testing and models carried out during this research with Chapter 6 providing a comparison and analysis of all the results. It is established that the results and predictions show excellent correlation when the limitations of measurement methods and environment are properly accounted for. In the later part of the chapter, further examination of an unexpected result relating to cable resistance dependency on the cable screen thickness is also carried out.

Chapter 7 presents areas of future work which stem from this research with Chapter 8 presenting conclusions of the work.

Chapter 2. Electrical Theory

In Chapter 1 it was seen that the subsea umbilical is a crucial component in the control of modern subsea oil wells. Although the propagation of electrical signals in cables and metallic media has been well researched and is well understood, surprisingly little information exists about the effects of inclusion of conductors in subsea umbilicals and their subsea deployment.

This chapter examines the known theory of umbilicals and cables at this time and sets the background from where the key questions of this research will be addressed: what is the effect on the electrical impedance of cables when incorporated into a subsea umbilical and what are the effects on impedance of the umbilical armouring, sea water and pressure?

Heaviside's telegrapher's equations are still the basis for modelling of data transmission in conductors today and these are outlined in section 2.1.

2.1 Transmission Line Theory

A lossy line i.e. a realistic model of a transmission line, where the cable resistance has significant impedance, as described by Paul C. (1994, p75-77), is represented by the equations 2.1 and 2.2

$$\frac{\partial}{\partial \mathrm{L}} \mathrm{V}(\mathrm{l},\mathrm{t}) = -\mathrm{L}\frac{\partial \mathrm{I}(\mathrm{l},\mathrm{t})}{\partial \mathrm{T}} - \mathrm{RI}(\mathrm{l},\mathrm{t}) \quad \text{2-1}$$

$$\frac{\partial}{\partial \mathrm{l}} \mathrm{I}(\mathrm{l},\mathrm{t}) = -\mathrm{C}\frac{\partial \mathrm{V}(\mathrm{l},\mathrm{t})}{\partial \mathrm{t}} - \mathrm{GV}(\mathrm{l},\mathrm{t}) \quad \text{2-2}$$

Where R is the resistance, L the inductance, G the conductance and C the capacitance per unit length, l is distance along the cable and t is time.

These equations tell us that:

- the rate of change of voltage along a transmission line is proportional to the inductance times the rate of change of current plus the resistance times the current, and
- the rate of change of current in a transmission line is proportional to the capacitance times the rate of change of voltage plus the conductance times the voltage.

Based on the transmission line element definition as shown in Figure 2.1,

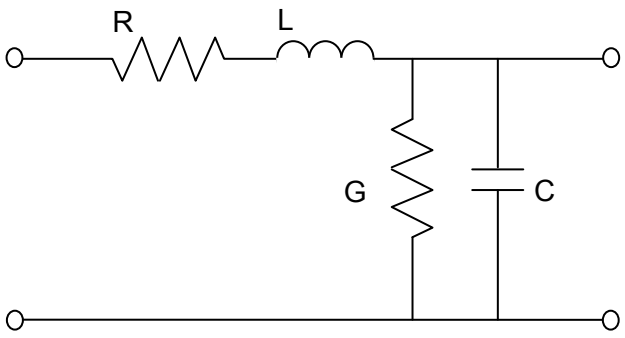

Figure 2-1 Transmission Line Element Definition

and using cable parameters defined per metre or kilometre, we can define line attenuation, phase shift and characteristic impedance from the cable elements of resistance (R), conductance (G), inductance (L) and capacitance (C). These parameters are then applied to the following formulae allowing calculation of the operational losses and reflections of the cables of the desired length (l) in the desired interconnection and loading arrangement to derive the propagation constant as described by Johnson and Graham (2003, p47) and shown in equation 2.3.

$$\gamma_o(R, G, L, C, l, s) = l\sqrt{(R + sL)(G + sC)} \quad \text{.....2-3}$$

Where s is the Laplace operator, the complex variable σ+jω. To derive the frequency response from such equations, s is replaced by jω, where ω=2πf and f is frequency.

This equation is used throughout this thesis in order to calculate the loss per km for an infinite length of cable or umbilical.

Result is in Nepers (1 Neper = 20 $\log_e$ dB), telling us the attenuation over length, l, in a transmission line with the given R, G, L and C parameters.

In a similar way, the Characteristic impedance of the cable section, which is used later in equation 2.9, is described by Johnson and Graham (2003, p42) and is shown in equation 2.4

$$Z_o(R, G, L, C, s) = \sqrt{\frac{R+sL}{G+sC}} \quad \text{2-4}$$

The use of two port network theory provides a very convenient and extremely useful system modelling tool as outlined by Johnson and Graham (2003, Appendix C). This allows us to define series and parallel impedances which can be easily and conveniently cascaded to form complex component arrangements such as used in filters and cable models. If we define

$$\text{Rshunt}(R) = \begin{pmatrix} 1 & 0 \\ \frac{1}{R} & 1 \end{pmatrix} \quad \text{2-5}$$

$$\text{Rseries}(R) = \begin{pmatrix} 1 & R \\ 0 & 1 \end{pmatrix} \quad \text{2-6}$$

then complex arrangements of series and parallel component impedances can be modelled.

Expressing the telegrapher's equation in a suitably compatible format, results in an extremely powerful and versatile means of deriving the frequency response of a cascaded sequence of impedances and cables. These definitions shown in equations 2.4 to 2.6, as described by Ramo, Whinnery, Van Duzer (1994, p251), are commonplace in modern engineering analysis and are used throughout this thesis as a means of calculating cable attenuation over distance within a desired network

configuration, with cable spurs and representative load and source impedances as seen on the equipment,

$$v(l) = v \cdot \cosh(\gamma l) - i \cdot Z_0 \cdot \sinh(\gamma l) \quad \text{2-7}$$

$$i(l) = i \cdot \cosh(\gamma l) - \frac{v}{Z_0} \cdot \sinh(\gamma l) \quad \text{2-8}$$

where l is the distance along the cable

From equations 2.7 and 2.8, the two-port network can be expressed compactly as the matrix:

$$\begin{pmatrix} \cosh(\gamma_o) & Z_o \cdot \sinh(\gamma_o) \\ \frac{\sinh(\gamma_o)}{Z_o} & \cosh(\gamma_o) \end{pmatrix} \quad \text{2-9}$$

Equation 2-9 now allows the transmission line propagation and attenuation performance to be accurately modelled and by using equations 2-5 and 2-6 to represent the source and load impedances of the transmitting and receiving modems, this allows calculation of the cable attenuation when used for subsea communications.

2.2 Deriving Cable R, G, L and C parameters

In order to make accurate predictions of the cable losses, it is necessary to establish a method for accurately calculating the R, G, L and C parameters, as outlined in Section 2.1, from the cable dimensions. These figures can then be applied to the transmission line model in equation 2.9 and will allow prediction of cable loss from the cable dimensions and material properties. Although with modern impedance analysers, such as the Solartron 1260 and Wayne/Kerr Model 6440, it is possible to measure cable RGLC parameters very accurately, so long as an awareness is kept of the interaction

of measurement length and test signal frequency, and that signal reflections may give misleading results, prediction of these parameters from the cable dimensions is not so straightforward. As far back as the 1920s equations were derived by Dwight (1921) and then again in the 1940s by Arnold (1941) to define transmission line resistance from cable dimensions and to understand the frequency dependency of these and the other G, L and C parameters of cables that dictate the operating performance. Sections 2.2.1 to 2.2.4 define methods for these impedance predictions which are used for comparison with the measurement data later, in Chapter 4.

2.2.1 Calculate R from cable dimensions

As the frequency of transmitted signals increases in the cables, the phenomenon known as 'Skin Effect' becomes apparent. This property, which causes the current in the core to concentrate towards the outside of the conductor, with the inside carrying very little, if any, of the current is a fundamental principle of the propagation of the electromagnetic waves associated with the transmitted signal. The significance of this property is dependent on the frequency of the transmitted signal, the dimensions of the copper cores and the conductivity and permeability of the conductors. This is described in many texts, e.g. Johnson, Graham (2003), Ramo, Whinnery, Van Duzer (1994), Arnold (1941) and Lago et al.(2009) and the impedance looking into a twin wire transmission line, with the conductors shorted at the far end, is defined below:

According to Ramo, Whinnery, and Van Duzer (1994, p182) the loop impedance of a transmission line pair is given by equation 2.10

$$Z(f) = j\frac{\sqrt{\frac{\pi f\mu}{\sigma}}}{\sqrt{2}\pi r_o}\frac{J_o\left(j^{0.5}\left(\sqrt{2}r_o\left(\sigma\sqrt{\frac{\pi f\mu}{\sigma}}\right)\right)\right)}{j^{0.5}J_1\left(j^{0.5}\left(\sqrt{2}r_o\left(\sigma\sqrt{\frac{\pi f\mu}{\sigma}}\right)\right)\right)} \quad \text{2-10}$$

Where μ = magnetic permeability of the signal conductor, typically $4.\pi.10^{-7}$ H/m,

$\sigma =$ conductivity of the signal conductor, typically $5.8x10^{-7}$ S/m and

$r_{o=}$ conductor radius and

$J_1(z)$ is a first-order Bessel function of the first kind

$J_0(z)$ is a zeroth order Bessel function of the first kind.

This loop impedance gives the resistance, from the real part of Z(f), and inductance, from the imaginary part of Z(f), per unit length of any pair of conductors in such an arrangement, with the penetrating depth of the propagating current from the conductor surface, known as the skin depth, defined by Johnson, Graham (2003, p60) by equation 2.11.

$$\delta(f) = \frac{1}{\sqrt{\pi\mu\sigma f}} \quad \text{2-11}$$

Figure 2.1 illustrates the resistance change in a twin wire conductor pair versus frequency. Similar simplifications and alternative methods of calculation outlined in several texts are also shown here and it is clear that these methods are consistent and reflect the same fundamental physical property.

Johnson, Graham (2003, p69, 70) states (again with definitions as above)

$$Z_i(\omega) = \frac{\eta(\omega) J_0\left(e^{(j3\pi/4)} r\sqrt{\omega\mu\sigma}\right)}{2\pi r\left(-j \cdot J_1\left(e^{(j3\pi/4)} r\sqrt{\omega\mu\sigma}\right)\right)} \quad \text{2-12}$$

where:

$$\eta(\omega) = \sqrt{j}\sqrt{\frac{\omega\mu}{\sigma}} \quad \text{2-13}$$

This text describes $\eta(\omega)$ as the intrinsic impedance of a good conducting material and, although the equation could be simplified by combining the two square root elements, it has been left as quoted in the text, illustrating that the phase angle of the intrinsic impedance is $\sqrt{j}$, or $\frac{\pi}{4}$ radians.

Calculations outlined in the paper by Arnold (1941) are also compared in the graph of Figure 2.1.

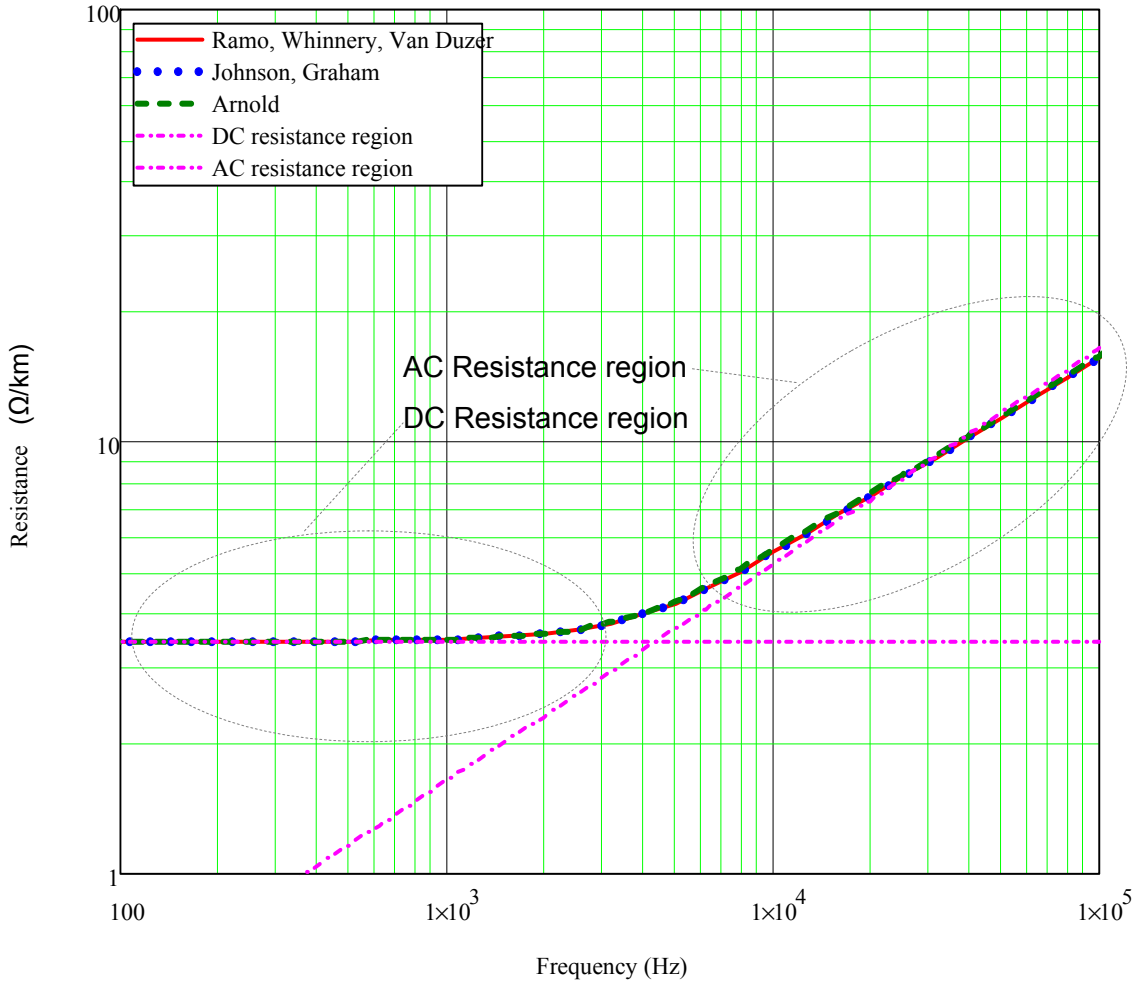

Figure 2-2 Comparison of 10mm^2 cable resistance calculation methods

As shown in Figure 2.1 this is made of up two regions: the DC resistance section where resistance remains constant until the skin effect corner frequency, as described by Johnson and Graham (2003, p65) and shown in equation 2.14, is approached,

$$\omega_\delta = \frac{8}{\mu\sigma r^2} \quad \text{2-14}$$

and the AC resistance, where the resistance increases from the corner frequency at a rate of $\sqrt{\omega}$.

It is noticeable here that the equations for resistance used do not include separation distance of the conductors, however in reality the currents in the two conductors also have an effect on the current distribution in each other.

In addition to the skin effect seen in a conductor caused by the interaction of the magnetic field from a current in the conductor itself, another effect exists when considering the conduction properties of transmission lines caused by the influence of each of the conductor's currents on each other. The currents flowing in the conductors of a twisted pair impact each other causing an asymmetric current density pattern across the cross section of each of the conductors and this is known as the proximity effect.

Proximity effect causes a redistribution of current such that in a transmission line there appears a higher current density in the parts of the cores facing each other and a lower density in the areas facing away from each other. This effect has been widely studied by such as Egiziano and Vitelli (2004), who develop an practical method for calculation of two dimensional proximity effect problems, Matsushima (1999) et al. who give a method for accurate calculation of the AC resistance in a series of identical conducting cylinders and in the paper by Murgatroyd (1989) which examines the proximity loss in multistranded conductor and considers the effect of each individual strand on the

others as well as the overall bunch geometry. Others, like Nan and Sullivan (2003), look at the packing density of the conductors on the prediction accuracy and introduce new methods to improve high frequency calculation accuracy while Tsai and Chen (1990), whose methods have been used later in this section to carry out representative calculations, develop a novel TEM model for calculating the current density and propagation constant in a multiconductor system with irregularly shaped conductors. Vitelli (2004) develops an computationally efficient method for calculating the proximity losses in adjacent conductors which is of particular relevance in the field of power electronics, Smith and Nordgard (1980) provide a formulation for the electrical parameters of a screened twisted pair transmission line which is shown to give accurate prediction of the capacitance, resistance and attenuation per unit length as well as the characteristic impedance and Kane and Auriol (1994) show how in close conductors the AC impedance parameters can change significantly dependent on the frequency and conductor spacing. In order to appraise the impact on the resistance from proximity effect, calculations were carried out using the methods outlined by Tsai and Chen (1990) and the plot shown in Figure 2.2 shows the current density across a section of one conductor of a transmission line pair.

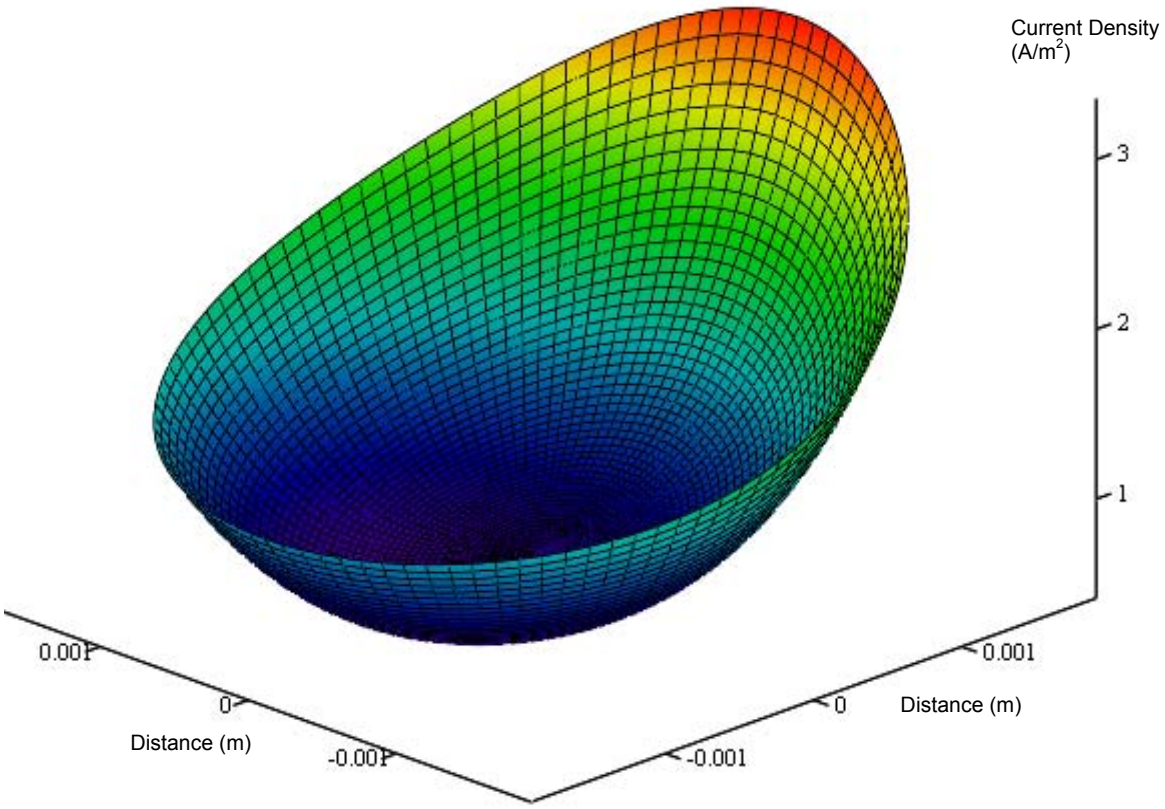

Figure 2-3 Plot of Current density in one conductor of a transmission line pair

Johnson and Graham (2003, p83) suggest a very general 'rule of thumb' solution to proximity effect scaling, which estimates, for the dimensions of the transmission line plotted here with conductor separation of 9mm and core diameter of 3.6mm, an increase in AC resistance of less than 10% above the skin effect resistance calculated before would be expected.

It seems that the proximity effect primarily causes a redistribution of the current over the copper cross section rather than causing any major increase in resistance.

2.2.2 Calculate G from cable dimensions

The impedance between the conductors in a transmission line is dependent upon the dimensions between the conductors and the materials of the insulating medium and thus the energy absorbed by the insulating dielectric medium from the transmission line conductors. In the case of our subsea cables being examined here which are typically insulated by polyethylene, according to Ramo, Whinnery, Van Duzer (1994, p252), the conductance for a transmission line in S/m is given by equation 2.15,

$$G = \frac{\pi\omega \cdot \tan(\delta) \cdot \varepsilon_r \varepsilon_0}{\cosh^{-1}\frac{d}{2r}} \quad \text{2-15}$$

Where:

r is the conductor radius, here equal to 1.784mm for a copper core with cross sectional area of 10mm^2;

d is the conductor separation, here equal to 6.74mm, from a 10mm^2 twin cable;

ε_r is the relative permittivity of the dielectric, typically around 2.25 for polyethylene;

ε_o is the absolute permittivity in free space, this is 8.854x10^{-12} F/m;

tanδ is the loss tangent, which is also equal to the dissipation factor and is taken from Kaye and Laby (2012), as 0.00025 ±0.00005 typically for polyethylene;

and cosh^{-1} represents the inverse trigonometric cosh function.

As dielectric loss factor is defined by equation 2.16,

$$\varepsilon_{dlf} = \tan\delta \cdot \varepsilon_r \cdot \varepsilon_0 \quad \text{2-16}$$

then an important relationship between conductance and capacitance is seen in equation 2.17

$$G = \tan\delta \cdot \omega \cdot C \quad \text{2-17}$$

Where the conductance is in S per unit length

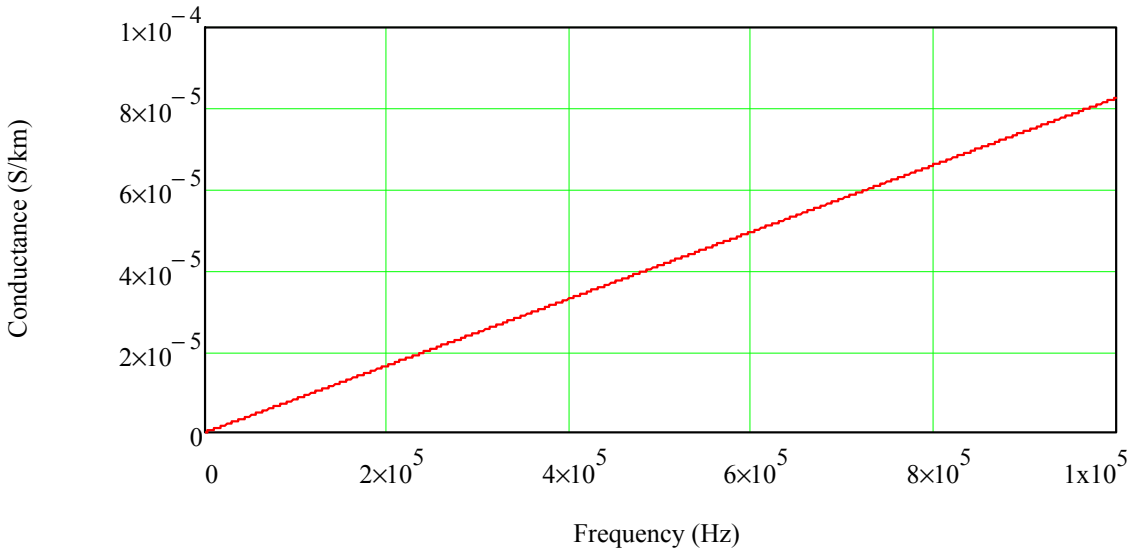

Figure 2-4 Calculated 10mm^2 cable conductance per km

Figure 2.3, shows a linear dependence of the conductance on frequency. Over the frequency range up to 1MHz, the permittivity and loss tangent figures are constant as described by Kaye and Laby (2012).

2.2.3 Calculate L from cable dimensions

The inductance in a transmission line pair is made up of the following constituent parts:

1) The internal inductance i.e. the imaginary self impedance of each wire in the pair;

2) The mutual inductance between the conductors and the loop prescribed by the pair.

The imaginary part of the loop impedance, as described in Section 2.2.1 in equation 2.14, gives the internal inductance of the conductors in the transmission line pair. Below the skin effect corner frequency, equation 2.18, the internal inductance remains more or less constant, dominated by the conductor internal inductance with a value of μ/8π. Above this frequency the internal inductance rolls off in the same way as resistance increases.

The mutual inductance is not frequency dependent and is defined by Ramo, Whinnery, Van Duzer (1994, p252), in equation 2.18

$$L_{dc} = \frac{\mu}{\pi}\operatorname{acosh}\left(\frac{d}{2r}\right) \quad \text{.....2-18}$$

With d, r and μ as defined in Sections 2.2.1 and 2.2.2

These two figures together give the overall inductance for the twin cable and this is shown in Figure 2.4 for a typical twisted 10mm^2 pair.

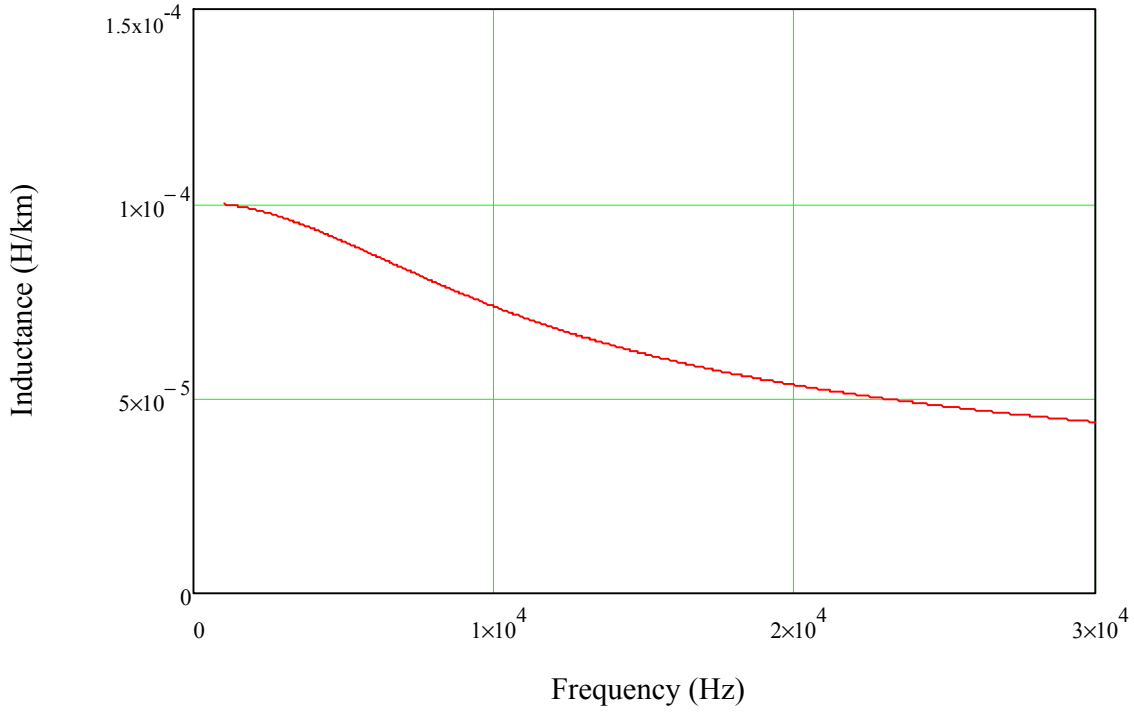

Figure 2-5 Calculated inductance for 10mm^2 cable

2.2.4 Calculate C from cable dimensions

According to Ramo, Whinnery, Van Duzer (1994, p252), the capacitance between a pair of parallel cylindrical conductors is calculated as shown in equation 2.19

$$C = \frac{\pi \varepsilon_r \varepsilon_0}{\cosh^{-1}\left(\frac{d}{2r}\right)} \quad \text{.....2-19}$$

Where the capacitance is in F/m, giving around 52nF/km for a $10mm^2$ quad cable where,

r is the conductor radius, here equal to 1.784mm from a copper core with cross sectional area of $10mm^2$

d is the conductor separation, here equal to 6.74mm, from a $10mm^2$ quad cable

ε_r is the relative permittivity, typically around 2.25 for polyethylene

ε_o is the absolute permittivity. This is 8.854×10^{-12} F/m

As can be seen, the capacitance is not frequency dependent in itself, however changes in the permittivity of the insulating materials surrounding the conductors at higher frequencies will cause a change in capacitance. Polyethylene has been selected for many years now as an ideal material for cable insulation, particularly for radio frequency cables, as it shows a uniform permittivity to in excess of 1 Gigahertz as defined by Kaye and Laby (2012). So in the case of the frequency range of interest of less than 1MHz for this thesis and our measurements, we would not anticipate seeing any frequency dependent change in capacitance.

2.3 Electromagnetic field solver modelling

The effects of cable dimensions and materials and their impact on the resistance, conductance, inductance and capacitance are all interdependent effects of the electric and magnetic fields generated by the flow of current and the presence of the voltages on the conductors. As computing power has increased, it has become practical to model the conductors and dielectric medium as an array of points with the complex interaction of the fields handled by iterative field solver methods. Techniques, such as described by Wu and Yang (1989), Tuncer et al. (1994) and Cristina and Feliziani (1989) can be used to perform these calculations according to the conductor geometry and electromagnetic modelling tools for commercial purposes are offered by companies such as Ansys Incorporated and Optem Engineering Incorporated, both of whose tools have been utilised in the later sections of the thesis. Such commercial tools and methods have been applied, such as by Shackleton D et al. (2007), for the modelling of subsea umbilicals. These electromagnetic field solvers allow us to analyse the impedances over a wide frequency spectrum giving accurate figures for skin and proximity effects in wires as well as the impact of induced eddy currents in the screens and armouring, and dielectric losses in insulation.

2.4 Measurement methods

2.4.1 Cable parameter measurement

The methods for measuring the cable parameters are straightforward in principle. With the remote cable ends connected together and the impedance ‘looking’ into the cables measured the resistance and inductance can be derived easily from the real and imaginary parts of the measurements. With the cable ends open circuit, the

conductance and capacitance are derived, again from the corresponding real and imaginary parts of the measurement.

In practice, though, much care is required in order to ensure accurate results. Cable lengths must be short enough to ensure any reflection effects seen from the end of the cable are not significant. Cable length should be less than a tenth of a wavelength at the maximum frequency of interest to ensure reasonable isolation from these effects. In addition the cable must be long enough to make sure impedances are practically measurable with the equipment available. With most modern impedance analysers, such as the Solartron 1260 and Wayne/Kerr Model 6440 Analyser as used in the measurements outlined in this thesis, 30m will allow accurate measurements up to a few hundred kHz. Beyond this frequency, or as the length of the measurement section becomes a significant part of a wavelength (typically around a tenth), signal reflections may be seen which will cause measurement error and ambiguity (see Chapter 4).

The impedance of the testing cables must be kept to a minimum and, as in the case of both instruments above, a four wire measurement method was adopted. This technique applies the test signal through a separate pair of wires from the monitor pair, ensuring that the source impedance, including the test cables, is not included in the resultant measurement of the cable under test. Figure 2.5, below, illustrates this technique and this was the basis for all measurements made in this thesis

Figure 2-6 Wayne Kerr Impedance Analyser showing 4-wire measurement method (Duco)

Further details of this measurement technique and of the instruments used in the measurements are given in Chapter 4.

2.4.2 Umbilical attenuation measurement

Again, although straightforward in principle, the measurement of the umbilical attenuation needs care to ensure accurate measurements are obtained. Four wire measurements at each end, and a precise measurement of the source and load impedance as well as umbilical length are necessary to derive an accurate figure for attenuation per unit length.

The ideal scenario would be to load the cable under test with the characteristic impedance at the frequency of interest and measure the attenuation under these conditions. It would be expected that this would give us the same figure as we would calculate in the propagation constant derived from the R, G, L and C parameters of the cable as outlined in section 2.1.

In practice though, this measurement, although it would give a cross check with measured R, G, L and C measurements is otherwise not particularly useful. Practical cables, particularly subsea communications cables, operate into fixed impedance loads and it is the attenuation into a realistic impedance that is useful. Good cable parameter measurements can be used to derive the attenuation into any load, using the two port network methods outlined in section 2.1 and these, along with a good umbilical attenuation measurement into a realistic impedance, give an equally good cross check of the measurements and also a more useful figure for the attenuation over the length of the cable.

In reality, cable and umbilical manufacturers quote the measured R, G, L and C figures on data sheets alongside derived attenuation and characteristic impedance calculations using the theory in section 2.1. Datasheets from manufacturers such as NSW, normally specify a 20% tolerance on the quoted values.

2.5 Chapter Conclusion

In this chapter some known theory of relevance to umbilical cables has been outlined, measurement methods described and some sophisticated electromagnetic modelling methods introduced. In the next chapter, some of the expected effects of deployment will be examined, and the measurements and calculations to be carried out in order to derive answers to the research questions will be presented.

Chapter 3. Effects of Cable Construction and Marinisation

This chapter outlines some known industrial working guidelines and then examines the main influences on cable impedance on deployment of an umbilical subsea and the main issues to be investigated in the later chapters.

3.1 Effects of deployment of cables in subsea umbilicals

There are certain agreed working principles and known areas of caution within the oil industry when it comes to system modelling which seem to be largely based on historical observation and have very little documented evidence for the background. This is thought to be largely due to the huge importance placed on company confidentiality of information and the potential cost of losing work to competitors.

- Aker Solutions analysis engineers are advised by their umbilical manufacturing department to add an additional 30% scaling to the stated core capacitance to take account of the effect of flooding of the umbilical after deployment. It is understood that capacitance will increase immediately by around 20% when deployed and that over the subsequent years, this will continue to rise due to water permeating the polyethylene insulation of the cables.

- AC resistance figures quoted by NSW in their cable data sheets suggest that the resistance of the cores in a screened cable is dependent on the screen material, i.e. two types of screen material are common, foil and tape, and typically cables with foil screens show a higher resistive component at high frequencies. The material used for foil screens is significantly thinner than tape.

- The proposed communications system for use in the BP Devenick subsea control system had to be abandoned, and a lower frequency system adopted, due to very high error rates. The poor communications performance was blamed on the presence of hydraulic steel tubes in the umbilical required because of the distance from the field to the platform.

3.1.1 Effects in the umbilical

How does the proximity of other cables, hydraulic steel tubes, hydraulic fluid or umbilical armouring affect the attenuation?

If the characteristics of an umbilical can be measured and compared against a representative electromagnetic model, a useful comparison of the two can be obtained. This will show the impact of skin effect, proximity effect, eddy current losses and the changes in insulation dielectric constant and loss tangent caused by the proximity of the other umbilical components.

3.1.2 Effects in the Sea

Due to the nature of the design of the subsea umbilical termination assemblies, when the umbilical is deployed it will flood such that the cables themselves are surrounded with sea water i.e. typically the copper cores each have an insulating polyethylene covering and these pair or quad arrangements are further surrounded by a insulating polyethylene jacket. This outer jacket will be surrounded by sea water once deployed.

What will be the effect of this flooding with sea water and the submersion of this umbilical under the sea on the cable impedances?

3.2 The effects on the cable of deployment in the sea

It would seem reasonable to expect a change in the copper conductivity due to the temperature gradient in the sea which would vary according to the depth and location in the world in which the umbilical is deployed. Similarly, due to the surrounding of the cable by seawater and since a screened cable already has a higher capacitance than an unscreened, due to the proximity of the screen to the cores, it would also seem reasonable to expect a change in capacitance as the surrounding dielectric is altered.

There are other factors to consider, e.g. since umbilicals are deployed at depths of up to 3000m, the pressure acting on them could be expected to cause a physical compression of the cables inside thereby changing the insulation dielectric constant as well as reducing the distance between the conductors. This change in geometry would be expected to affect the capacitance as well but we also know inductance will be affected by the loop prescribed by the conductors. If the geometry has changed, this loop area will also have changed and therefore inductance will be altered as well; but by how much? What about the resistance? Is it similarly affected? And will variations in the sea water salinity have any effect on the cable impedance? Clearly changes in the water conductivity will have a huge effect on any electromagnetic properties of the water with an inevitable impedance change and a potential mismatch between wet and dry parameters. If this 'salinity dependent' impedance change in the seawater has a significant impact on the cable impedance causing a mismatch to the source impedance, there could well be a significant loss of power and poor signal communications.

According to Stewart (2010), the relationship between sea water pressure, temperature, density and salinity is defined by The International Equation of State (1980) published by the Joint Panel on Oceanographic Tables and Standards (1981).

If a test can be performed on a bare quad cable, measuring the impedance when dry, when immersed in fresh water and when immersed in seawater, it will be possible to assess the dependence of the impedance on the properties of the surrounding water conductivity. In addition, measurement of a short length in a pressure chamber will give a good basis for understanding the impact of submersion of our cables in a subsea environment.

3.2.1 Temperature

Seawater temperatures vary greatly throughout the world and therefore the region in which the umbilical is deployed must have a bearing on the electrical properties of the conductors. Surface waters are heated by sunlight through the day and this heat is distributed by the effect of the waves and currents over the top 100m or so. Therefore, throughout the world a similar pattern with a reasonably flat gradient over the top 100m is seen. This can be in the region of 20°C to 25°C in tropical waters whereas in Arctic and Antarctic regions can be as low as 0°C or even lower. In some cases, due to the salinity and other impurities, this can be lower than -2°C and, since water has highest density around 4 degrees above its freezing point, sea water temperature gradients can easily show a higher temperature at depth than on the surface, where ice and sub zero conditions dominate.

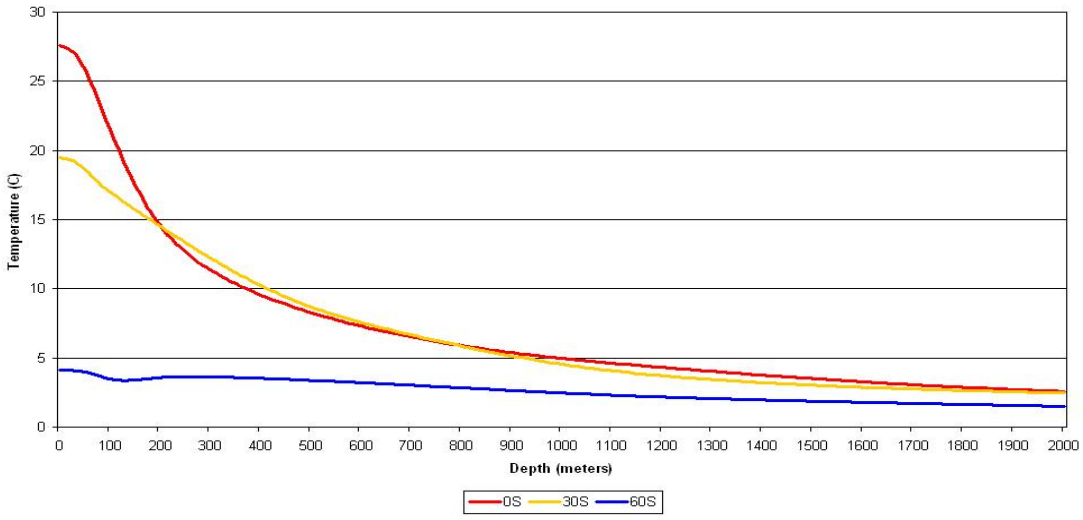

Figure 3-1 Ocean Temperature vs Depth at various Latitudes of the World

Joseph (2010) graphs the variation in subsea temperature at a selection of latitudes, shown in Figure 3.1.The three curves show the temperature versus depth at different world latitudes. The 0°S group includes latitudes -15°S to 15°N. The 30°S group includes -45°S to -15°S. The last group includes -75°S to -45°S

This temperature variation with depth shows how, over the first 100m, temperatures are relatively constant but beyond this, there follows a rapidly changing temperature region, between 100 and around 300m, known as the Thermocline.

Since copper conductivity changes with temperature, it would be expected therefore, that the other complex parts of the impedance would be similarly affected. Also, as seawater temperature varies across the deployment length of the umbilical, it would seem likely that the resultant impedance must also vary over the length.

3.2.2 Pressure due to depth

Pressure within the ocean increases with depth and for a given sea water density, a linear relationship exists between depth and pressure. For every 10.2 meters increase in depth, approximately, the pressure increases by 1 bar. Subsea equipment and cables designed to operate at 3000m, for example, will therefore have to withstand

pressures of around 300 bar which requires very careful and detailed mechanical design.

The density of the sea water is not so straightforward, however. Sea water density varies greatly throughout the oceans and often very rapidly in localised areas. These areas of rapid change are known as Pycnoclines. Pycnoclines are seen at the mouths of rivers, where fresh water mixes with sea water, or similarly in areas with unusual current flows or heating or cooling effects. As density varies also with depth and temperature, this calculation and indeed the relationship between pressure, salinity, temperature and depth is an extremely complex one and is modelled by the equation of state for sea water, Stewart (2010). Analysis at this level of detail is beyond the scope of this thesis, and is in fact unnecessary for the investigation being carried out in this thesis. It is sufficient at this stage to assume the linear depth/pressure relationship as defined above.

As the pressure will alter the physical dimensions of the deployed umbilicals, it would seem inevitable that, as a consequence, the cable impedance would be affected too. Also, as pressure varies across the deployment length of the umbilical, it would seem likely that the resultant impedance must also vary over the length.

3.2.3 Salinity

As outlined in Section 3.1.2, the equation of state for sea water, Stewart (2010) defines the relationship between salinity, density and temperature.

Salinity of the oceans at depth, again, varies greatly throughout the oceans. Depth, temperature, density and locality e.g. at the mouths of rivers or narrow inlets such as fjords, are just some of the influences which can have an effect. However, in general according to data from US National Oceanographic Data centre (2012), the salinity, in

grammes per litre, varies with depth over the oceans approximately as per the curve shown in Figure 3.2.

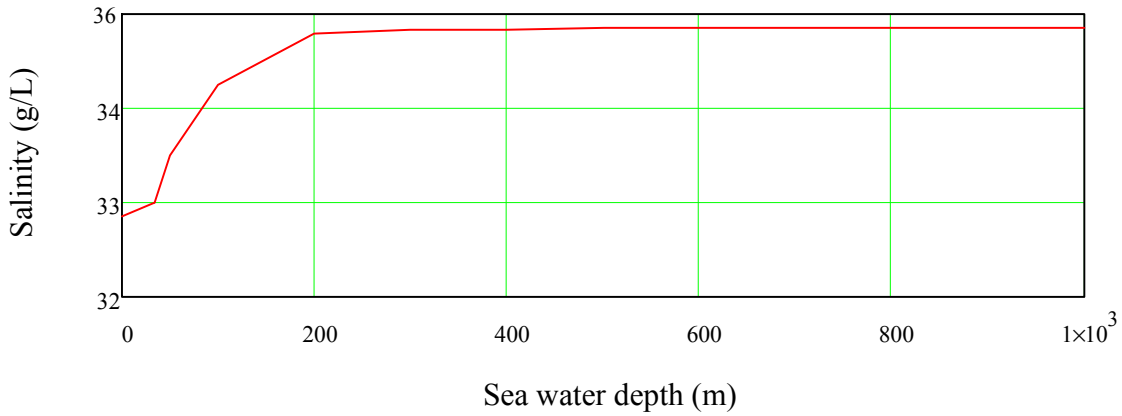

Figure 3-2 Typical graph of sea salinity versus depth

The concept of sea water 'saltiness' or salinity as graphed above again is not straightforward but the term really refers to dissolved salts, rather than salt. The most abundant dissolved ions are: Sodium, Magnesium, Calcium, Potassium, Strontium, Chlorine, Sulphate and Bromine, and the mixing of seawater and fresh water, for example at the mouth or rivers, will produce an averaging in the concentrations of these ions. Similarly changes in salinity will occur due to evaporation in high temperature regions of the ocean, however the constant composition rule, a fundamental rule in oceanography states that the relative ratios or concentration of these ions will always remain constant.

As the conductivity of the sea water surrounding the cables will alter as the salinity changes, a change in the radiated electric and magnetic fields from the propagating fields would be expected. Also, as salinity varies across the deployment length of the umbilical, it would seem likely that the resultant impedance may also vary over the length.

3.2.4 Water ingress/flooding

In discussion with Aker Solutions umbilical engineers in Norway, it was suggested that a 20 to 25% increase in cable capacitance would be expected when the umbilical is deployed. It was also suggested that this would continue to increase over subsequent years. At the time, these figures could not be substantiated, but it was believed that the water penetrated the polyethylene insulation over time.

No evidence could be found for this from installed subsea cable data, however information obtained from a manufacturer's screened cable test for a major subsea project showed that, while no change takes place in the cable characteristic when submerging a screened cable, if the four conductors are exposed by stripping back the outer insulation and screen over a short section and then submerging and testing under pressure, an increase of just under 25% in capacitance is indeed seen as the water permeates through the cable under the outer insulation, as shown in Figure 3.3. Tests were carried out in a pressure vessel at 250 bar and used fresh water.

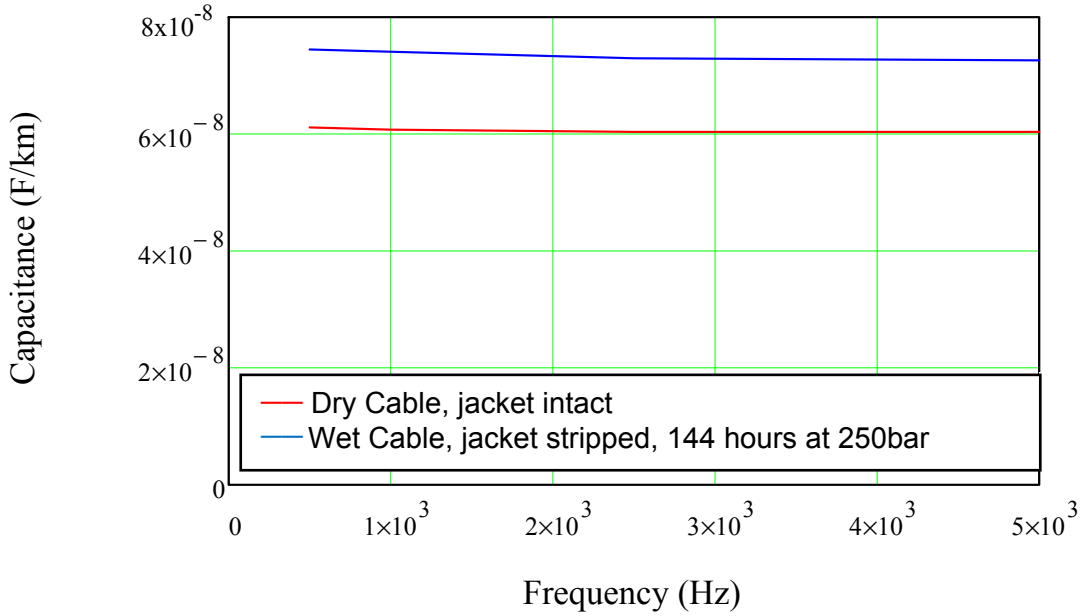

Figure 3-3 Effect of flooding on cable capacitance

The photograph shown in Figure 3.4 clarifies the arrangement.

As the screened cable would have a higher capacitance than the equivalent unscreened cable, it is reasonable to expect that an even higher percentage increase would be seen on submersion of an unscreened cable.

Figure 3-4 Cable jacket stripped back to allow water access (Duco)

In all subsea cable designs, it is required that two water barriers are provided between any conductor and the sea. In the test above our conductors would normally be isolated from the sea by the individual conductor jackets and the outer overall polyethylene insulating layer. It would not be normal for water to surround the individual conductor's insulation under normal operation of subsea equipment. This, however, is a very clear indication that a significant change in capacitance can be expected when an unscreened cable is submerged and water surrounds the outer jacket.

3.2.5 Water Treeing

Following on the thoughts from Aker Solutions engineering, the concept of water ingress into the polyethylene jacket is explored some more in this section. Much work has been done to explore the effects of water penetration of cable insulation such as that done by Steenis and Kruger (1990) who examine the effects of cable aging on the growth of water trees and a consideration of the growth mechanism, Platbrood et al.

(2009) who demonstrate that the growth of trees is very dependent on the insulation material and provides a method for stimulating rapid tree growth for the purpose of assessing new insulation, Sun et al (2009) who look at the effects of electrical field, age and dielectric properties on the growth of trees in a variety of materials and provides a means of comparison with the resistance of new developed materials to this phenomenon and Hvidsten,et al.(2005) who assess the impact of very high temperatures on the electrical properties of XLPE. Others such as Thomas and Saha (2005) explore methods of detecting the presence of water trees in deployed cables over their lifetime and how to assess the cable condition while Stancu C et al. (2009) examine the degree to which the semiconducting layers in high voltage cables affect the likelihood and type of trees that will grow, and the resultant acceleration of dielectric breakdown.

Ozaki et al. (2001) assess the impact on capacitance and dissipation factor of the insulation of cables under stress at 1KV, Nilsson et al. (2010), show that the means of crosslinking LDPE insulation affects the electrical degradation of cables and resistance to water treeing and Hai and Thank (2006), evaluate the eventual failure of the cables caused by water tree degradation and assess the ability of degraded cables to withstand voltage stress in humid environments.

Sarkar et al. (2010) examine the impact of ethylene content on the growth of bowtie tree formation and the long term performance of cables in a wet environment. Here it is also demonstrated that under test the ac breakdown strength are comparable in the higher and lower ethylene content insulation materials, Czaszejko (1998), studies the statistical distribution of the length of water trees that grow after the short exposure of a XLPE insulated cable to a DC voltage and Ciuprina et al. (2004) consider the difference in the length of water trees that grow in chemically XLPE and LDPE and show that there is no significant difference in the lengths of trees that develop.

From the earliest days of subsea telecommunications cables, engineers were well aware of the ability of water to penetrate the insulation materials. Burns (2009) reports on issues found with the 1947 Anglo-Dutch and 1948 Anglo-Belgian telecommunications cables insulated with early polyethylene, branded as Telcothene. It was found that the cables would flood with water at depths exceeding 250m but at less than this, the flooding effect was not seen. Studies showed that due to osmosis, the salt in the seawater was able to draw the water from the cable until the pressure became too high, hence the two effects of water penetration and osmotic 'suction' worked in opposition with the resultant depth limit.

This ability of water to penetrate polyethylene has subsequently been studied by many and it is now recognised that, dependent on the material construction and applied voltage, the penetration of the insulation by water is expected. The effect was first formally brought to light by Miyashita (1969) and is known as 'water treeing'. As pointed out by Steenis and Kreuger (1990, p994) 'Trees' primarily take two different forms.

1) Vented trees grow in the direction of the insulation material boundaries to the other side of the insulation, predominantly in the direction of the electrical stress, and are accelerated by voltage potential and frequency. Figure 3.5 shows a vented tree.

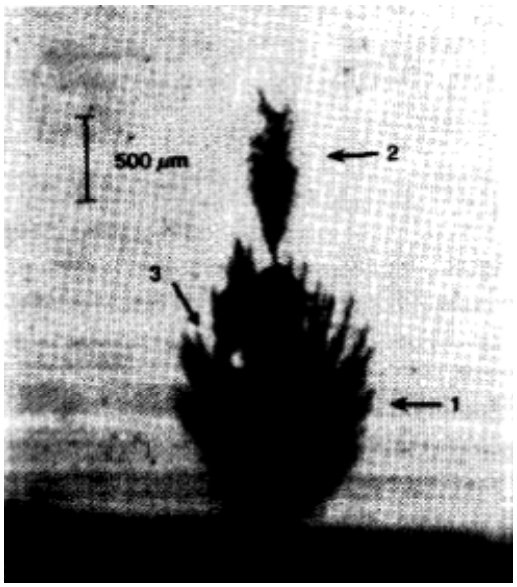

Figure 3-5 Vented Tree, Steenis and Kreuger (1990)

2) Bow tie trees: initiating in the insulation, volume and grow in opposite directions along the electric field lines. Figure 3.6 shows this effect

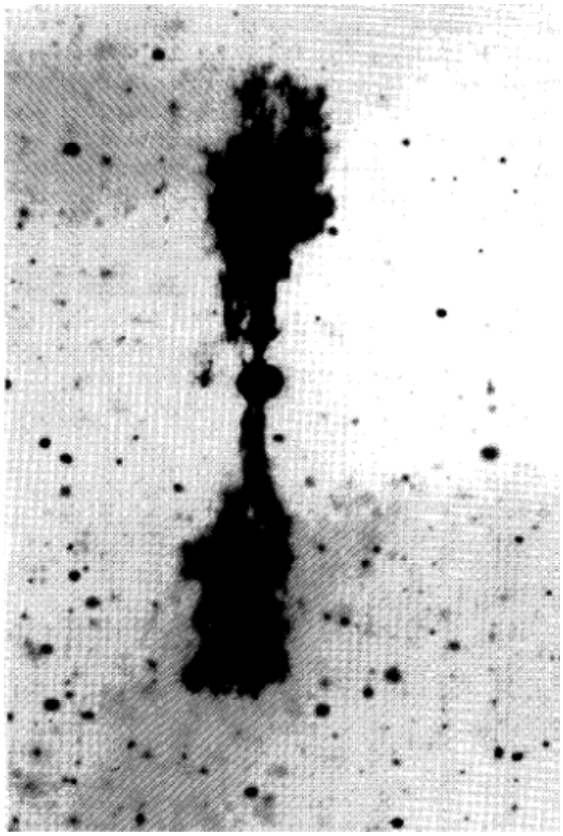

Figure 3-6 Bow tie Tree, Steenis and Kreuger (1990)

Since water trees grow in discontinuities in the polyethylene molecular structure, the higher the density of polyethylene, the less the effect. High Density Polyethylene has longer chain structures with lengths of 7000 to 14000 molecules compared with Low Density Polyethylene with chain lengths of 1500 to 3500 molecules and, as a result, the ability for trees to grow is substantially reduced.

The effect has been shown to be dependent on applied voltage, frequency and temperature, Steenis and Kreuger (1990), Hvidsten,et al.(2005). Trees start to grow with applied voltages of greater than about 1kV/mm with the rate of growth increasing as voltage is increased. In a similar way growth rate and magnitude of trees is dependent upon frequency and temperature with growth rate and magnitude of trees increasing rapidly above a few kHz and above 30°C.

Although higher density polyethylene with greater molecule lengths are available to help reduce the effect of water treeing, and prevention using tree retardant cross linked polyethylene (XLPE), has been used successfully in Asia as outlined by Barber and Marazzato (2005), it still seems the only way to prevent treeing completely is to produce a completely impervious water barrier around the conductors. With current technological capability, the only way in which this can be done is with a continuous metal jacket or a tube. This technique is currently used for the distribution of optical fibres subsea, where a steel tube is used to prevent water ingress through to the fibres and thereby ensure hydrogen darkening of the fibre is avoided. However, although this technique is also used with subsea cables operating at high voltages i.e. for power distribution between platforms or for subsea power lines operating at several kV, it is not generally used for power connections below 1kV as is normal for connection to subsea well control equipment for the oil industry.

So there is continual water ingress into the cable taking place over many years, although there are many factors: frequency, voltage, temperature all have a bearing on the magnitude of the problem. Analysis of water treeing and its impact on the energy industry is the subject of much ongoing study. As the trend towards offshore wind, subsea tidal and wave power systems grows and companies like Nexans increasingly supply long distance, high voltage subsea cables, as described in Angoulevant O (2010), it is becoming increasingly important for the energy companies to fully understand the impact of water treeing on power transmission.

However, for the purposes of this thesis, as the majority of subsea control systems used within the industry are still designed to operate below 1kV due to the limited availability and high cost of high voltage subsea wet mate electrical connectors and standardisation of subsea cable specifications, and since power frequencies are typically 50 or 60Hz and subsea temperatures are typically less than 10°C, water treeing effects are not considered further in this research as these do not significantly impact the type of subsea control systems being considered in this research.

3.3 The effect of construction on cable parameters

From data received from umbilical and cable manufacturers, it can be seen that cables with the same cross sectional area can have significantly different attenuations, dependent on the construction of the cable. As shown in Figure 3.7, screening or armouring a cable will have a dramatic effect on the attenuation at higher frequencies and even the number of cores grouped closely together will have an impact on the attenuation. Standard quad and twin cable architectures are shown in Figure 3.7, with the quad attenuation measured between the conductors forming a diagonal pair.

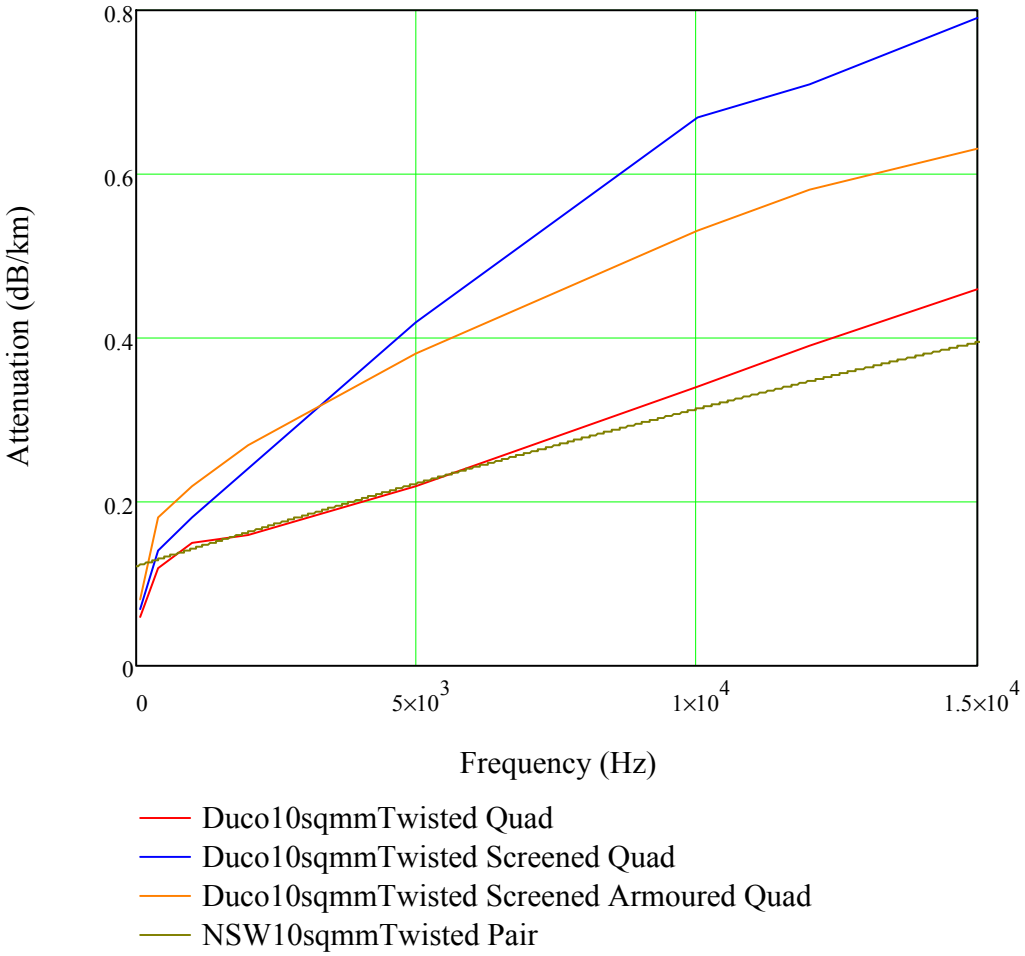

Figure 3-7 Attenuation of Various 10mm^2 Cable Types

From the plots in Figure 3.7, it is clear that the construction of the cables and the surrounding materials themselves have a significant effect on the cable attenuation. Noticeable here is the difference between the attenuation of a twisted pair and a twisted quad. Is this due to an effect caused by the proximity of other cores or is this due to the difference in separation of the two cores being measured?

Similarly the resistance of a twisted screened quad is significantly higher than an unscreened quad. Is this due to dimensional differences or does the screen itself cause the increase in resistance?

Since it is seen from these figures that the general construction of the cables will affect the losses of the cable, what other effects would be expected when the cable is incorporated into an umbilical and deployed in the sea? How does the construction affect the primary R, G, L and C parameters and how significant are these effects? What is the effect on the cable of the hydraulic steel tubes and umbilical armouring?

If the impedance of a section of cable in isolation can be measured and compared with figures when in proximity to a steel surface, the degree of influence of neighbouring material on the impedance can be assessed. Measurement of the cable impedance remote from and near a steel plate will give a good indication of the effect of the neighbouring metalwork and similarly the test in the steel pressure vessel outlined in section 3.1 above, will give further backup to any changes that may be seen.

3.4 Chapter conclusions

In this chapter, the effects of deployment subsea have been outlined and bringing together some of the tests suggested in sections 3.1.1, 3.2 and 3.3, tests are proposed where the impedance of a bare quad cable when dry, when immersed in fresh water and when immersed in seawater is measured in order to assess the dependency of the impedance on the properties of the surrounding water conductivity. In addition, measurement of a short length of cable in a steel pressure chamber will give a good basis for understanding the impact of submersion in a subsea environment when in the proximity of umbilical armouring and hydraulic tubes, and the application of pressure to this chamber will allow us to measure the effect on impedance of submersion at depth. These tests, which are followed up in Chapter 5, should provide answers to the research questions of the effects of umbilical construction, flooding and pressure on cable impedance in an umbilical.

As the area of water treeing described in section 3.2.5 is an area where meaningful study may in fact take years to complete, this has not been examined further as part of this research but is raised again in the section on recommended future work.

Chapter 4. Methods and Models

In the last chapter some of the influences and known effects on the umbilicals were outlined and in this chapter, tests methods and measurement integrity tests are carried out before the main research tests investigate the issues of flooding, pressure, construction and salinity in Chapter 5.

Section 4.1 examines the methods and equipment used in measuring the cables and umbilicals in the further tests carried out in this research.

The tests to be performed will be:

1) In section 4.2, manufacturer's supplied measured data for various cables will be compared with different prediction methods in order to ensure a good picture of the losses in a bare quad cable is obtained. In Section 4.2.3, specific manufacturer's measurements are examined to assess the effect of screening on the cable parameters;

2) In Section 4.3 measurements are carried out to provide some essential checks on interpretation of equipment results and check for measurement errors;

3) In section 4.4 further measurements are taken to investigate other potential sources of error to further ensure results are not misleading.

4.1 Test Equipment

Two impedance analysers are used for measurement in this section, primarily due to availability from companies where work was carried performed. These are the

Solartron 1260 and the Wayne/Kerr Model 6440. An outline of the specifications and limitations of these devices is as shown in Table 4.1:

	Solartron 1260	**Wayne/Kerr 6440**
Frequency range	100μHz to 32MHz +/-100ppm	20Hz to 3MHz, ±0.005%
Resistance	Accuracy at 100KHz ±0.1% up to 10kΩ, ±0.2% to 1MΩ, ±1% to 10MΩ, ±10% to 100MΩ,	0.01mΩ to >2GΩ, ±0.02%
Conductance	Refer to resistance accuracy specifications	1nS to >2kS
Inductance	Accuracy at 100KHz – ±0.1% down to 20μH, ±0.2% to 2μH,	0.1nH to >2kH, ±0.05%
Capacitance	Accuracy at 100KHz – ±0.1% down to 200pF, ±0.2% to 20pF,	1fF to >1F, ±0.05%

Table 4-1 Impedance Analyser Performance Comparison

The Wayne/Kerr 6440 provides a temperature compensation function to allow for variation in copper conductivity. By recording of the measurement temperature, the conductivity figure is adjusted and an appropriate scaling of derived parameters is carried out.

Other data was supplied by cable manufacturers Duco and NSW and is measured and supplied to industry for use on projects, however as this data is not verifiable, is quoted purely for information purposes. All these figures were measured by adopting the 4-wire measurement method as outlined in section 2.4.1 and shown in Figure 4.1.

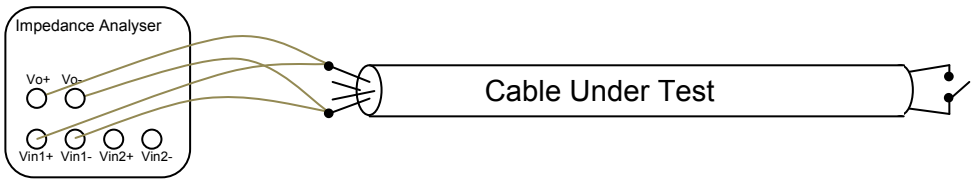

Figure 4-1 Four Wire Impedance Measurement Method

This technique ensures minimum error in the measurement at the equipment under test (in this case, a cable) by:

- Minimising current, therefore voltage drop, in sensing wires;
- Test waveforms applied and measured differentially;
- Impedance measurement is carried out on a short length to minimize error from reflections.

For impedance measurement, a measurement of the cable impedance looking in to the cable with the end open circuit will give a measure of the capacitance and conductance of the cable.

Similarly, if this measurement is repeated with the far end of the cable short circuited, a resistance and inductance measurement is obtained.

Measurement of attenuation is shown in figure 4.2. Here, cables used for test should be kept as short as possible or if this is not practical, as is the case when umbilicals are measured and ends may be fifty meters from each other, a calibration file can be obtained, measuring the losses in the test cables only and subtracting these from the final measurements.

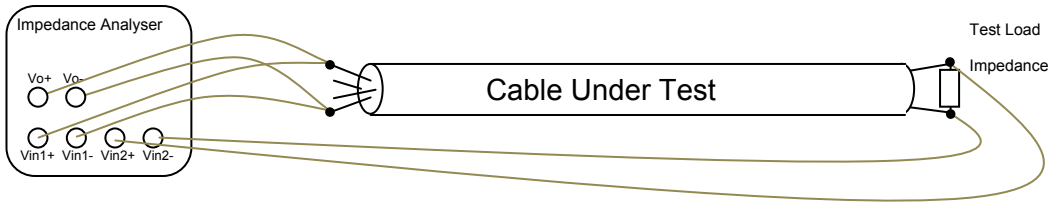

Figure 4-2 Attenuation Measurement Method

When the test load impedance is equal to the Characteristic Impedance of the line, as described in Equation 2.4, the measured attenuation will equal the theoretical loss per metre for an infinite line, as outlined in Equation 2.3. In reality though, as

manufacturer's equipment is designed with particular fixed source and load impedances and as generic solutions are produced to work with a large variety of cable types and cross sections, these measurements are made to reflect the requirements of the equipment that will be deployed. In the case of the umbilical measurements made in Section 6.5, this impedance is set at 94Ω as defined by the particular manufacturer of the equipment being evaluated.

4.2 Measurement of quads and twins to show skin effect

The modelling technique described by Ramo, Whinnery, and Van Duzer (1994) for predicting cable losses is based on a resistance, conductance, inductance and capacitance (RGLC) model as outlined in section 2.2 over the frequency band of interest, to 1MHz:

Capacitance is defined as a function of the conductor geometry and the material properties of the insulation, and remains constant over the frequency band.

Conductance, again, is a function of conductor geometry and the material properties but is also a function of angular frequency so increases linearly over the frequency band.

Resistance and inductance are still functions of the conductor geometry (core separation and dimensions) and frequency, however this is a much more complex mathematical relationship, with skin effect and proximity effect also having a significant impact on the results.

4.2.1 10mm^2 Twisted Pair vs Quad

Figure 4.3 shows a prediction of the resistance according to Ramo, Whinnery, and Van Duzer (1994), for the 10mm^2 cable compared with measured resistance figures supplied by a cable manufacturer for the same type of cable. As the theory for the

cable resistance takes no account of conductor separation, the same calculation is applied to the twin and quad cable.

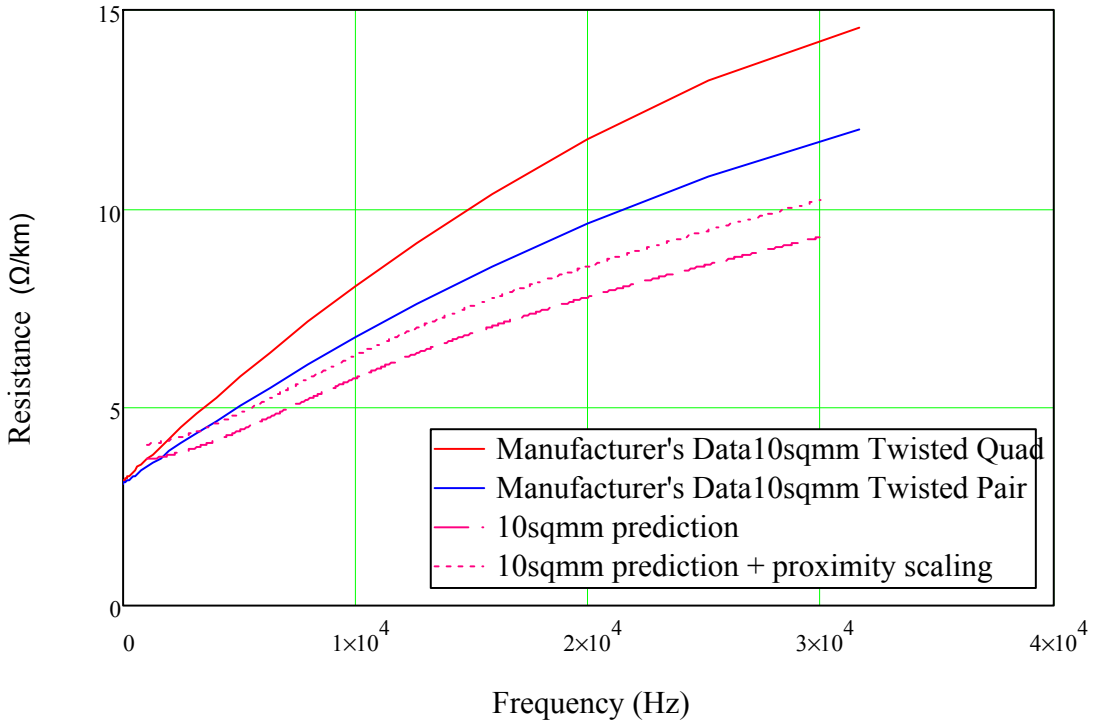

Figure 4-3 Resistance comparison - Manufacturer's data and resistance prediction (Ramo, Whinnery, Van Duzer (1994))

From Figure 4.3 three things can be clearly observed:

1) The resistance measured is significantly higher than that predicted

2) The error in the calculation is greater for the quad cable than for the twin cable.

3) The measured rate of change is higher for the quad than the twin

Johnson, Graham (2003) give a proximity effect factor scaling figure in the order of 1.1 for the case where conductor separation is 6.74mm and diameter is 1.78mm. With this applied, the predicted resistance is higher, however still insufficient to reflect the measurements.

Similarly, figures for the predicted and manufacturer's measured inductance are shown in figure 4.4:

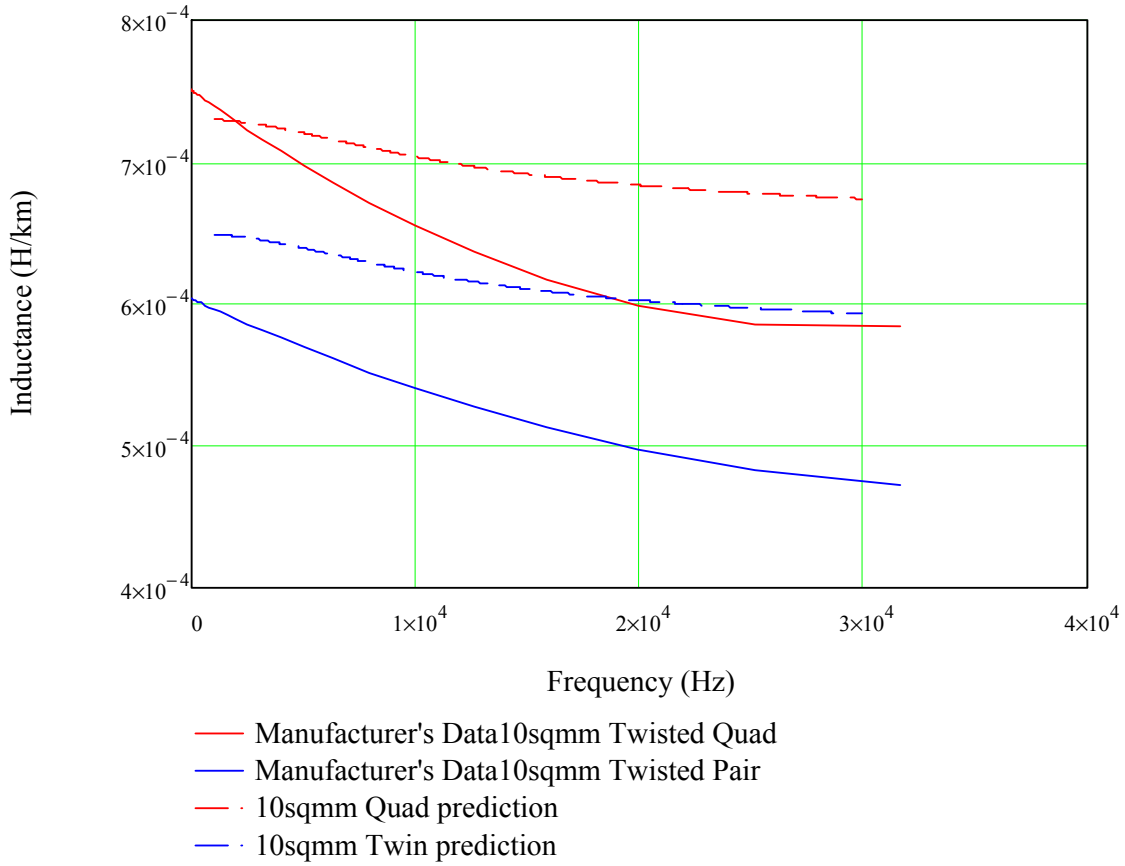

Figure 4-4 Inductance comparison - Manufacturer's data and inductance prediction (Ramo, Whinnery, Van Duzer (1994))

Here it can be seen that, while the prediction is within 10% at low frequencies, below around 4KHz, and the overall shape of the curve is correct, the rate of roll off, as defined by the skin effect part of the inductance calculation, is insufficient both for the twin and the quad cables, to properly track the measured data.

Noticeable here, again, is that, after the skin effect corner frequency, the rate of change of inductance with the manufacturer's quad and twin cables, is more rapid with the quad cable than with the twin, showing around a 150μH difference at DC compared with about 110μH at 30kHz.

The manufacturer's stated capacitance for the Twisted Pair cable in Figure 4.4 is around 51nF/km for the quad and 58nF/km for the twin. The prediction for a similar $10mm^2$ twin with separation of 6mm would give around 56nF and for a quad with separation of 8.5mm, about 41.5nF.

Conductance is quoted at DC only by the manufacturer and is given as a DC resistance (the reciprocal of conductance) greater than 10GΩ. Prediction would give around $1.7x10^{13}$ S. Conductance is exceptionally hard to measure accurately over our frequency band due to the effect of leakage currents in the air so measurements have to be treated with a certain amount of caution before their inclusion in the models. This is considered again in section 6.5 and this issue plays a major part in the alignment of the various measured and calculated predictions.

4.2.2 Comparison of alternative resistance calculation methods

As covered in section 2.2.1, the methods outlined by others: Johnson, Graham (2003); Ramo, Whinnery, Van Duzer (1994) and Arnold (1941) as shown in Section 2.2.1, all show similar findings for resistance and are shown in Figure 4.5 against manufacturer's data for twin and quad cable.

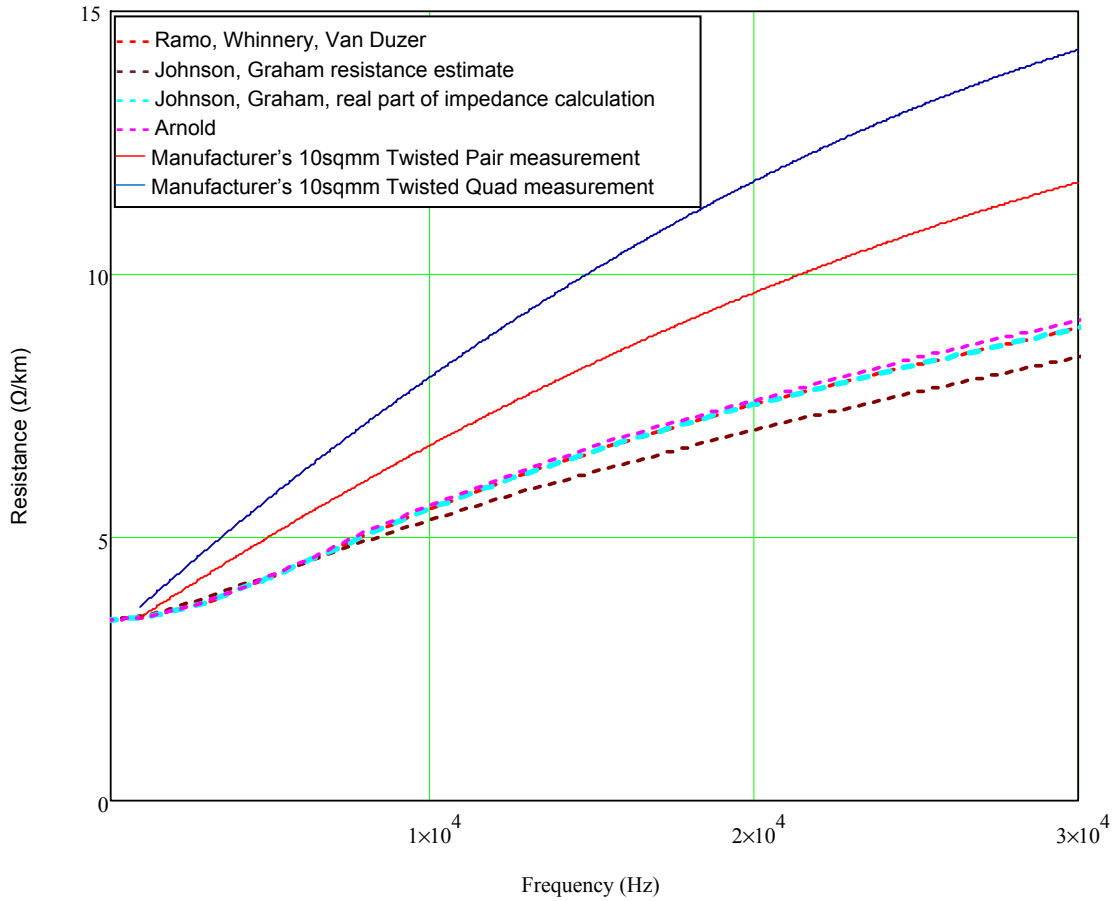

Figure 4-5 Comparison of resistance calculation methods vs sample measurements

Again, all the methods for calculation of resistance utilised show similar results with the following observations:

1) The resistance measured is significantly higher than that predicted;

2) The error in the calculation is greater for the quad cable than for the twin cable;

3) The measured rate of change is higher for the quad than the twin.

4.2.3 10mm² twisted quad vs screened twisted quad

A comparison of manufacturer's measurements obtained for a screened and unscreened cable shows a further area of uncertainty against the calculations outlined so far. The addition of a screen to a cable could be reasonably expected to cause an increase in capacitance and this is seen in the case of the twisted quad whose resistance is plotted Figure 4.6, where the capacitance for the quad is around 55nF for the unscreened quad and around 87nF/km for the screened version of the same quad. However, as well as the observed discrepancy outlined already between the measured cable impedance parameters and those predicted with the quad and twin cables showing different figures, there is also seen here a difference in the manufacturer's measured resistance for a screened quad and a unscreened quad as shown in Figure 4.6.

The graph of Figure 4.6 shows the resistance measured for a 10mm^2 twisted quad and twisted screened quad versus the predicted resistance as described by Johnson, Graham (2008).

This illustrates that the resistance of the cable is affected by the screen although this is not described in the texts, Johnson, Graham (2003), Ramo, Whinnery, Van Duzer (1994) and Arnold (1941).

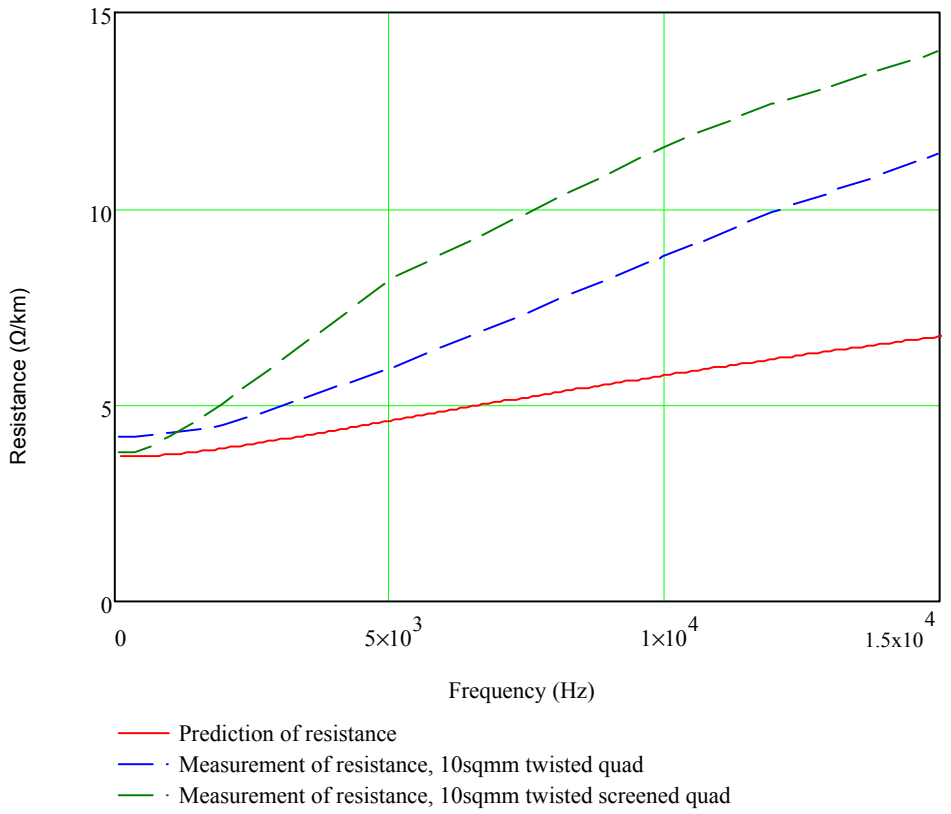

Figure 4-6 Comparison of predicted and measured resistance for various 10mm^2 quad cables

In a similar way, the inductance for the screened and unscreened quads gives different results, as shown in Figure 4.7

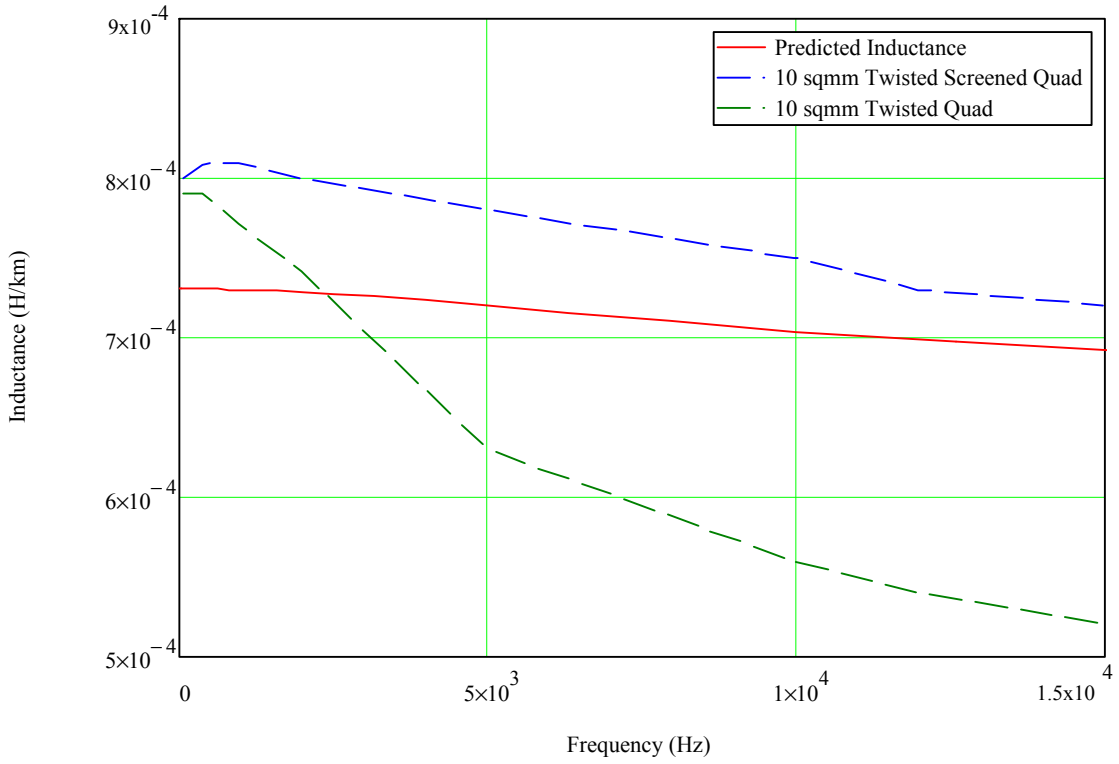

Figure 4-7 Comparison of predicted and measured inductance for various 10mm^2 quad cables

As a result of these unexpected effects, cable attenuation is much higher than prediction has shown to date so that on several occasions, subsea systems designed and manufactured were unable to achieve acceptable communications without substantial rework. Oil fields such as Shell Penguins in 2002/3 and Mobil Arthur in 2003/4, showed such problems.

4.3 Measurement error checks

While the methods employed for measurements are recognised techniques within the industry and generally regarded as good practice, in order to make sure measurement

anomalies were not giving misleading results, some other possible sources of error and measurement cross checks were carried out.

4.3.1 Coiling of cables

For convenience, many of the measurements had to be carried out with cables in a coil on the floor of a workshop or in a manufacturing yard. For example, frequency response measurements on full umbilicals, in the main, are only really possible before deployment of the umbilical, while it is store on a carousel in the manufacturer's yard. Access to both ends of the umbilical with the one instrument is often awkward although in some cases 'double length' attenuation measurements can been made, in order to minimise measurement error, by looping back cores at the remote end of the umbilical.

With RGLC measurements however, since these are done on relatively short lengths of cable, it is possible to lay out the cable to suit the measurement method and the following test, carried out using a 19m unscreened quad core aimed to assess whether the act of coiling the core had any impact on the measured RGLC values. All cable parameters were measured, but shown in Figure 4.8 are the measured resistance values.

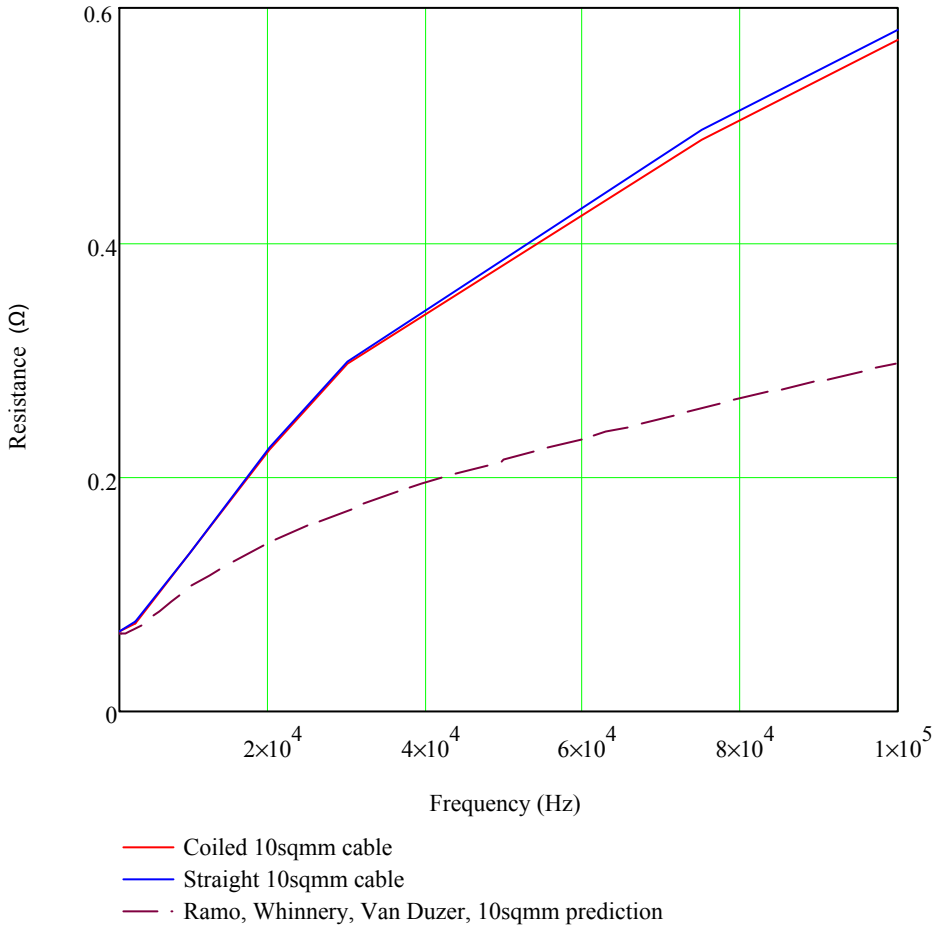

Figure 4-8 19m Coiled vs Straight resistance measurement

As shown, the resistance is consistent, showing a difference of less than 1 ohm between measurements up to 100kHz, suggesting that the large cable drums on which the measurements were made are not having a significant impact on impedance or attenuation measurements, at least up to 100kHz, with the derived attenuation, calculated from the measured R, G, L and C parameters having no significant observable difference, shown in Figure 4-9.

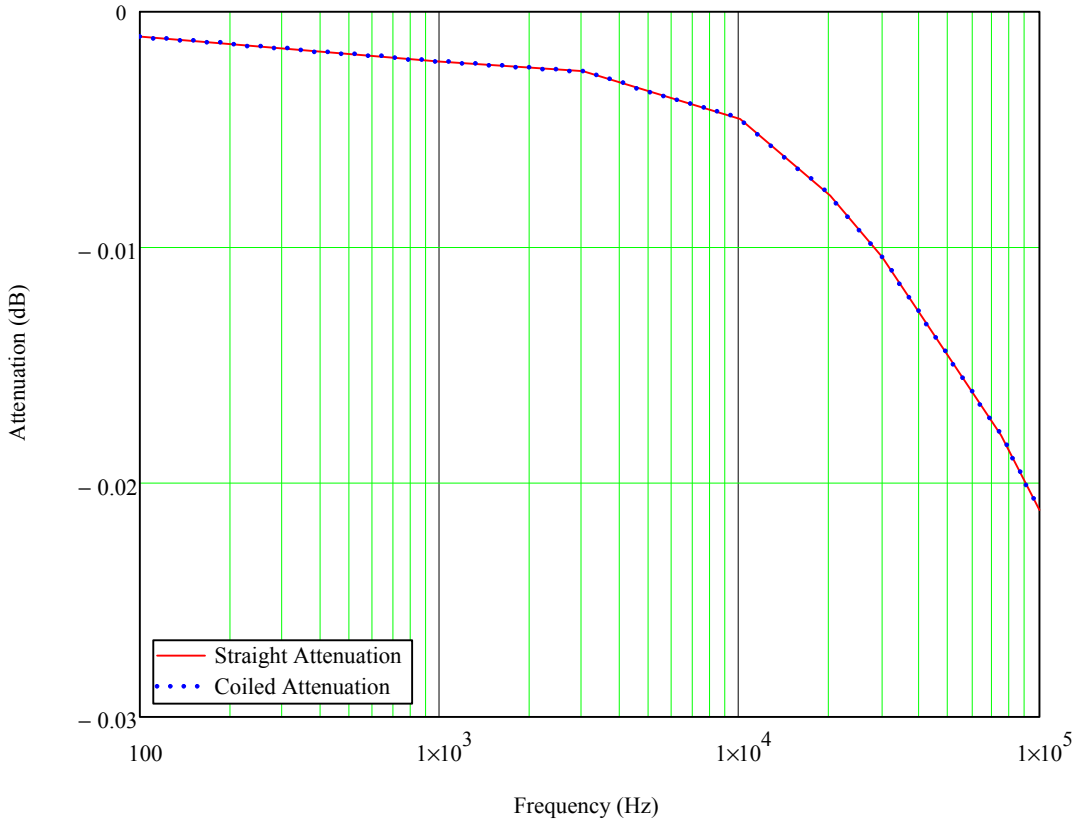

Figure 4-9 Attenuation of 19m 10mm^2 Cable – Derived from RGLC Measurements

4.3.2 Calibration checks

As the impedances being measured are extreme, being in the order of mΩ in some cases to hundreds of MΩ or more in others, some measurements were carried out to assess the accuracy of the measurements of the Solartron 1260 with some known representative impedances.

The following components were measured: a 0.1Ω Resistor, a 10μH inductor, a 6.8MΩ resistor and a 1nF capacitor. These components were off the shelf laboratory parts, with resistor tolerance 5%, capacitor tolerance 10% and inductor, 15%

Figure 4.10 indicates the measured resistance, showing expected results to about 200 to 300kHz. It is felt that around this point there may have been some limitations in the measurement accuracy due to the test leads which utilised ‘crocodile clips’ to provide connection to the components. This connection method, while giving reasonably low contact resistance at up to a few kilohertz, is however not so reliable above this perhaps increasing measured impedance and causing discontinuity in the characteristic impedance and thereby perhaps also causing resonant effects in the measurements. However, given the limitations specified for the equipment, these figures show good correlation with the component specification, within the equipment limits.

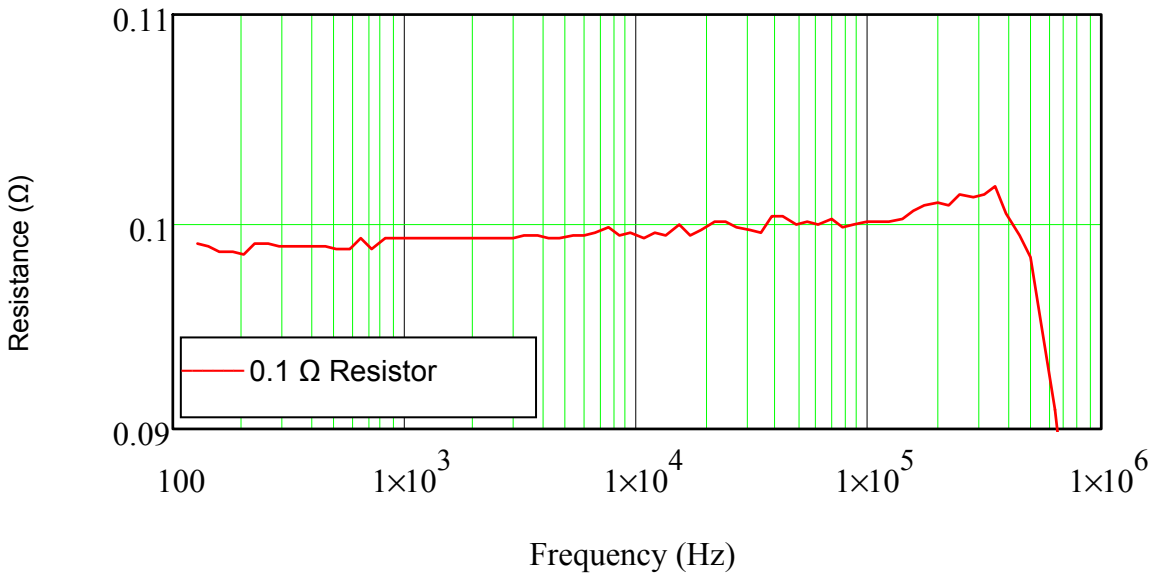

Figure 4-10 0.1Ω Resistor Measurement

Figure 4.11 indicates the measured inductance, showing inductance between 11.5µH and 1.09µH up to around 300kHz. As the measured impedance is within the 15% specification for the inductor, this would seem to be quite plausible. Again above 200 to 300kHz, results become dubious; whether due to measurement method, instrument limitations or component resonance is not clear, but whatever the cause, the measurements to greater than 100kHz are within the tolerance of the component.

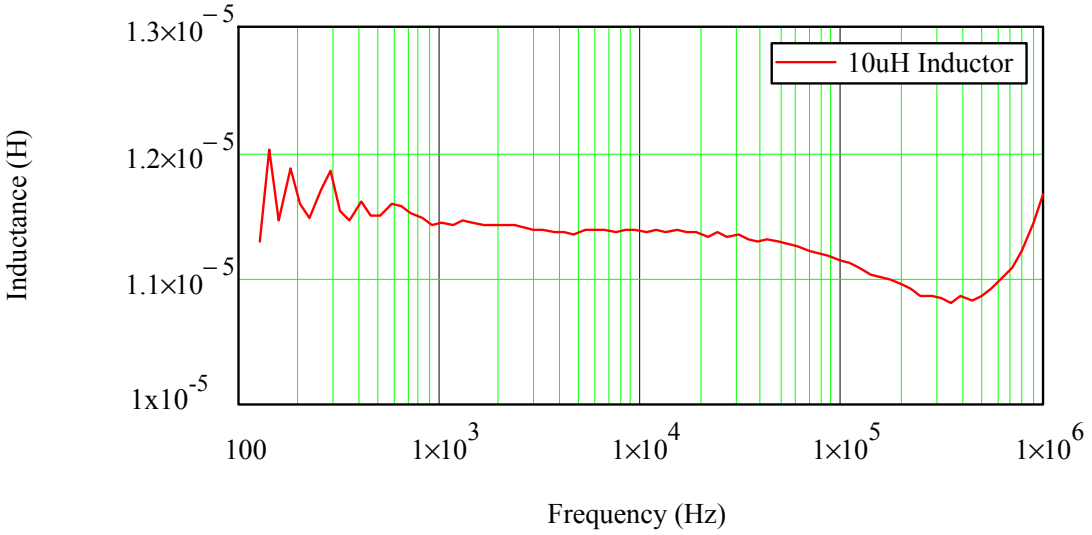

Figure 4-11 10µH inductance Measurement

Figure 4.12 indicates the measured capacitance, showing between about 1.12nF and 1.09nF up to around 150kHz. The measured impedance is slightly outside the 10% specification for the component, but within 11.5%. Component leads and stray effects in cables could be contributing factors again, as the method adopted to measure the capacitance was as per the cable measurement set up, and is not really conducive to precision measurement of electronic components. Again, above 200 to 300kHz, results become dubious; whether due to measurement method, instrument limitations or component resonance is not clear, but whatever the cause, the measurements to greater than 100kHz look reasonable.

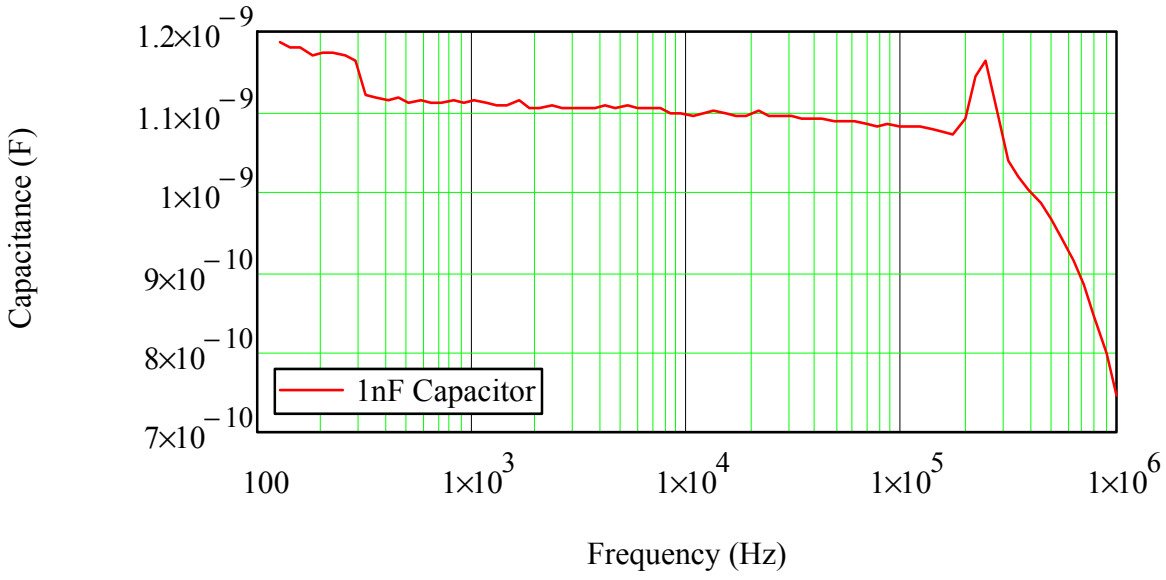

Figure 4-12 1nF Capacitor Measurement

Figure 4.13 shows the measured 6.8MΩ resistance, and for convenience of comparison with the measured component, this is displayed as resistance rather than conductance. Measurements are between 2.8 MΩ and just under 4MΩ under 30kHz and then drop off dramatically. The Solartron 1260 specifications show it is capable of reading this impedance with 1% accuracy up to 10kHz and has a specification of 10% accuracy to 100KHz. As stated in section 4.2.1, measurements of conductance are extremely difficult to make accurately due to the very small currents measured by the equipment, in this case in the order of 440nA for the specified 3V output. Given that the minimum range for the equipment for current measurement is 6μA, the equipment is certainly operating at the bottom limit of its capabilities, although with a stated resolution of 200pA, it should still be getting better figures. It is felt that this error is probably mainly down to leakage currents in the air and through limitations in the electrical isolation between the test connections, again 'crocodile clips'.

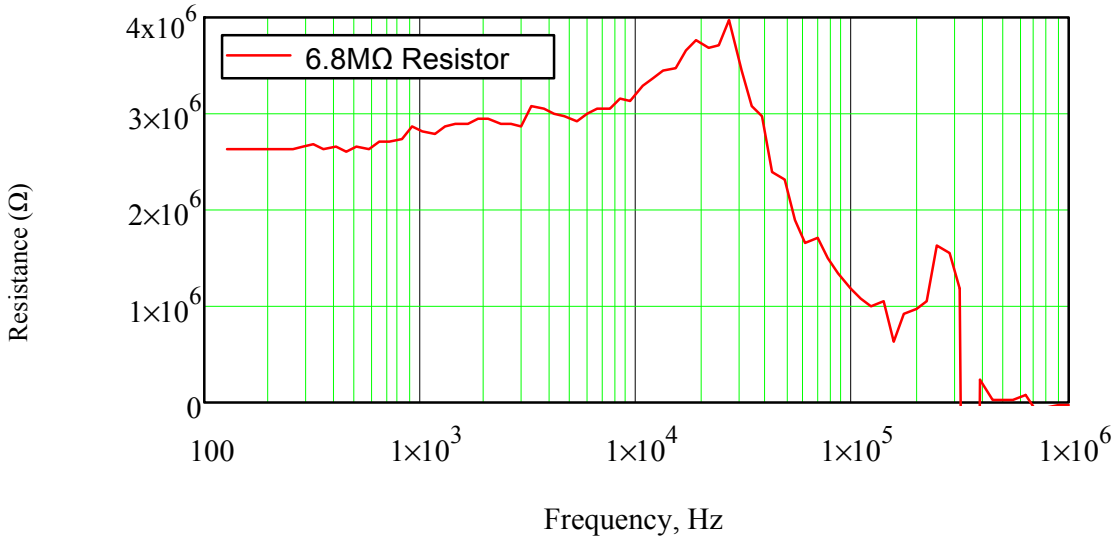

Figure 4-13 6.8MΩ Resistor Measurement

So whether these measurement inaccuracies and resonant peaks are due to limitations in the parts or in the measurement method at the high frequencies, the measurements are sufficient to show that the Solartron itself and the measurement method adopted, is capable of accurate measurements down to mΩ, μH, and nF up to around 200kHz. Measurement of high impedances as seen in the conductance measurements will have to be treated with caution, though, as due to the extremely small currents being measured, the limitations of the measuring instruments and the potential for leakage currents between measurement leads, accuracy of results is very difficult to guarantee.

4.3.3 Impedance Analyser vs Oscilloscope measurement

A 19m length of 10mm^2 cable was obtained and the impedance measured using a HP33120A signal generator and two channels of an HP54602B oscilloscope to make measurements as shown in Figure 4.1. Similarly the impedance parameters would also be measured using the Solartron 1260 by way of direct comparison of the results.

These measured R, G, L and C values can then be used to predict the attenuation in the cable length and these predictions compared with an impedance analyser attenuation measurement, the premise being that if results are reasonably consistent between measurement instruments and give reasonable prediction of attenuation, then the fundamental principles of the attenuation measurement and prediction methods are reliable. These measurements are shown in Figures 4.14 to 4.17.

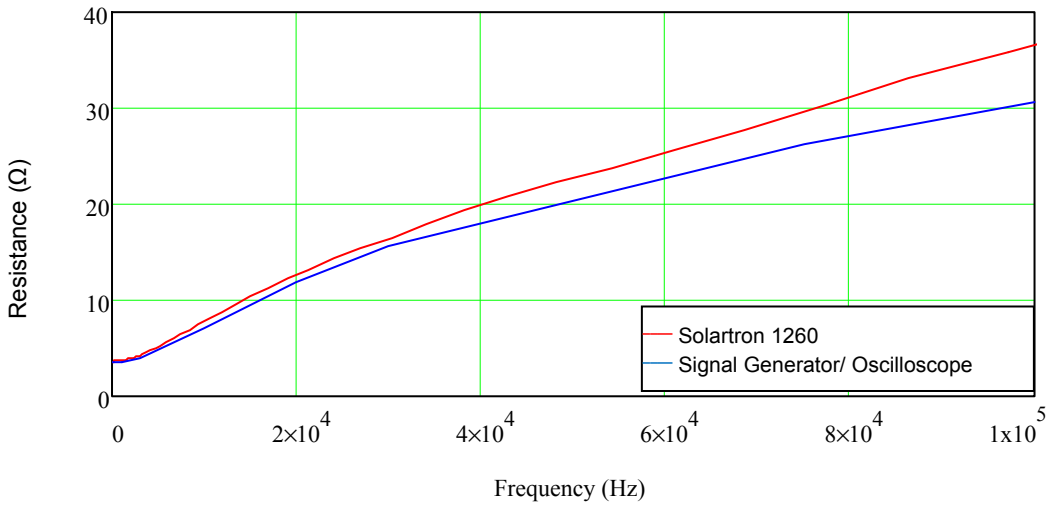

Figure 4-14 Resistance measured with impedance analyser and oscilloscope

Resistance values measured by both methods are within 2% of the mean of the measured values up to 50KHz and better than 10% to 100KHz

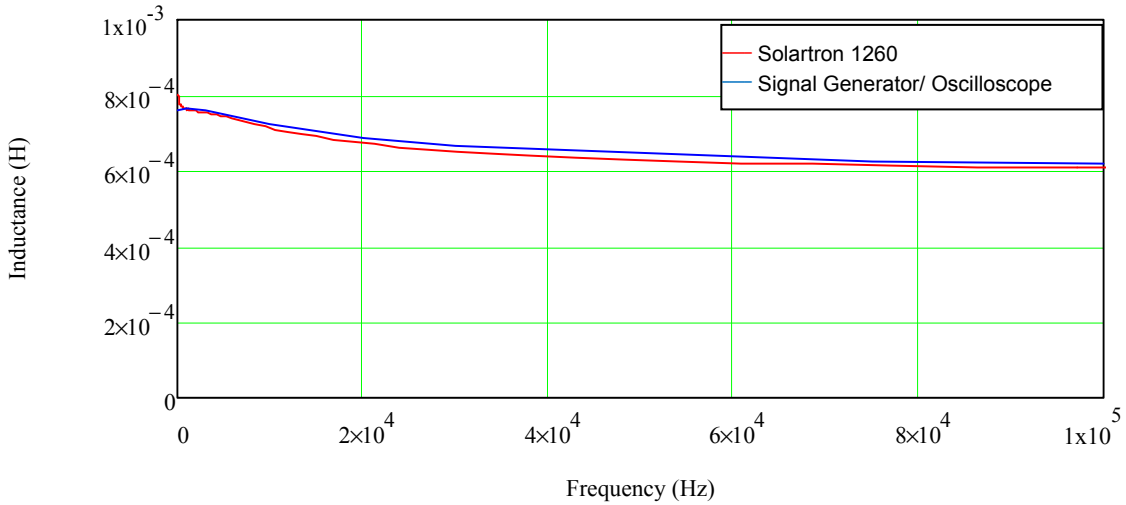

Figure 4-15 Inductance measured with impedance analyser and oscilloscope

Measured inductance shows good correlation between both methods with results within 2% of the mean of the measurements from the two methods up to 100KHz.

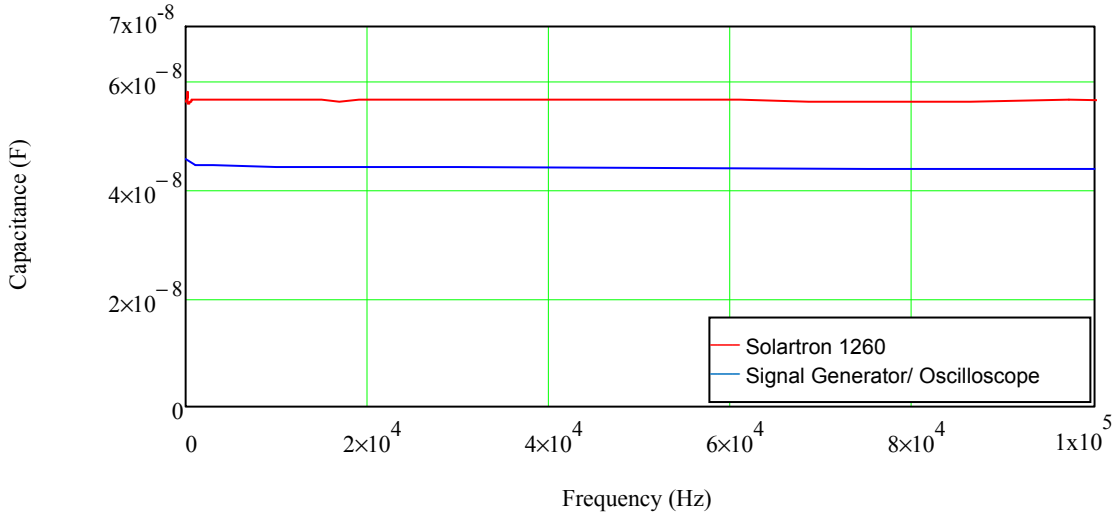

Figure 4-16 Capacitance measured with Impedance Analyser and Oscilloscope

Capacitance measured seems to have a definite offset between results from each method showing around a 12% error from the mean of the measured values from the two methods.

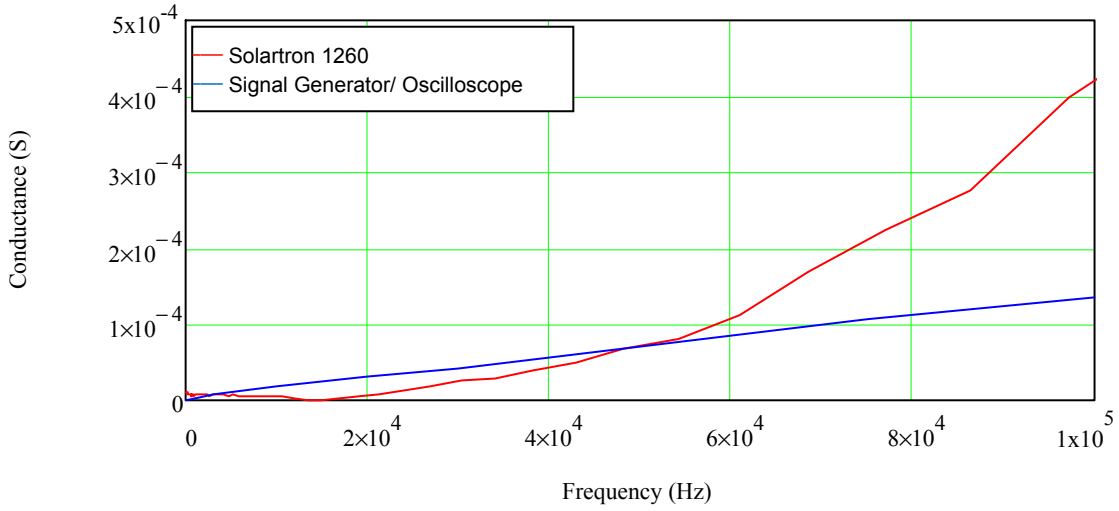

Figure 4-17 Conductance measured with impedance analyser and oscilloscope

The conductance measurements show significant differences in results from the two methods across the frequency band of interest.

It is clear from figures 4-16 and 4-17 that there are significant differences between the measured figures for capacitance and conductance with the two methods. In section 4.3.2 it was demonstrated that the very small measurement currents and instrument accuracy along with effects such as stray capacitance and air leakage currents all act to make precise measurement of the parallel impedances extremely difficult.

It should be noted that as the capacitance and conductance are measured together, up to around 50kHz the lower capacitance (higher impedance) measured by the oscilloscope method, is mirrored by a higher conductance (lower impedance). As seen below in Figure 4-18 it would appear that, to some extent, these measurements errors compensate each other when used together to derive the cable attenuation prediction. Above 50kHz the difference in conductance is significant, however the impedances being measured, currents employed in the measurements and the test set up are all likely contributors to these differences in measurement.

Using the figures for R, G, L and C measured by the two methods, the attenuation can be predicted and compared with an attenuation measurement as outlined in Figure 4.2. As the Solartron 1260 and a Signal Generator/Oscilloscope combination were used to acquire the RGLC measurements in two different ways, this should give a good cross check that all impedance and attenuation measurements and methods are trustworthy.

Figure 4.18 shows the attenuation predicted from the measurements taken with the oscilloscope and the Solartron 1260, and compares these with the measured frequency response of the cable section.

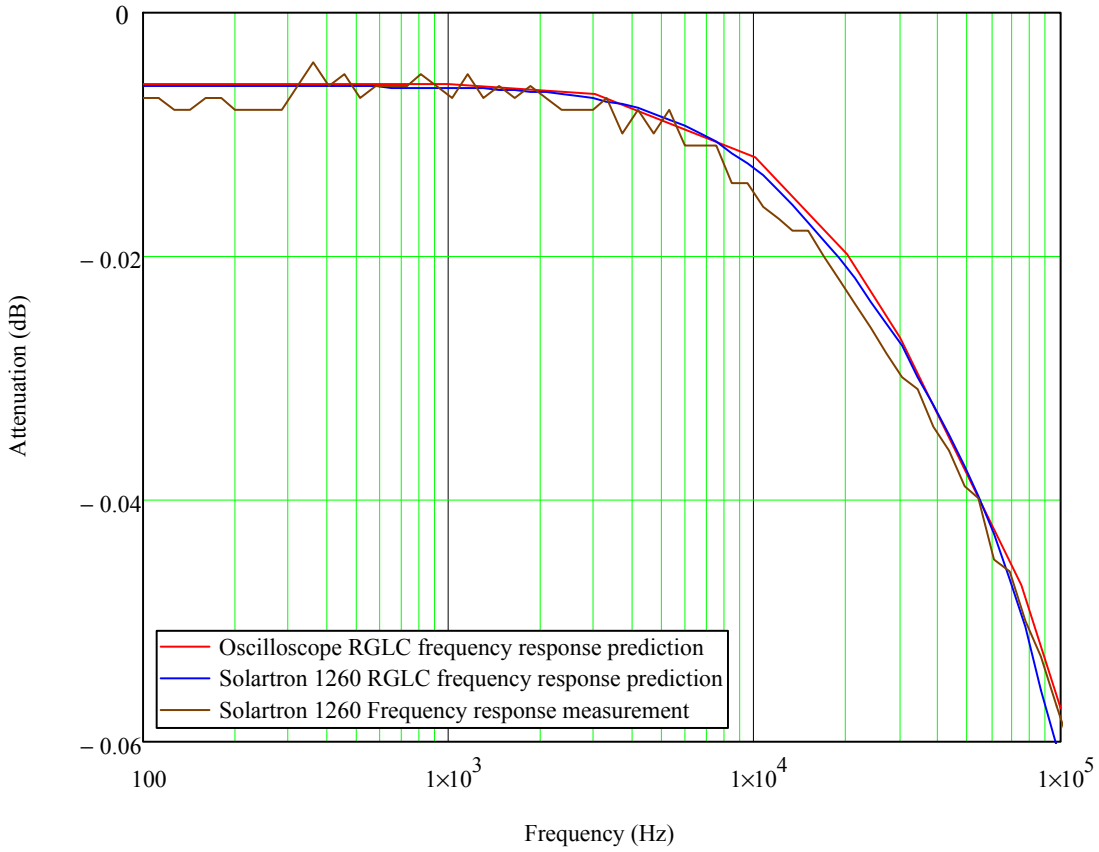

Figure 4-18 19m Cable frequency response - measured and predicted from RGLC data

The principle of accurate RGLC figures giving accurate attenuation prediction is justified by these measurements and was reflected in many other of the measurements taken in this research.

Accurate frequency response predictions can be made if accurate impedance measurements of the cables can be obtained. There is now confidence that the instruments and measurement methods are producing dependable results.

4.4 Other sources of error

Consideration has to be given to other potential sources of error between the measurements of cables obtained and the predictions using the various modelling methods available.

4.4.1 Cable Twisting Rate/ Lay length

Due to the longitudinal twist of conductors in twin and quad cables and also of these in the umbilicals, the actual copper length, known as the lay length of the cable, can be up to 5% longer than the usable length of the cable.

The theoretical loop DC resistance, R_{dc}, for a 10mm^2 cable pair would be 3.68Ω/km at 20°C, calculated from

$$R_{dc} = 2 \cdot \frac{1}{\sigma A} \quad \text{4.1}$$

σ is the conductivity of copper 5.435x10^{7}S/m

and A is the cross sectional area of each cable core, in m^2

4.4.2 Fill factor

As the conductors in the bulk of our subsea cables are made of seven strand bundles, it would seem possible that the impact of using partially separated conductors rather than a cylindrical solid core would affect the measured resistance. As illustrated in figure 4.19, although the overall cross sectional area is still the same, small gaps between the strands could mean the onset of skin effect will occur at a different frequency due to the effective use of seven cables with smaller diameter. If, for example, oxidation of strands had taken place, would it be possible that a kind of Litz wire effect is being seen, where individual conductors in a bundle are separately insulated to reduce the impact of skin effect on cable resistance?

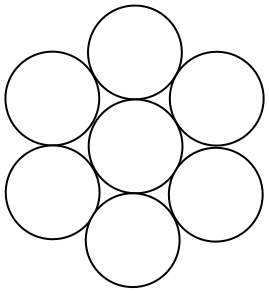

Figure 4-19 Cable Stranding and resultant gaps

Lesurf J (2009) suggests that the effective resistance of a bundled cable is typically 0.9069 times the otherwise calculated value, although clearly the degree of compression of the copper will affect this. This is a very 'intuitive' kind of approach and any scaling factors are very much dependent on conductors being circular and uncompressed, however more detailed calculation methods described by Murgatroyd (1989) give similar results.

If this effect is exaggerated to its extreme, a situation is approached where each conductor is separated, in a similar way to Litz[1] wire. Methods for calculation of Litz wire losses are described by Rossmanith et al. (2011) and Xi Nan and Sullivan (2005), and Tang and Sullivan (2003) describe a technique for calculation of the loss in a non-insulated multistrand bundle. However, if this was the effect being seen here then since, as conductor diameter decreases, skin effect does not start to operate until a higher frequency, it would then be expected that the resistance of a bundle would increase at a lower rate with frequency than would be the case with a solid conductor, and this is opposite to measurements taken. This would then imply that the actual

[1] as outlined by Lesurf J (2009), Litz wire comprises cable bundles where strands are individually insulated and bundled together in such a way that skin effect is not seen until a much higher frequency as conduction takes place over many smaller cables. In addition, in practical cables, like those manufactured by New England Wire (2012), a continual 'shuffling' of the conductors' positions in the bundle takes place to ensure no one conductor spends any more time than any other at any specific position within the cable.

resistance at high frequency of the stranded copper cable would approach that of the sum of the separate strands. In reality, the resistance measured is much higher than that expected e.g. as shown in section 4.1.1, implying that the stranding of the cables is not the cause of the increased cable resistance measurements.

4.4.3 Surface area

In addition to the fill factor outlined, where gaps between conductors affect resistance, it can also be seen in Figure 4.19 that the resultant cross section is now a different shape with a 'flower' shaped perimeter. Most calculations of cable impedances are based on an assumption of a circular perimeter. If the perimeter is in fact made up of semi-circular (or slightly larger) conductors with interspaced indentations due to stranding, then impedance could well be affected. This would effectively give the conductor a larger circumference, pushing the skin effect corner frequency lower, while at the same time not affecting the DC resistance.

However, while the graph of Figure 4-20 does show the same DC resistance and a lower corner frequency, more isolation between strands would also be expected to bring the resistance closer to that of an ideal 'Litz' arrangement with a lower AC resistance.

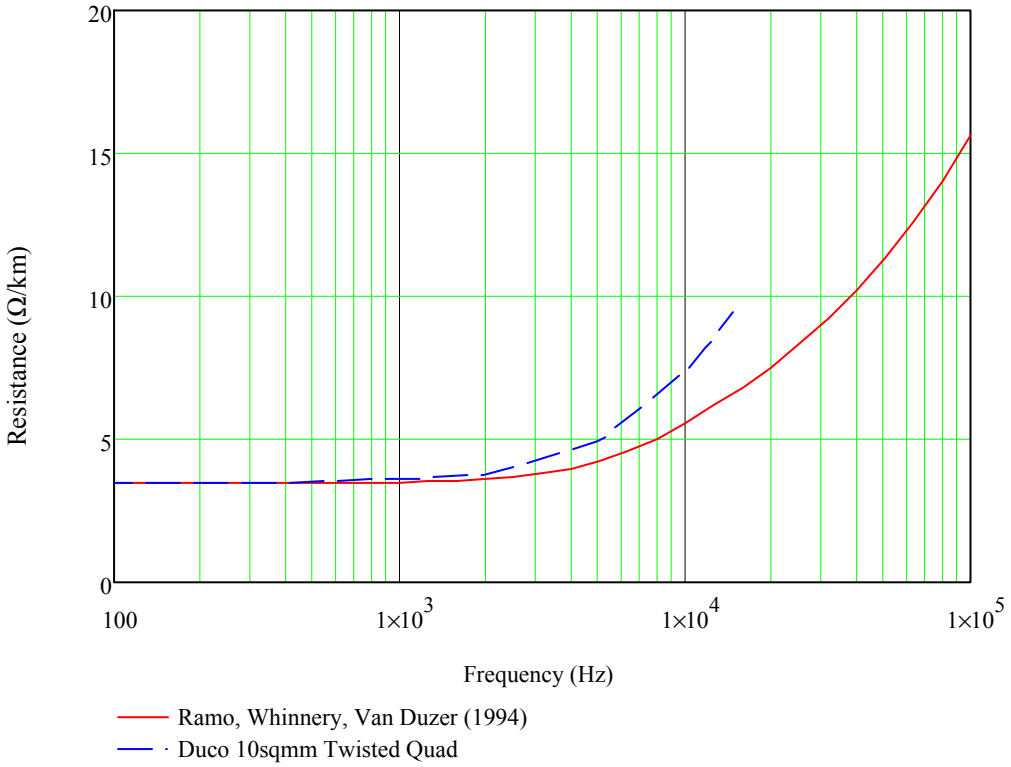

Figure 4-20 Comparison of theoretical and measured resistance showing the shift in corner frequency caused by a non-circular cable perimeter

This is the opposite of the trend seen in the measurements where resistance is generally higher than that of the solid circular conductor, implying that this physical construction constraint is not having a major effect on the resistance.

4.4.4 Strand oxidation

There are two forms of copper oxide: cuprous oxide and cupric oxide. Cuprous oxide forms the greenish oxidation layer often seen on copper conductors exposed to weather.

If exposed to high temperatures, cupric oxide will form, showing a black layer around the copper conductor.

Cuprous oxide is classified as a semiconductor, while cupric oxide is an insulator, but in either case oxidised copper strands would mean a reduction in the usable conduction cross section and would affect the conduction at DC. Tang and Sullivan (2003) discuss the possibility of utilising oxidised strands as a low cost alternative to fully insulated Litz wire and provide a means of predicting the loss in such cases. Again, as conductive cross section is reduced due to the oxidation, the DC resistance will be higher and a change in the skin effect corner frequency, detailed in equation 2.14, from the theoretical point would be seen.

4.5 Chapter conclusions

In this chapter it has been shown that the resistance and inductance measured consistently deviate significantly from the figures predicted in the texts referenced, Johnson, Graham (2003); Ramo, Whinnery, Van Duzer (1994) and Arnold (1941). Good measurement methods have been established and other sources of error have been examined.

Chapter 5 now describes a series of measurements made and modelling done to examine and assess the effects of pressure, salinity and surrounding materials on the impedance of cables and to establish reasons for the consistent difference seen in this section between measured and predicted results.

Chapter 5. Detailed Measurement and Electromagnetic Predictions

It is apparent from the measurements made and the data examined in Chapter 4 that the theoretical models adopted to this stage of this thesis i.e. Johnson, Graham (2003); Ramo, Whinnery, Van Duzer (1994) and Arnold (1941), are insufficient to accurately model the impedance parameters of the cables types being examined and that the prediction of loss in a cable is a complex issue and more sophisticated modelling techniques are required to derive more accurate figures. In Chapter 2, the use of electromagnetic field solver tools was introduced. In this Chapter, a series of tests are performed to assess the effects on cable impedance of subsea deployment in an umbilical, and a corresponding series of electromagnetic models are carried out to give a cross comparison of results.

As outlined in section 2.3, an electromagnetic field solver can be used to model cable parameters and Figure 5.1 illustrates the difference between the prediction described by Ramo, Whinnery, Van Duzer (1994), a prediction using Optem Incorporated's field solver model and a bare quad cable, measured using the Wayne/Kerr Model 6440 Analyser as outlined in Chapter 2.

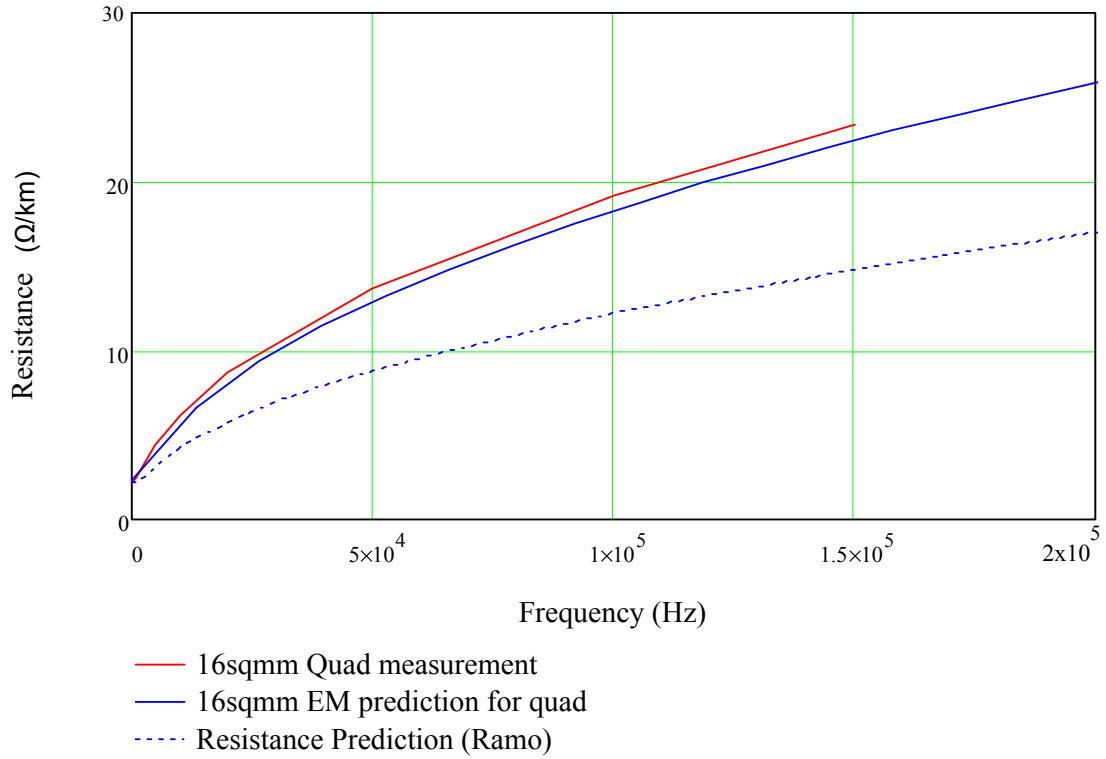

Figure 5-1 Comparison of Measured and Predicted Resistance for 16mm^2 Cable

During the development of a subsea control system by a major UK oil company, it became apparent that the cable losses were going to be higher than the communications equipment would be capable of handling, as initial measured losses showed attenuation beyond the acceptable communications transmit/receive margins for the equipment's communications frequency band. The umbilical, shown in Figure 5.2, was made up as follows:

- Cores A to F are the 16mm^2 electrical quad cables used for power and communications.
- Cores 1 - 3, 11 - 13, 15 - 17 are 12.7mm, 345 Bar hoses for hydraulic or chemical fluids

- Cores 4 - 8, 20, 21 and 23 are 19mm, 345 Bar Hoses for hydraulic or chemical fluids
- Cores 9, 10, 14, 18, 19, 22 are 12.7mm, 690 Bar Hoses for hydraulic or chemical fluids

Based on the tests outlined at the end of Chapter 3, extensive testing and modelling was undertaken to assess the problem as part of this research and the following methods were employed in an attempt to derive an accurate prediction and comparison of the cable losses when deployed in the umbilical:

1) Transmission line theory using the two port network modeling method as described in section 2, is used to establish attenuation predictions from measured or modeled RGLC values derived in 2 and 3, below.

2) An Electromagnetic model of the 16 mm^2 quad in three of the locations in the umbilical was prepared (A, C and F in Figure 5.2), and the results applied as appropriate. As well as a model for a section of bare quad cable, each of the cores was also modelled in two conditions: with adjacent hydraulic hoses air filled, and with adjacent hydraulic hoses water filled.

3) Measurement of the Cables in a variety of environments and results used to predict losses on full umbilical. Measurements included:

    - In free space;
    - In a plastic tank surrounded by sea water;

- Measurement of a sample of cable on a steel plate to simulate the proximity to hydraulic steel tubes and steel wire armouring as seen in the umbilical;
- Measurement of a sample of cable in a pressure chamber under pressure and surrounded by fresh water;
- Measurement of RGLC parameters from a sample of the umbilical;
- Measurement of the attenuation over the complete umbilical (this set of data is included in Chapter 6).

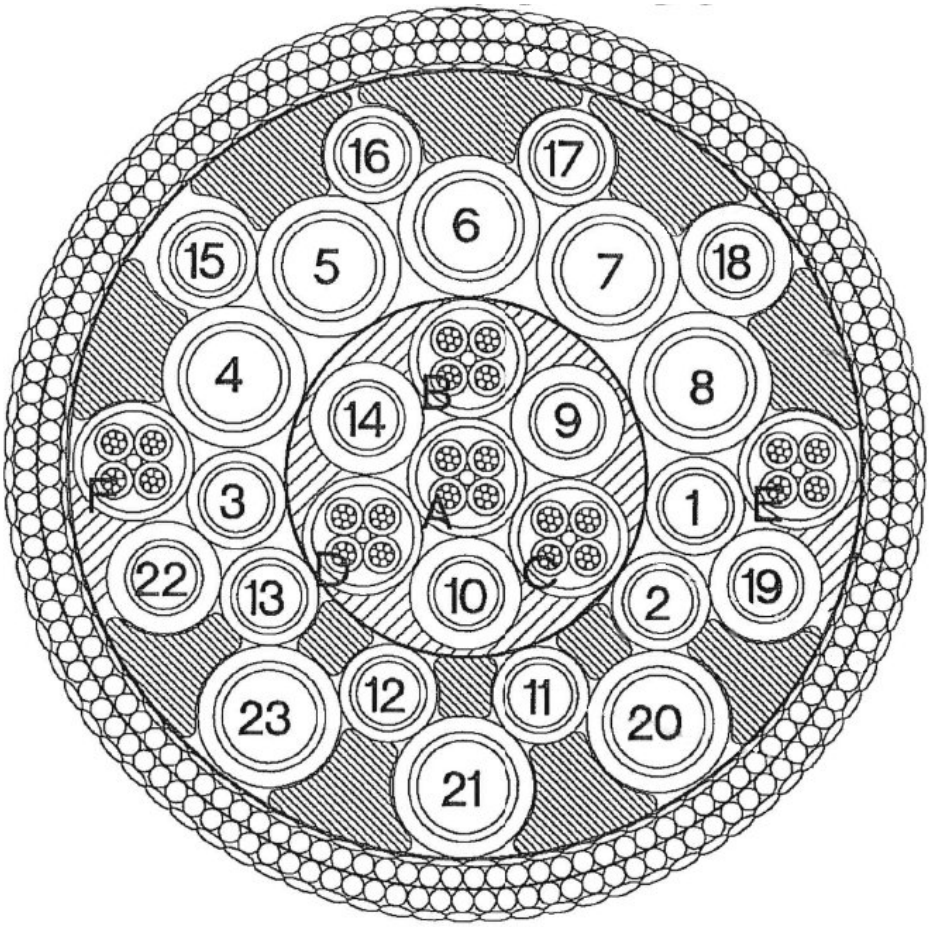

Figure 5-2 Cross Section of 187.1 mm diameter Umbilical Cable Analysed and Measured

As this was a commercial project, and since the field solver that had been used to this point in this research work was a free student version of a comprehensive industrial piece of software by Ansys Inc., called Ansoft Maxwell SV, it was not acceptable for this to be used for commercial purposes. Instead, the electromagnetic model was carried out using software by Optem Incorporated in Canada.

These three sets of data are compared and illustrate the effect on each of the fundamental RGLC parameters of pressure, surrounding metalwork and immersion in water.

5.1 Comparison of EM modelled cable parameters

As outlined at the beginning of chapter 4, electromagnetic modelling of the umbilical was also carried out and the results of this are shown below. The bare quad is modelled and also the effect of its being located in positions A, C and F in the umbilical. In positions A and C the effect of the adjacent copper conductors on the cable impedance is modelled. The modelling carried out for core F, on the other hand, predicts the effect of the adjacent copper conductors and the surrounding steel wire armour on the cable impedance. The properties of the steel wire armour and copper, in particular permeability and conductivity are not exactly known for the umbilical examined, however for the sake of the models, typical values of conductivity are taken as 5.8×10^{-7}S/m for copper and 1.1×10^{-6}S/m for the steel wire armour. Similarly, permeability is assumed as 1.2566290×10^{-6} (or $4.\pi.10^{-7}$ H/m x 0.999994) for copper and $4.\pi.10^{-7}$ H/m for the steel armour. Two conditions of each location are considered: when the adjacent hydraulic hoses are air filled and when they are seawater filled.

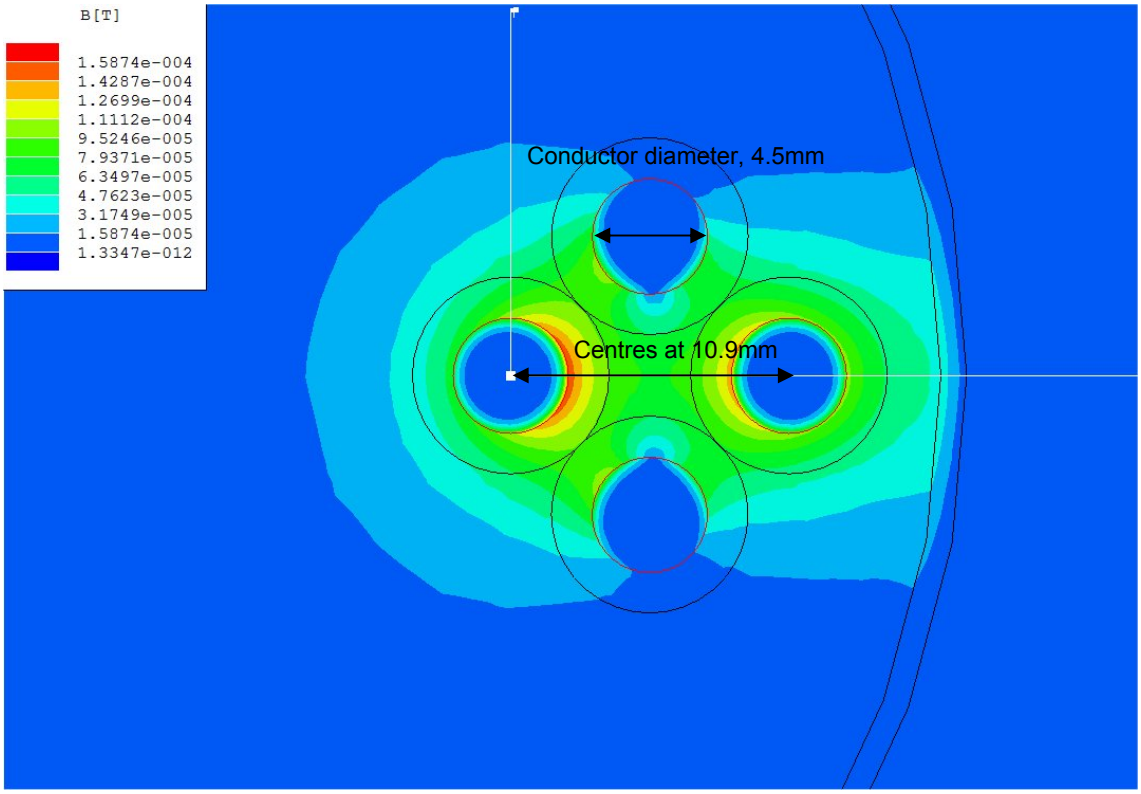

Figure 5-3 Plot of model used to derive impedance parameters of cables in proximity of steel wire armour

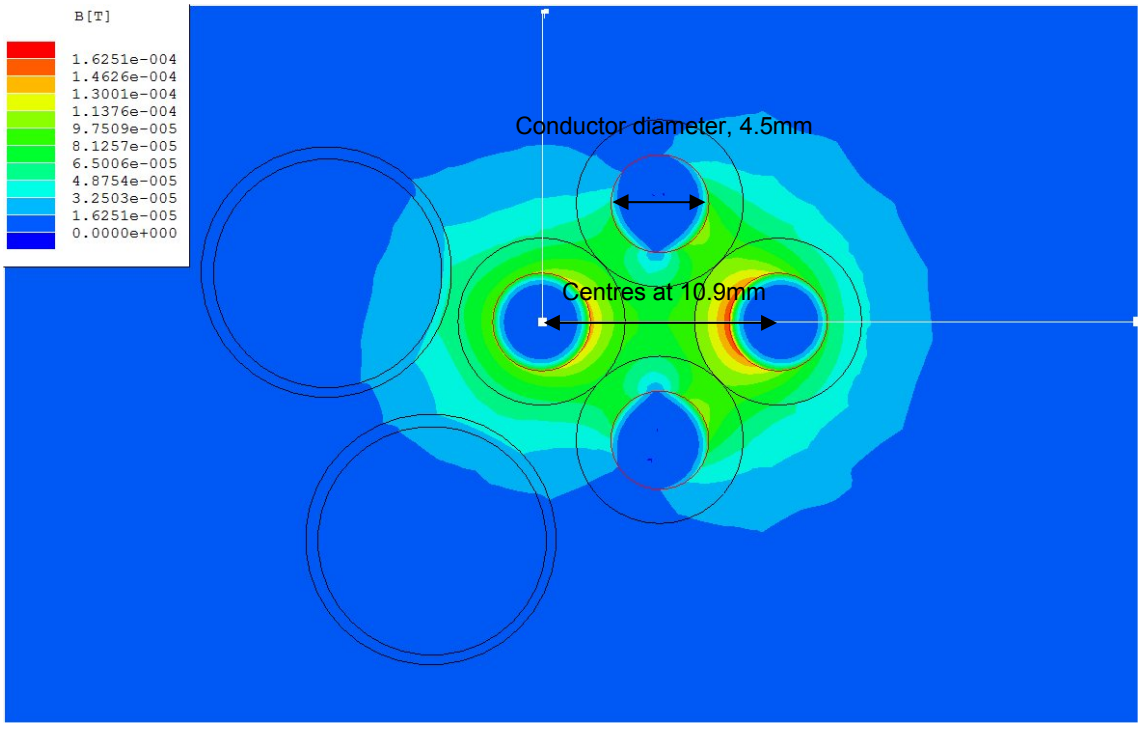

Figure 5-4 Plot of model used to derive impedance parameters of cables in proximity of hydraulic tubes.

As shown in Figure 5.5, resistance increases with frequency due to the skin effect and at higher frequency, the rate is proportional to the square root of frequency as expected, as discussed in section 2.2.1. There is a clear increase in the resistance measured with core F, adjacent to the armouring, compared with Cores A and C, with the addition of sea water to the hoses having very little effect on the resistance.

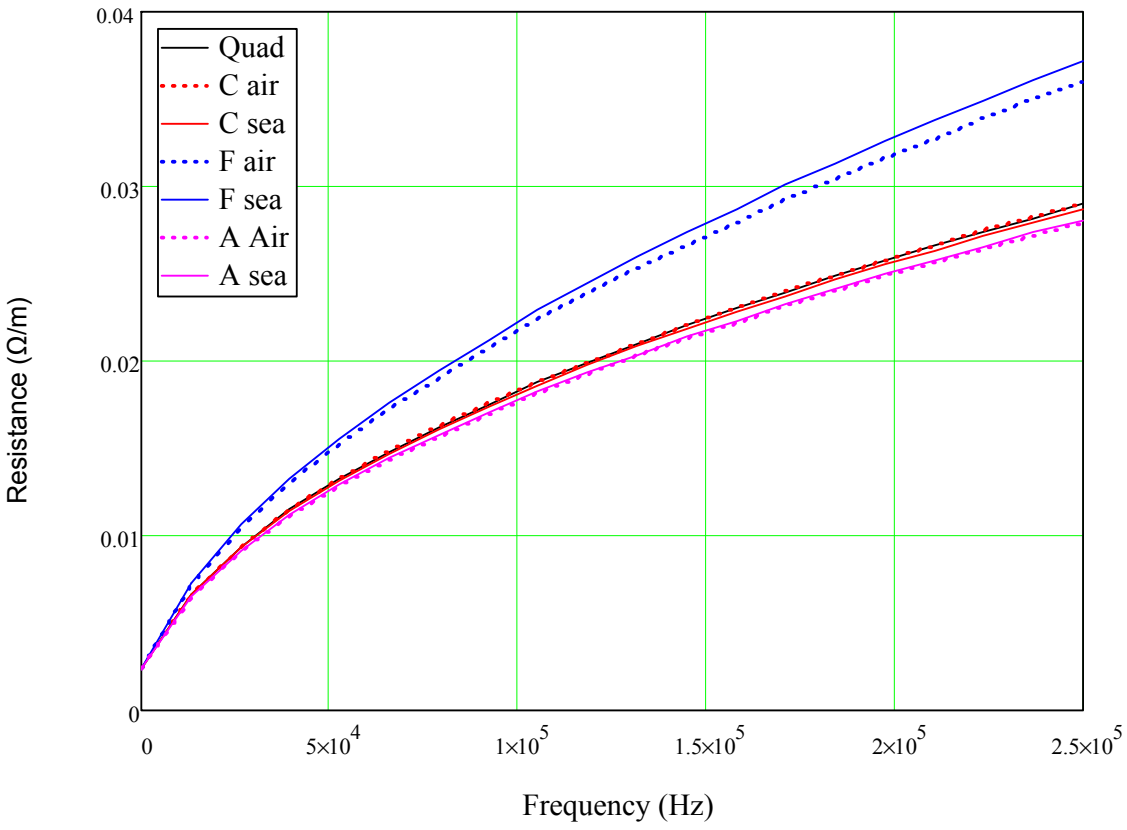

Figure 5-5 Resistance calculated for various conditions using Optem Field Solver

Inductance similarly, in Figure 5.6, is affected by the skin effect, showing the highest inductance at low frequencies and dropping off as frequency increases. It seems, though, that only at very low frequencies has the armour any major impact on inductance as seen for core F.

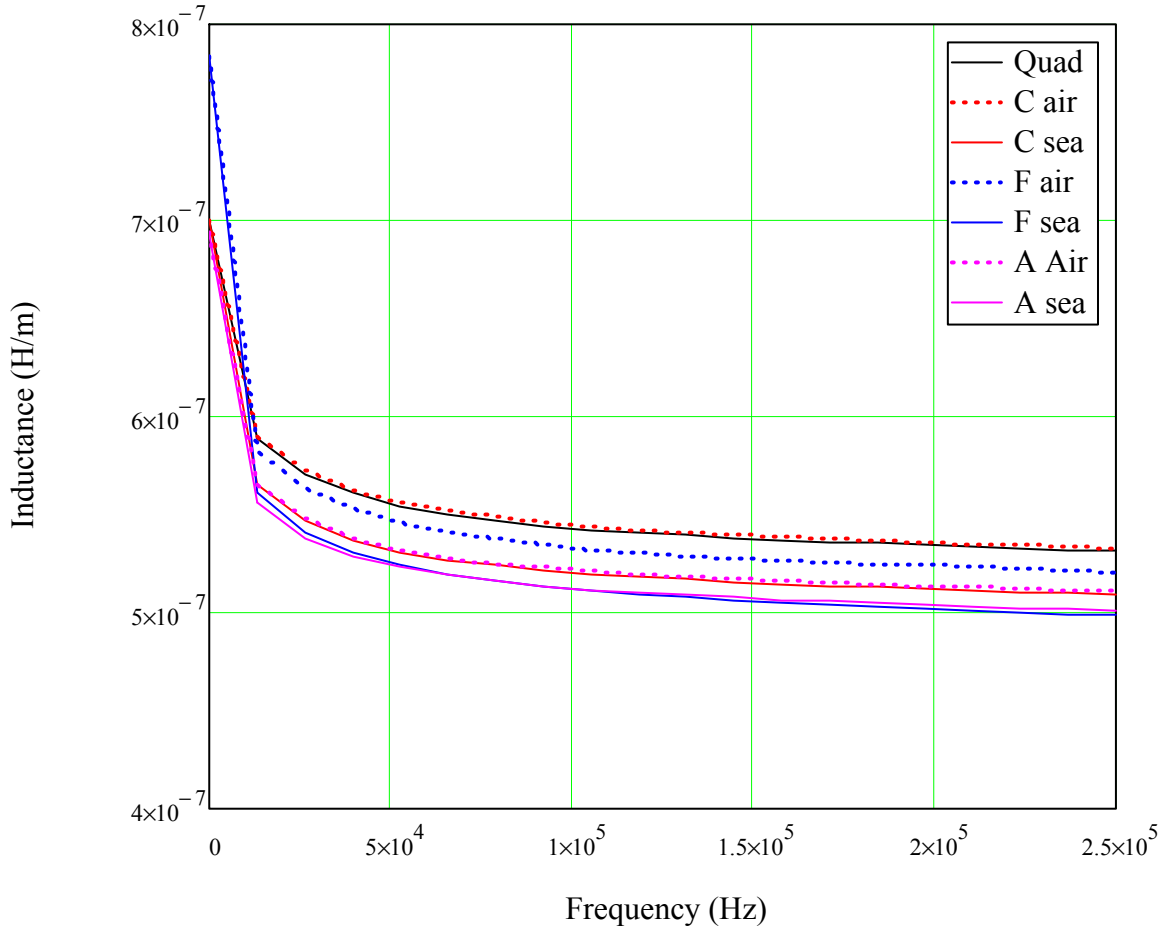

Figure 5-6 Inductance calculated for various conditions using Optem Field Solver

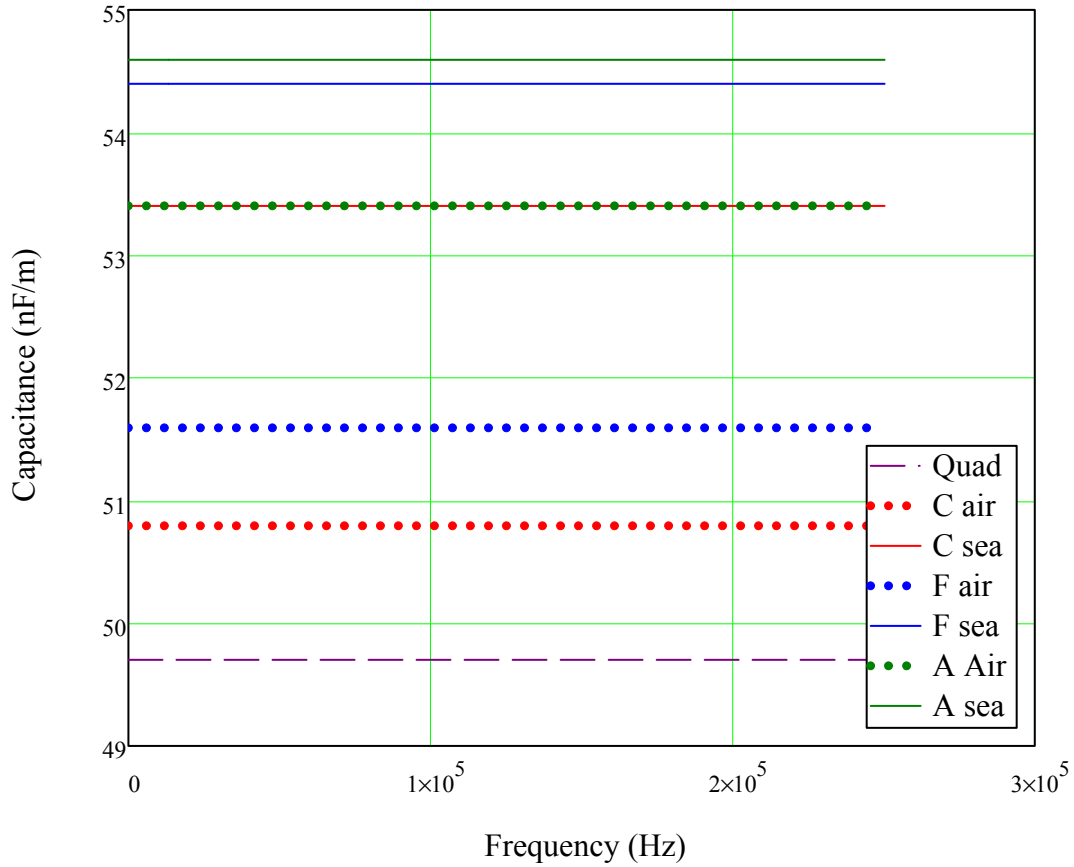

Figure 5-7 Capacitance calculated for various conditions using Optem Field Solver

It can be observed in Figure 5.7 that, since the dielectric constant and loss tan are approximately constant below 1 GHz, C is constant over the whole range of calculation. Capacitance does not seem to be significantly affected by the proximity of the armouring, however the incorporation of water into the hydraulic hoses in each case causes a rise in the conductance.

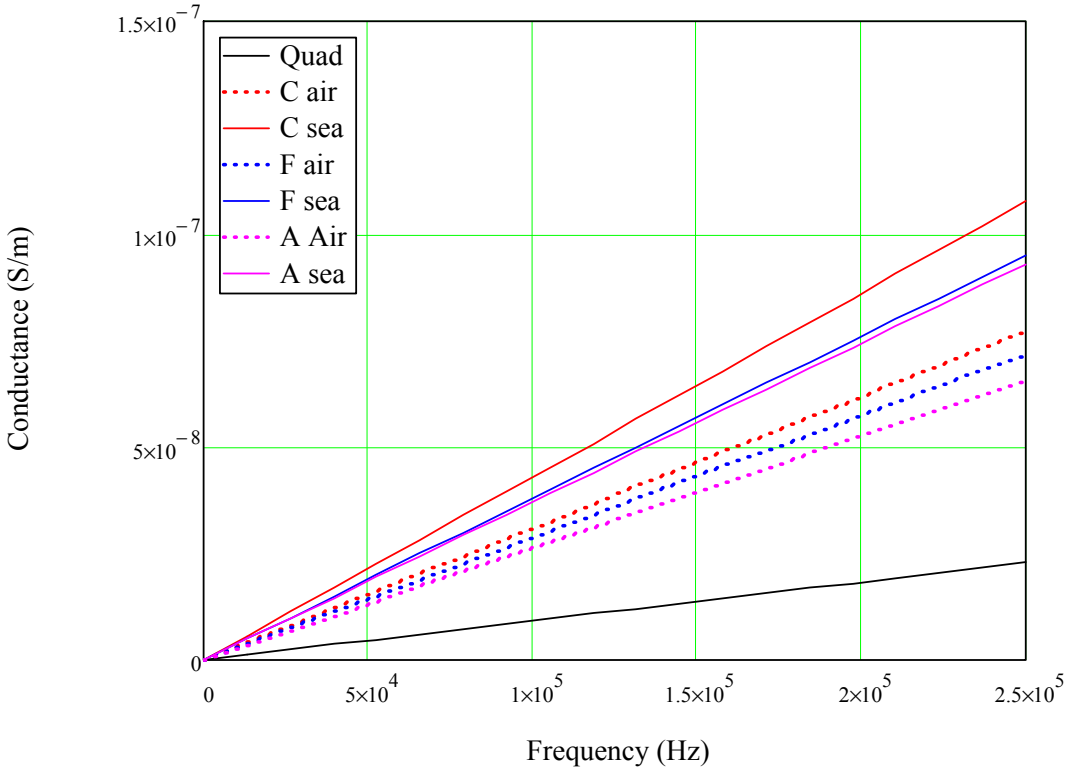

Figure 5-8 Conductance calculated for various conditions using Optem Field Solver

Similarly, in Figure 5.8, since the dielectric constant and loss tan are approximately constant below 1 GHz then conductance, G, is proportional to frequency. Conductance does not seem to be significantly affected by the proximity of the armouring, however the incorporation of water into the hydraulic hoses in each case causes a rise in the conductance.

5.2 Comparison of measured RGLC parameters

The following measurements were made on a length of 16mm^2 quad cable in the following situations and were carried out using a Wayne/Kerr Model 6440:

1) 20m quad cable impedance measured on the floor of the warehouse, temperature 18.7°C

2) Quad Cable impedance measured on a length of steel plate, Figure 5.9, temperature 18.7°C

Figure 5-9 Impedance measurement of quad cable measured on steel plate (Duco)

3) 10.8m Quad Cable impedance measured in a dry pressure vessel, Figure 5.10, temperature 18.7°C

Figure 5-10 Impedance measurement of quad cable in pressure vessel (Duco)

4) 10.8m Quad Cable impedance measured in a flooded pressure vessel, temperature 17.2°C

5) 10.8m Quad Cable impedance measured in a pressure vessel, flooded and pressurized to 300 bar, temperature 18°C

6) 10.8m Quad Cable impedance measured after 22hours in a pressure vessel, flooded and pressurized to 300 bar, temperature 17.7°C,

7) 10.8m Quad Cable impedance measured 1 hour after pressure vessel pressure returned to ambient, still flooded, temperature 19.6°C,

8) 10.8m Quad Cable impedance with pressure vessel drained, temperature 18.7°C,

9) 10.8m Quad Cable removed from pressure vessel, temperature 18.6°C,

10) 15m section of cable in air and flooded with seawater

Dependent on operating temperature, a temperature adjustment scaling factor was applied to the Wayne Kerr measurements as outlined at the beginning of Chapter 4 and, for sake of comparison, impedance values per km recorded.

The pressure vessel itself was 10m in length, so cable was cut as short as possible, to 10.8m, in order to minimise the amount of cable not exposed to pressure vessel conditions. As vessel measurements are mainly used for comparison with each other under the different conditions, values are compared without adjustment for this error, although it should be borne in mind that the magnitude of any pressure or flooding effects may be less than the actual figures by a factor of 10.8/10 = 1.08

This series of measurements show the effect of the steel housing in proximity to the quad cable, simulating the effect of the steel wire armour of the umbilical and also the effect on the loss when the cable is flooded.

5.2.1 Resistance Measurements

The resistance variation when subjected to the tests outlined is shown in Figure 5.11:

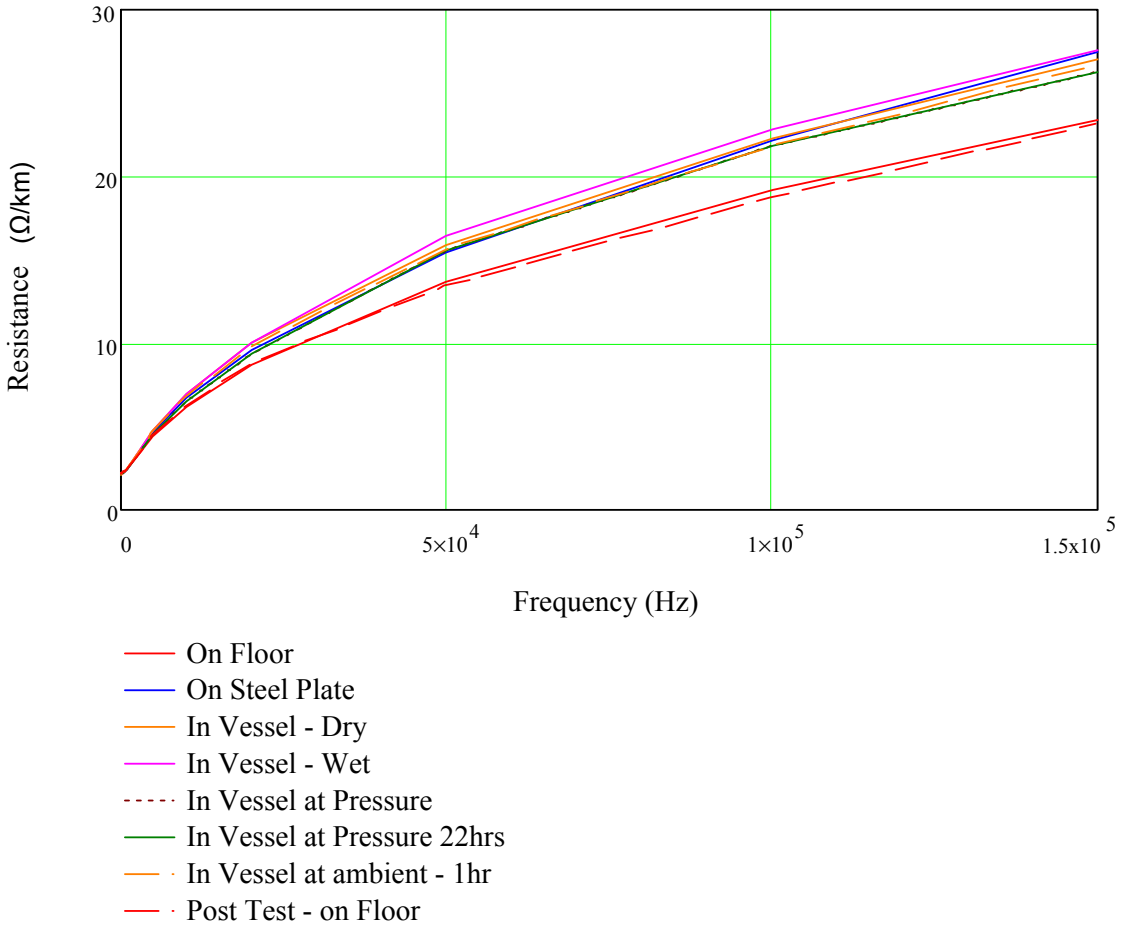

Figure 5-11 Measurement of Resistance in various pressure vessel tests

And zooming in a bit to the data in order to see the details, Figure 5.12 shows

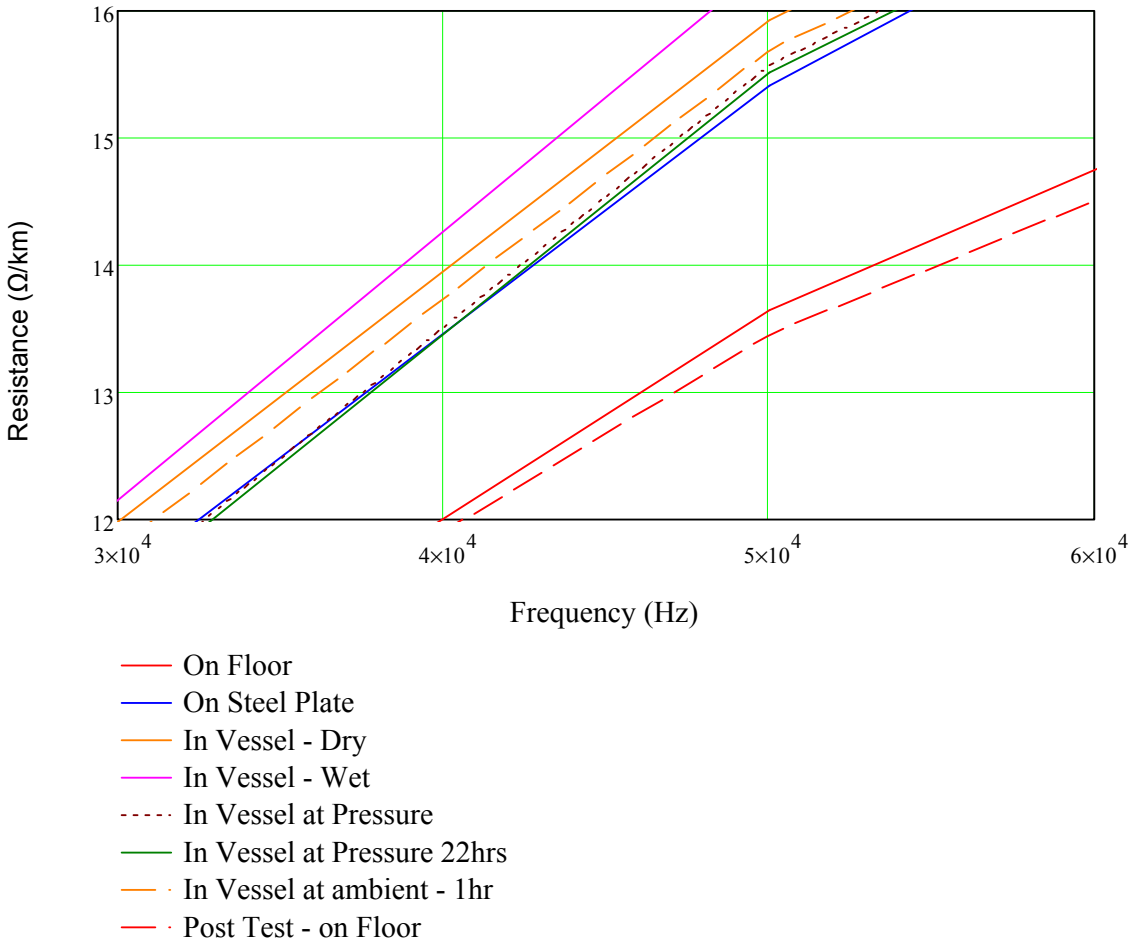

Figure 5-12 Measurement of Resistance in various pressure vessel tests

It can be seen that:

1) in proximity of any steel surface, whether the steel plate or the pressure chamber, the resistance increases significantly;

2) The addition of water to the vessel appears to increase the resistance measured;

3) When subjected to pressure the resistance drops but doesn't significantly change from this value as pressure is maintained;

4) When pressure is released, resistance increases again but not to the same value it had before pressurization;

5) When the vessel is drained after the tests, the resistance returns, more or less to the value before the pressure had been applied or the vessel had been flooded, and after removal from the vessel seemed to have returned to a value beyond (lower than) the pretest value.

5.2.2 Inductance Measurements

Similarly the inductance variation when subjected to the same tests is shown in Figure 5.13:

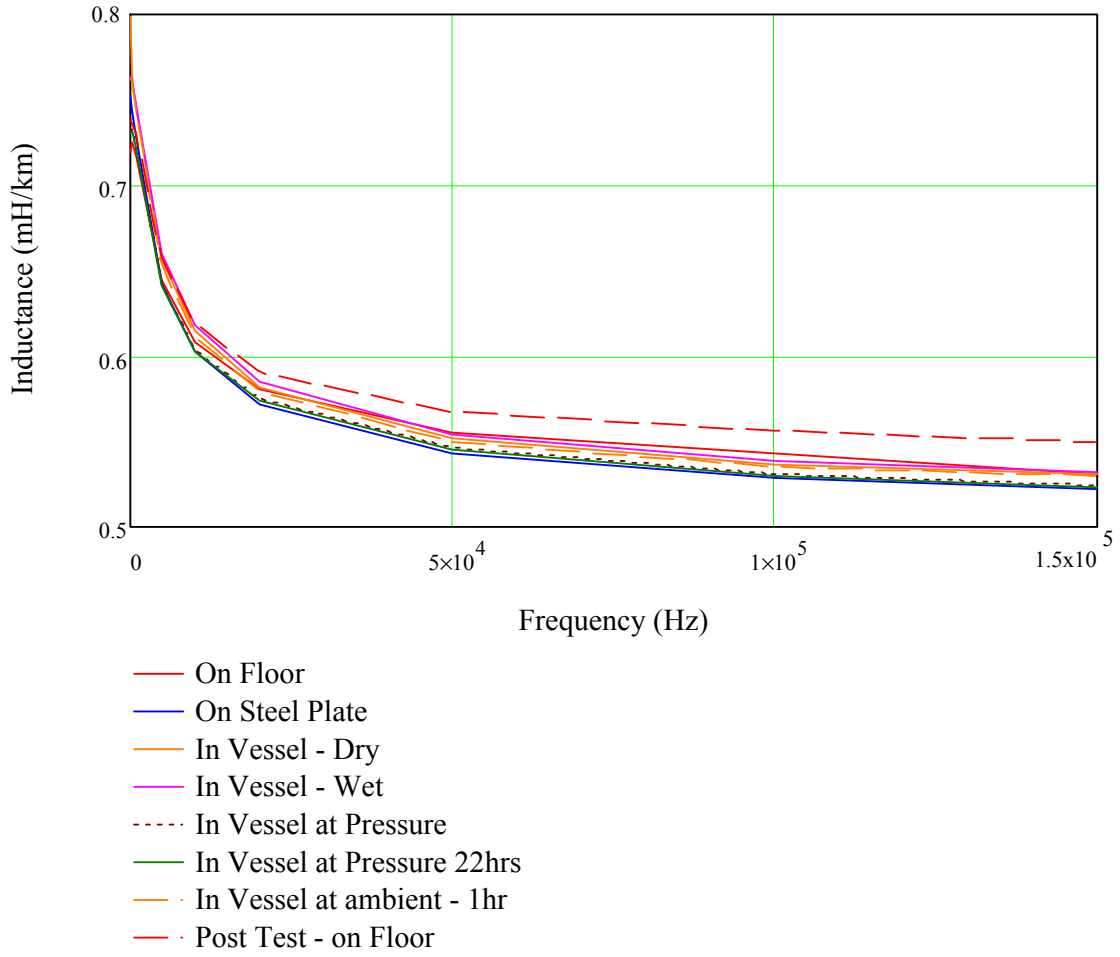

Figure 5-13 Measurement of inductance in various pressure vessel tests

And zooming in a bit to the data in order to see the details, shown in Figure 5.14

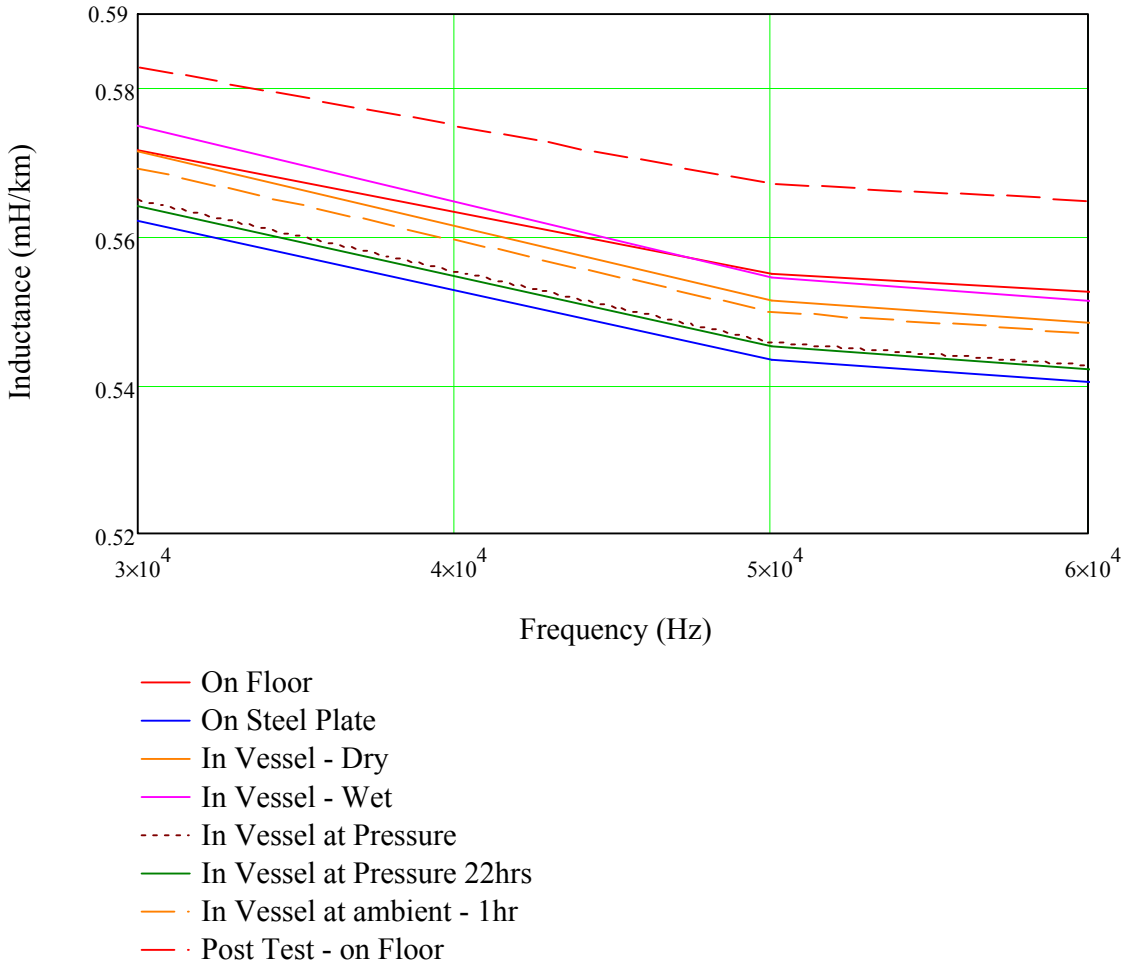

Figure 5-14 Measurement of inductance in various pressure vessel tests

It can be seen that :

1) in proximity of any steel surface, whether the steel plate or the pressure chamber, the inductance decreases;

2) The addition of water to the vessel appears to increase the inductance measured slightly;

3) When subjected to pressure the inductance drops slightly and doesn't significantly change from this value as pressure is maintained;

4) When pressure is released, inductance decreases slightly but not to the same value it had before pressurisation.

5) When the vessel is drained after the tests, the inductance returns to slightly above the value measured before the pressure had been applied or the vessel had been flooded, and after removal from the vessel, seemed to have returned to a value beyond (higher than) the pretest value.

5.2.3 Capacitance Measurements

The effect on capacitance is shown in Figure 5.15

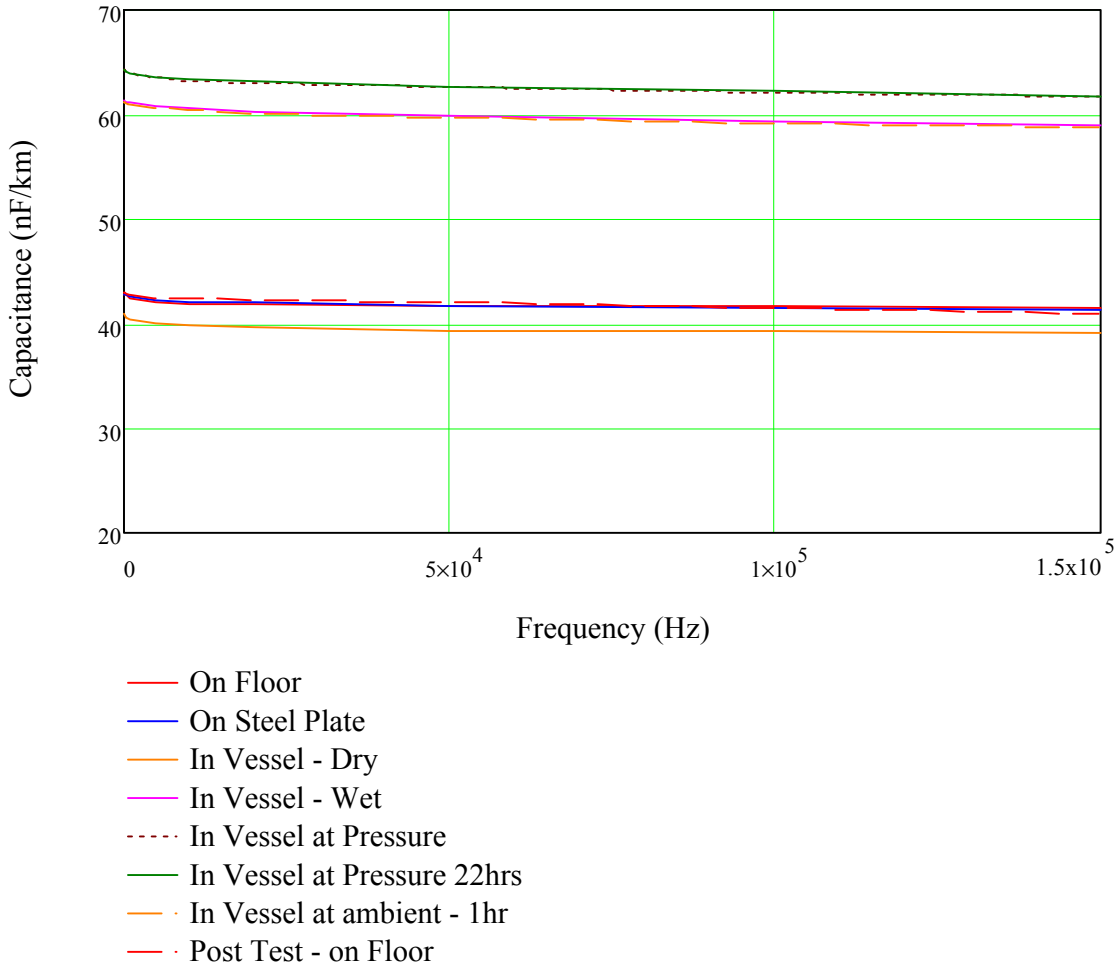

Figure 5-15 Measurement of capacitance in various pressure vessel tests

And zooming in to better see the details, shown in Figure 5.16

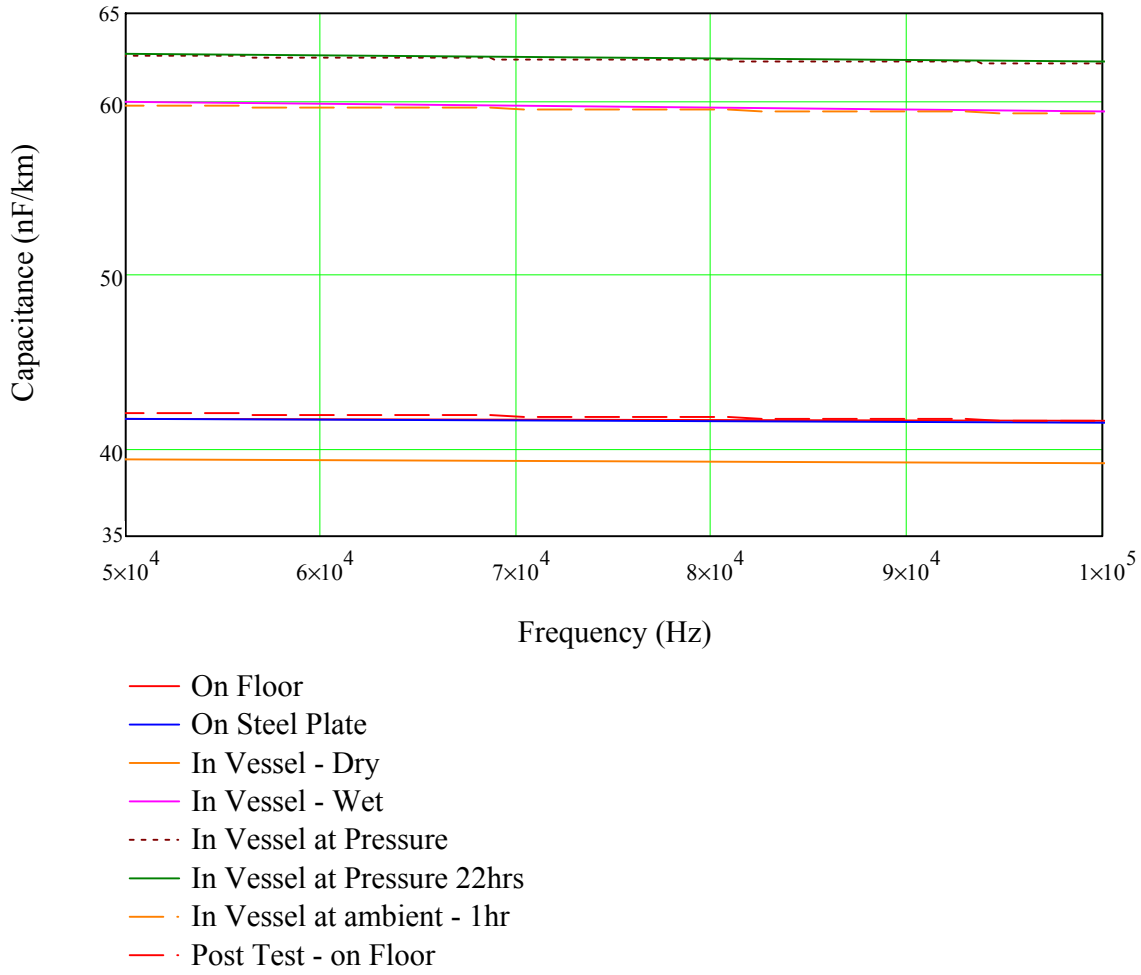

Figure 5-16 Measurement of capacitance in various pressure vessel tests

It can be seen that:

1) in proximity of any steel surface, whether the steel plate or the pressure chamber, the capacitance is not really affected;

2) The addition of water to the vessel appears to increase the capacitance measured;

3) When subjected to pressure the capacitance increases slightly but doesn't significantly change from this value as pressure is maintained;

4) When pressure is released, capacitance decreases slightly to around the same value it had before pressurization;

5) When the vessel is drained after the tests, the capacitance returns, more or less to the pretest values.

5.2.4 Conductance measurements

The effect on conductance is shown in Figure 5.17.

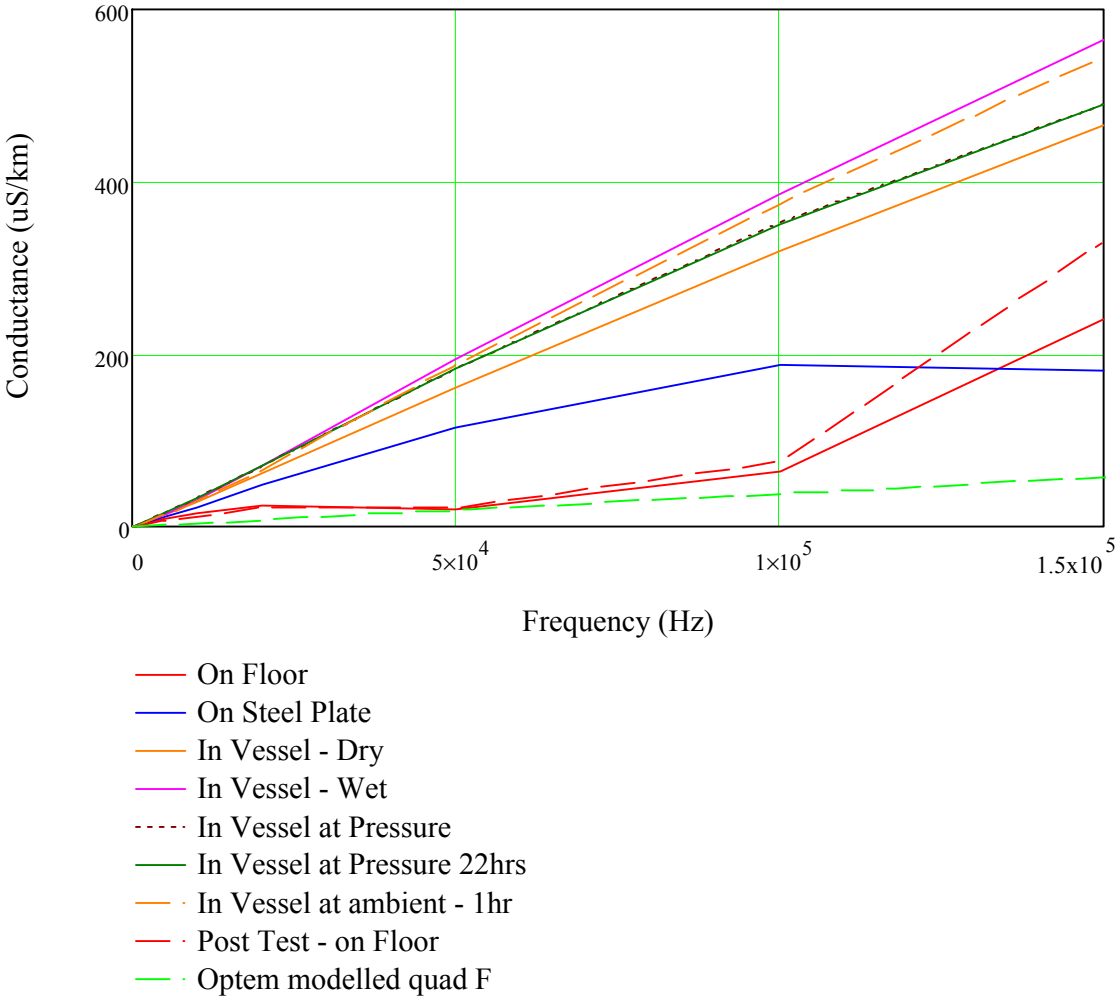

Figure 5-17 Measurement of conductance in various pressure vessel tests

And zooming in to the data to clarify the relationship between the measurements, Figure 5.18 shows

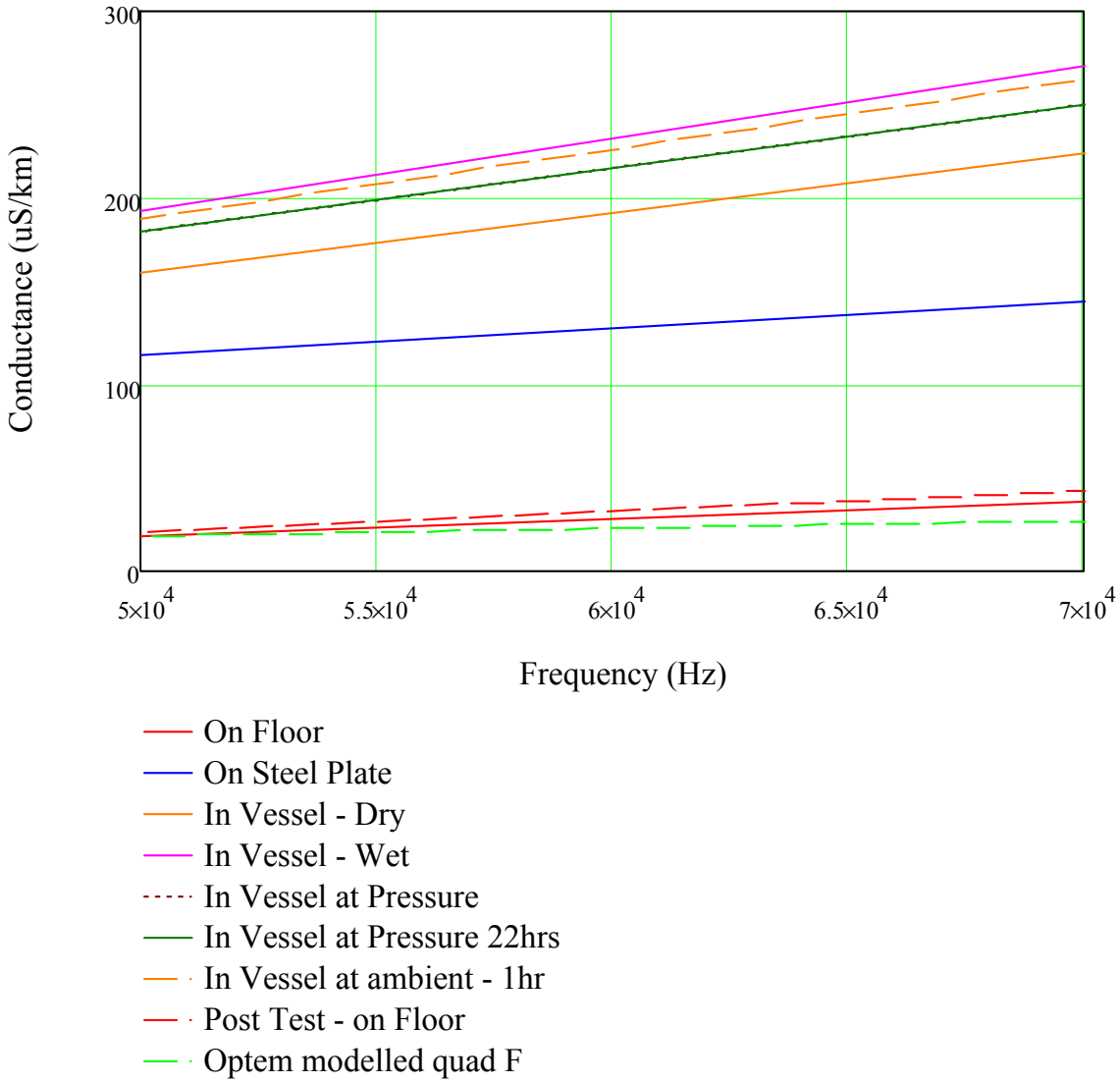

Figure 5-18 Measurement of conductance in various pressure vessel tests

The conductance measurements, shown in Figure 5.18, increase linearly with frequency but are significantly higher, by about a factor of 10, than the EM modelled figure for core F. As mentioned before in sections 4.2.2 and 4.2.3, accurate measurement of conductance is extremely difficult due to the very low measurement

currents so, at this stage these measurements are presented for reference. This is discussed later in section 5.1.7. In general it can be observed that:

- There is an increase in conductance by locating the quad on the steel plate or in the chamber;
- The addition of water to the chamber further increases the conductance;
- The application of pressure increases conductance further still, however little difference is seen over time. Before and after the application of pressure, conductance is higher;
- Removal from the water, pressure and the chamber, returns the conductance value to around the same value as before the test.

5.3 Measurements in air and sea water

In addition to the pressure chamber measurements above, tests were carried out in order to assess the impact of sea water on the impedance parameters of the quad cable. The following measurements indicate the difference seen in R, L, G and C when the cable is introduced to a plastic tank filled with sea water. The two diagonal pairs in the 15m 16mm^2 quad were measured, Pair A and Pair B with Pair A measured in air at 16°C, Pair B measured in air at 15.2°C and the two pairs measured in the sea water tank at 13°C.

Again, a temperature adjustment scaling factor was applied to the Wayne Kerr measurements and for sake of comparison, impedance values per km recorded.

5.3.1 Resistance

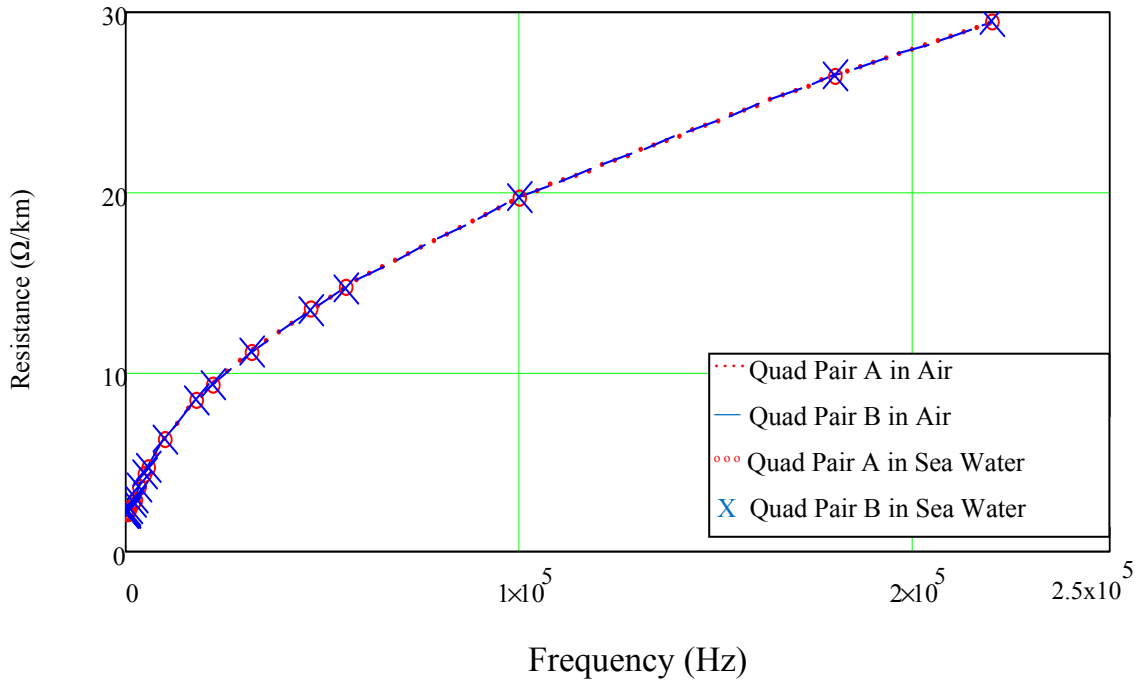

Figure 5-19 Effect of sea water on resistance

Figure 5.19 shows that, with wet results within 0.2% of the measurement in air, there is no perceivable effect on the measured resistance whether the cable is measured in air or in sea water.

5.3.2 Inductance

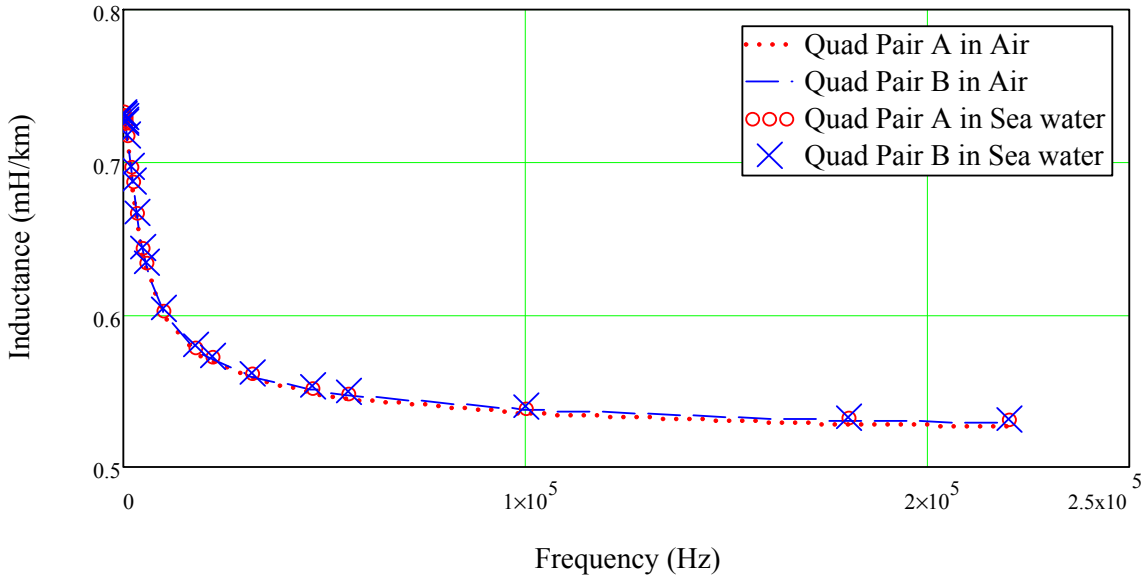

Figure 5-20 Effect of sea water on inductance

Figure 5.20 indicates again that there is very little effect on the measured inductance, with an increase of less than 2% seen when the measurement is made in sea water compared with air.

These resistance and inductance measurements suggests that, although sea water has significant conductance, with a figure of typically 4S/m, when compared with copper at 58 million S/m this is fairly insignificant, and so the magnitude of induced eddy currents is relatively small and the resultant effect on the conductor resistance and inductance, are minimal.

5.3.3 Conductance

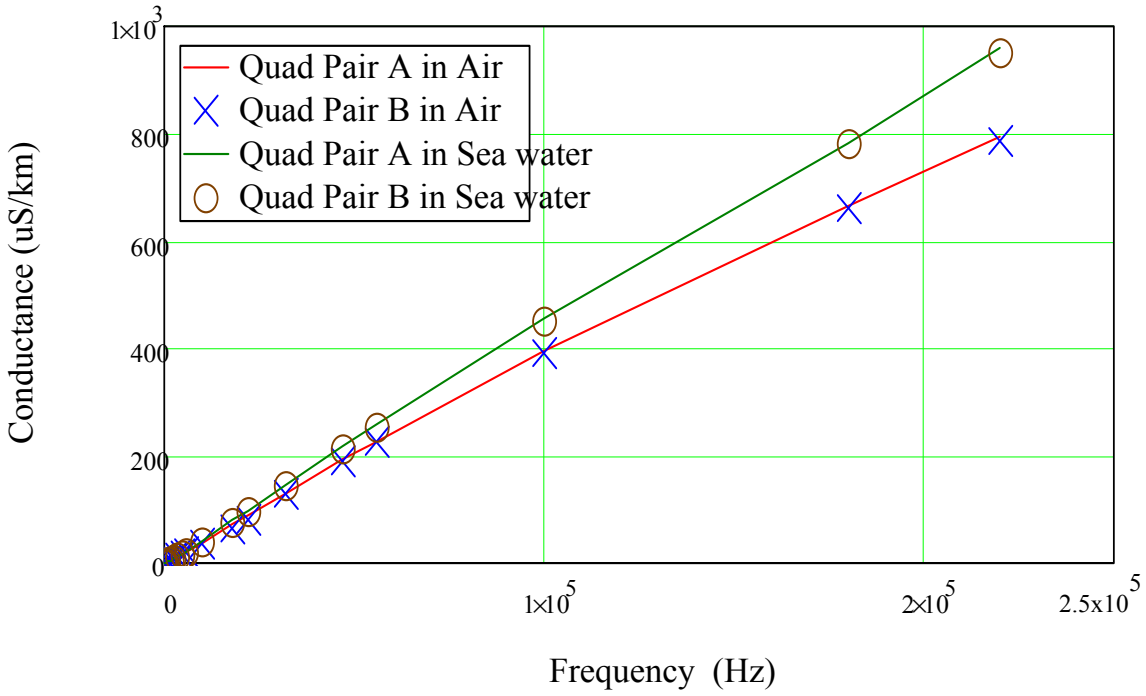

Figure 5-21 Effect of Sea Water on Conductance

Conductance in Figure 5.21 can be seen to increase by the submersion of the cable in sea water and shows around a 20% increase across the whole frequency band measured.

5.3.4 Capacitance

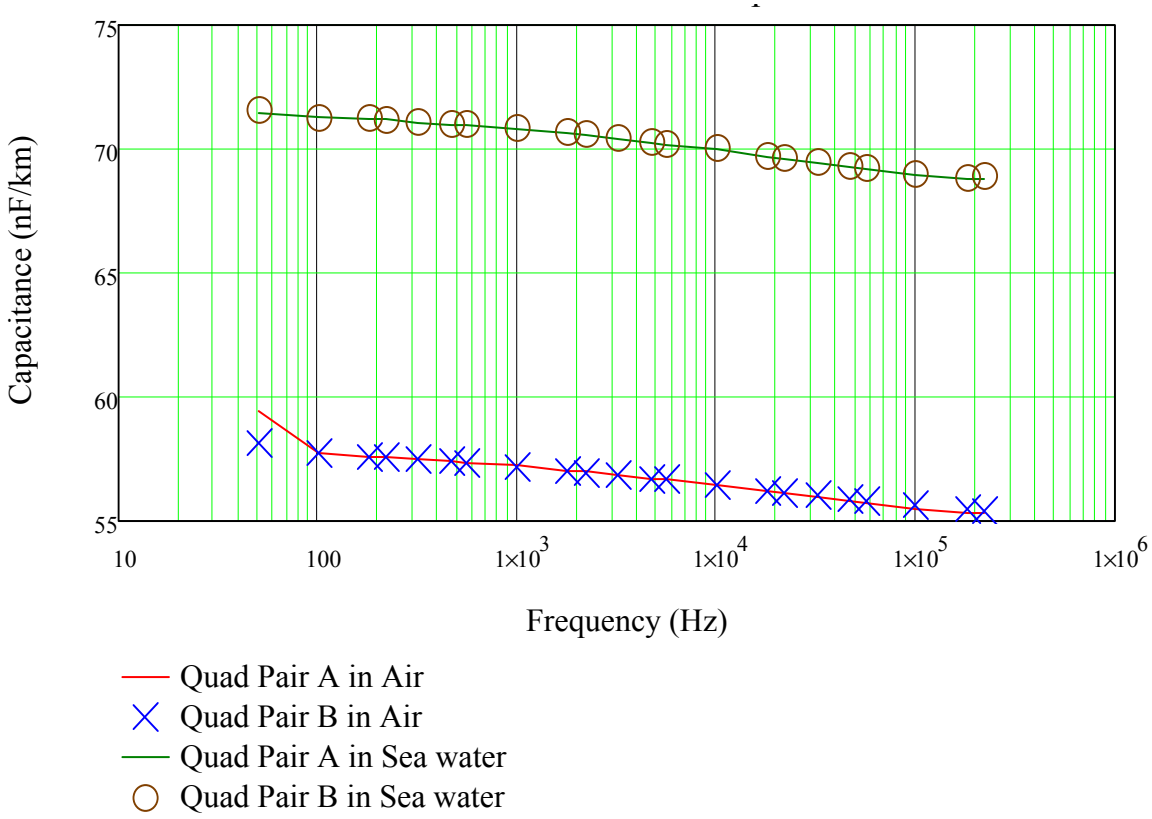

Figure 5-22 Effect of sea water on capacitance

And in Figure 5.22 it is clear that the capacitance is similarly affected and again shows an increase of around 20% with submersion of the cable in sea water.

5.4 Conclusion

In this Chapter measurements and modelled data were presented for the cables in a large variety of cases, and these examined the effects of pressure, steel surfaces and sea and fresh water on the impedance of the cables. These data will be examined along with full length umbilical attenuation measurements in Chapter 6, and will establish the accuracy and dependability of the modelling methods and the impedance and attenuation measurements and techniques.

Chapter 6. Comparison of Modelled and Measured Results

This chapter examines the many measurements and models of Chapter 5 and shows how predictions of attenuation made from these modelled and measured impedance parameters compare with attenuation measurements made on the full length umbilical. In section 6.6, the impact of a cable's screen thickness on the R, G, L and C parameters of the cable is also explored by further electromagnetic models.

6.1 Comparison of measured vs. EM prediction for bare quad

This series of measurements and predictions, shown in Figures 6.1 to 6.4, compares the electromagnetic prediction of the quad cable with the measured bare quad cable used for the pressure tests.

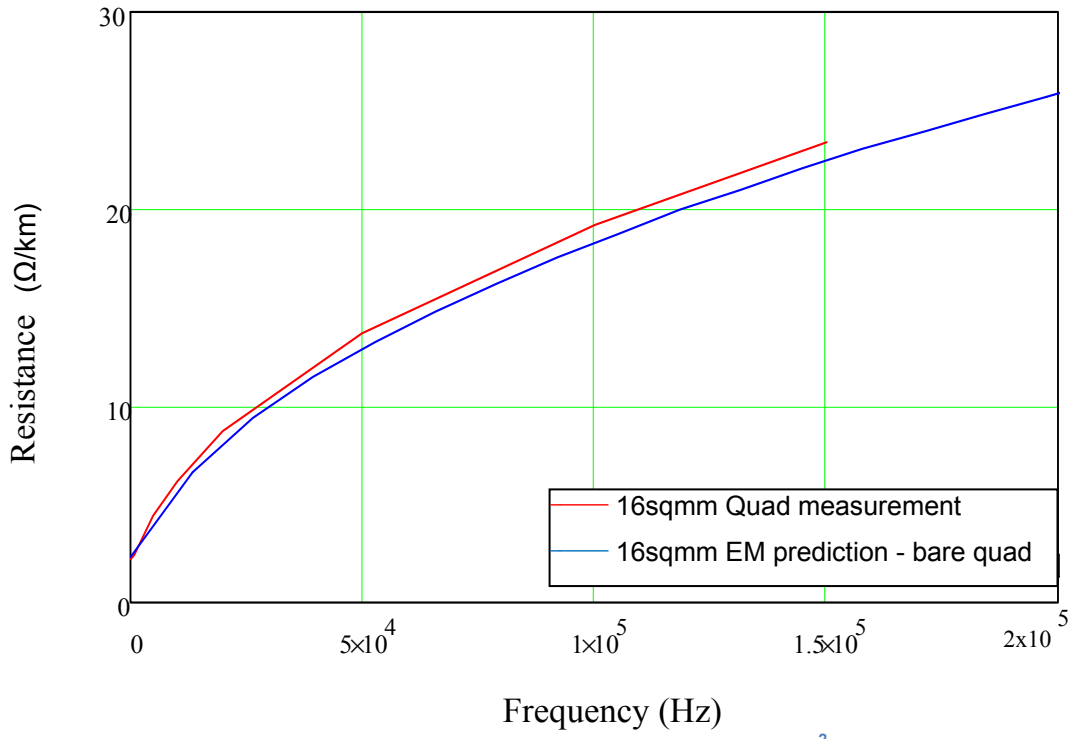

Figure 6-1 EM modelled and measured resistance for 16mm^2 quad cable

Figure 6.1 shows the modelled cable resistance is within 5% of the measured figures up to 100kHz. The skin and proximity effects, examined in section 2.2.1 are seen here to cause an increase in resistance as the frequency increases. Eddy currents induced in the adjacent copper conductors of the quad themselves generate a magnetic field opposing the flow of current in the conductors being examined, thereby increasing the resistance in the cores. The EM model provides an accurate calculation of the impact of the adjacent copper conductors on the resistance of the quad cores being used.

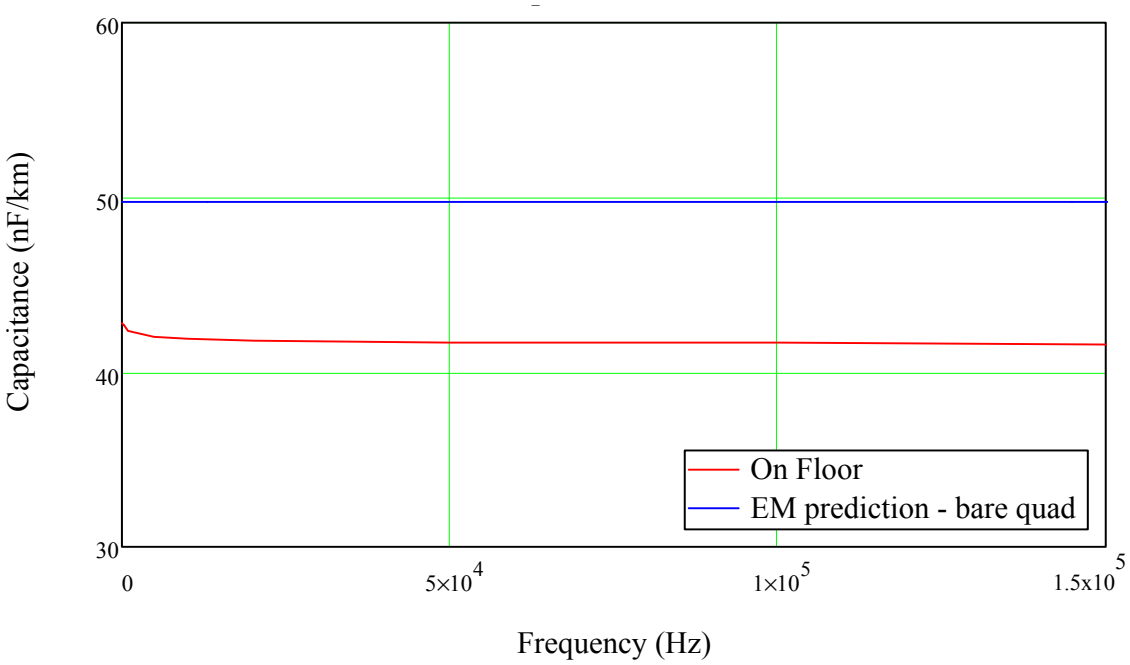

Figure 6-2 EM modelled and measured capacitance for 16mm^2 quad cable

The data plotted in Figure 6.2 shows the modelled cable capacitance is within 20% of the measured figures up to 100kHz. This deviation is not insignificant, however it must be remembered that, as described in section 2.2.4, capacitance is dependent on the electrical properties of the insulation material and the exact figure for dielectric constant of the measured cable is unknown. Also, as described in sections 4.2.2, 4.2.3 and 5.2.4 accurate measurement of capacitance and conductance can be prone to error due to

stray coupling between the measurement leads. This issue of conductance and capacitance measurement is dealt with in more detail in section 6.5.1.

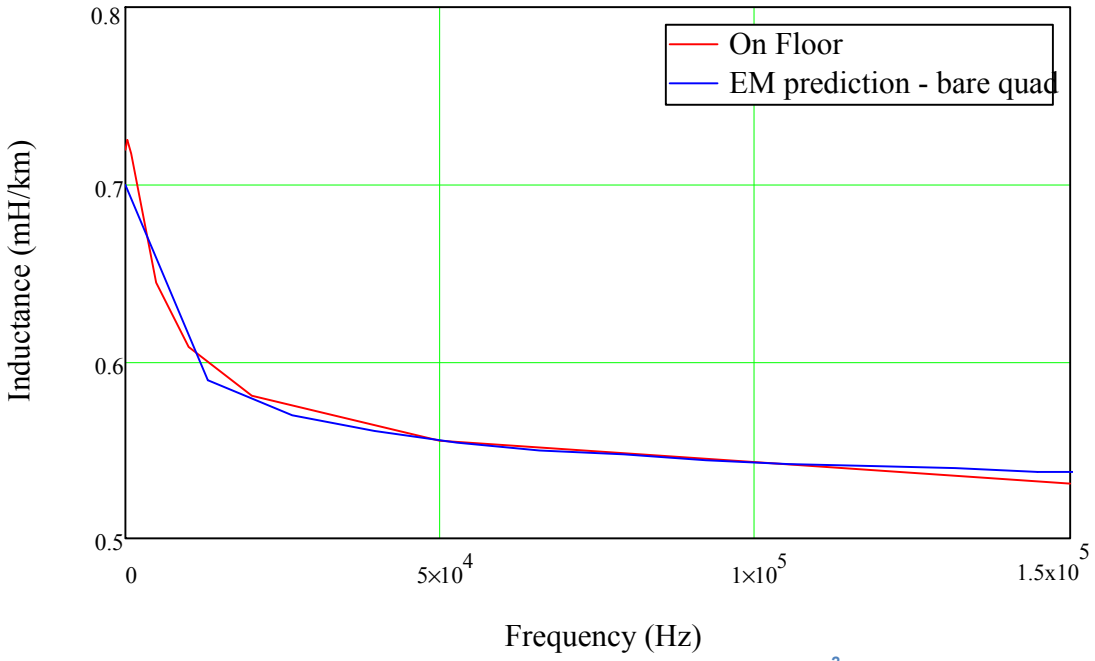

Figure 6-3 EM modelled and measured inductance for 16mm^2 quad cable

It is shown in Figure 6.3 that the modelled cable inductance is within 4% of the measured figures at 60Hz and within less than 1% at 100KHz.The EM model provides an accurate calculation of the impact of the skin effect as well as the induced eddy currents in the adjacent copper conductors on the inductance of the quad cores being used.

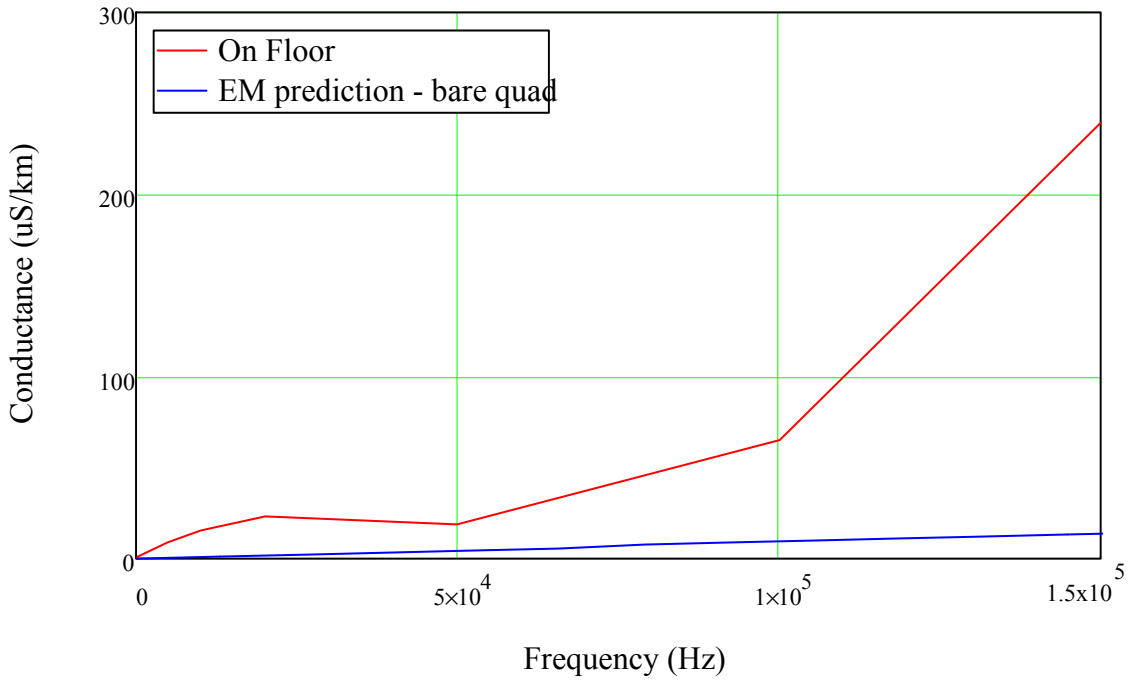

Figure 6-4 EM modelled and measured conductance for 16mm^2 quad cable

Figure 6.4 shows there is significant difference between the modelled cable conductance and that measured right across the full frequency band.

As discussed before, in sections 4.2.2, 4.2.3 and 5.2.4, capacitance and conductance measurements are much more affected by the measurement configuration and parasitics, than those for resistance and inductance. The very small measurement currents, in the order of 900 nA, required to measure a cable with conductance of 10μS/km (100kΩ) with a 3V signal on a 30m length, and the stray capacitance effects caused by leads, seem to be the main contributors to the errors. This issue is further discussed in section 6.5.1.

6.2 Comparison of measured vs. EM predicted RLGC parameters with cable in proximity to steel armouring

This series of measurements and predictions in Figures 6.5 to Figure 6.8 show the effect of the steel housing in proximity to the quad cable, simulating the effect of the steel wire armour.

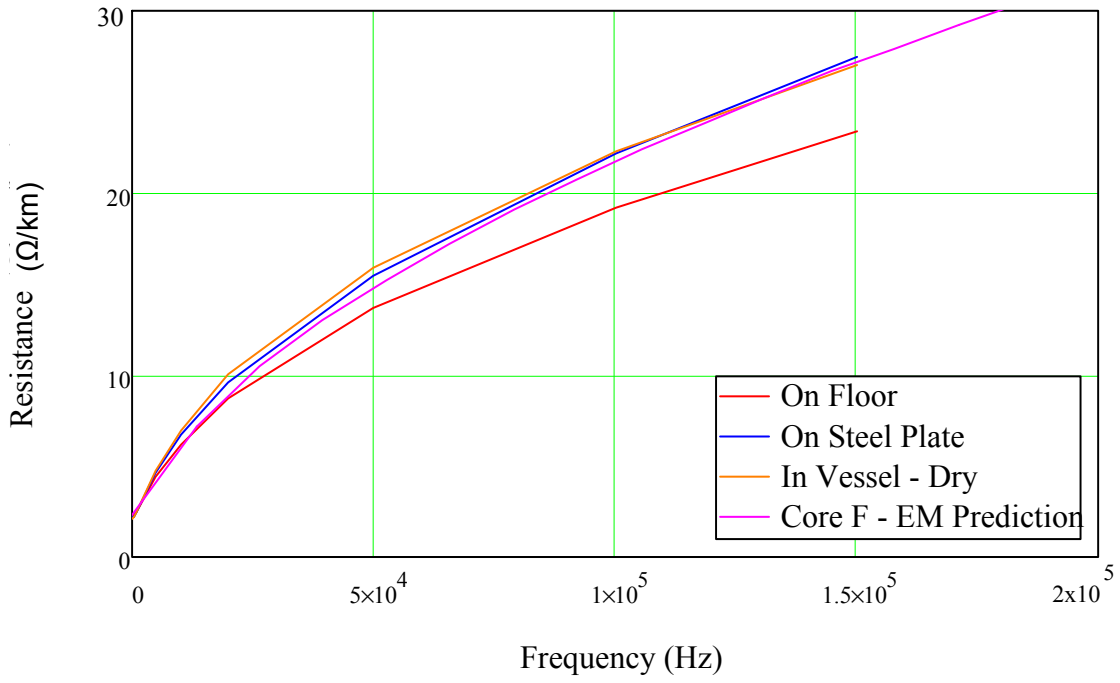

Figure 6-5 EM Modelled and measured resistance for bare16mm^2 quad cable and in proximity to steel surface

The measurements made on the floor are remote from the influence of any metallic objects. The EM model for core F derives figures for the quad in proximity to the umbilical steel wire armour, while the Vessel and Steel Plate measurement show the effect of proximity to the corresponding metallic surfaces on the resistance. It is clear from Figure 6.5 that when the quad cable is brought near to a steel surface, whether the pressure vessel, or the test steel plate there is a significant increase in resistance due to the induced eddy currents in the surrounding materials. This is reflected accurately in the EM model with results at 150kHz all within 2%.

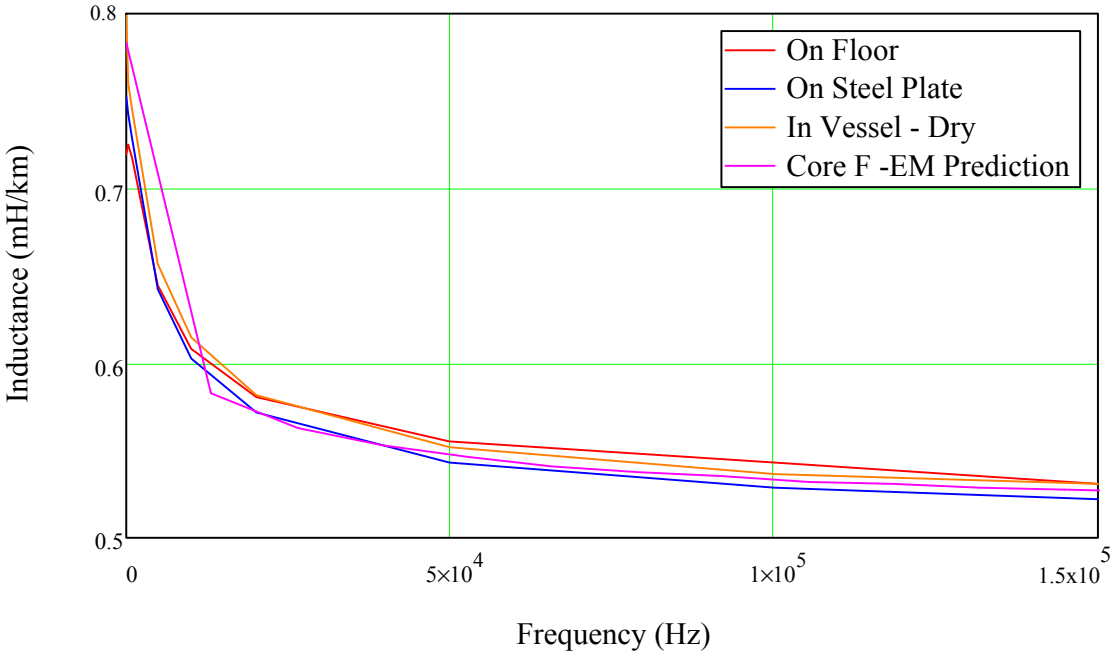

Figure 6-6 EM Modelled and measured inductance for bare16mm^2 quad cable and in proximity to steel surface

There is less of an impact on the inductance when the quad cable is brought in proximity of the steel surface as shown in Figure 6.6, however the effect of induced eddy currents in the nearby conducting materials is again reflected accurately in the results of the EM model with the results all within about 3% at 100KHz.

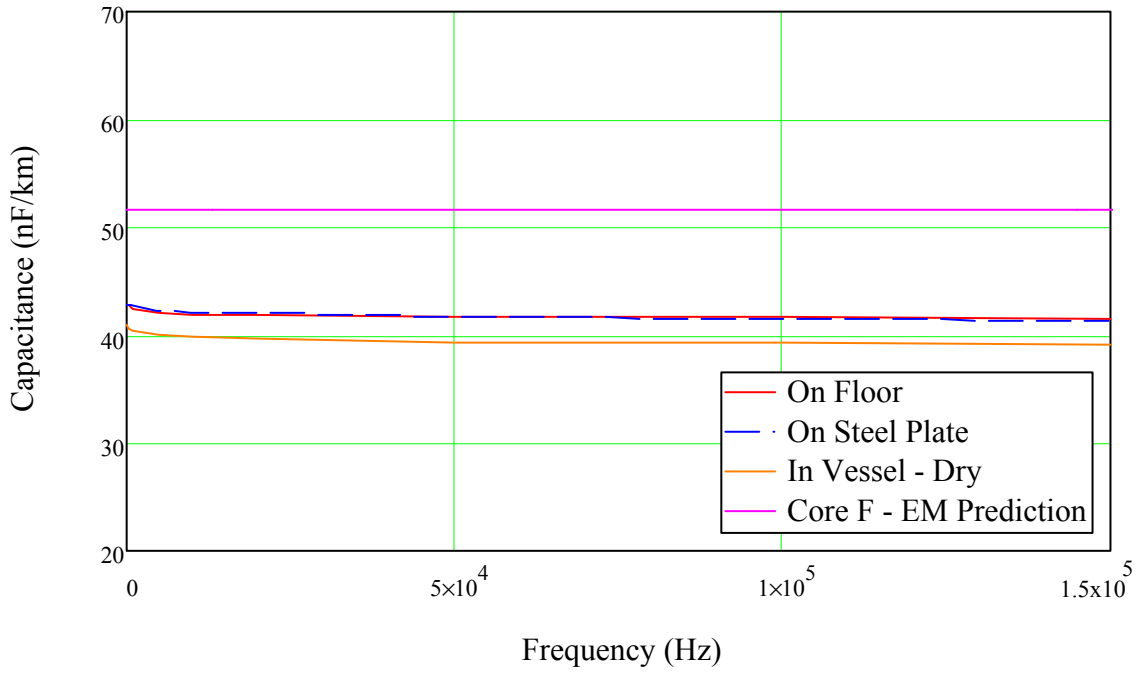

Figure 6-7 EM Modelled and measured capacitance for bare 16mm^2 quad cable and in proximity to steel surface

Figure 6.7 shows the capacitance is not greatly affected by the presence of the steel plate or pressure vessel, showing no change in the proximity of the steel plate and less than 5% variation due to the pressure vessel. Although the presence of the conductive material inevitably disturbs the radiated electric field from the conductors at its location, there is little change to the dielectric property providing storage between the conductors. This would suggest the change in capacitance caused by the hydraulic steel tubes or umbilical armouring will be minimal.

The difference in the EM model as noted in section 6.1 is again clear.

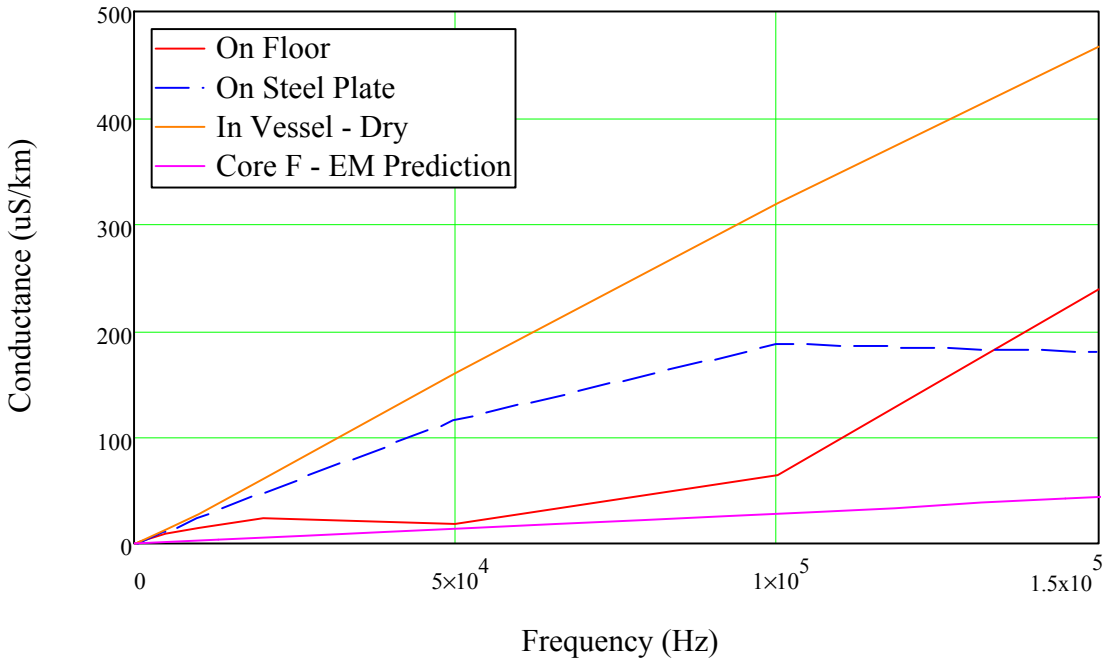

Figure 6-8 EM Modelled and measured conductance for bare16mm^2 quad cable and in proximity to steel surface

Figure 6.8 shows the proximity to the steel surfaces does appear, on the face of it, to increase the measured conductance, however again as noted in section 6.1, measurement currents are extremely small and the additional conductive surfaces and the possible effect on the measurement leakage currents would allow extra possible paths for parasitic coupling between the measurement probes. Results will have to be used with caution.

6.3 Comparison of measured vs. EM predicted RLGC parameters with pressure chamber flooded

This series of measurements and predictions in Figures 6.9 to 6.12 show the effect of the steel housing in proximity to the quad cable, simulating the effect of the steel wire armour of the umbilical and also the effect on the loss when the cable is flooded.

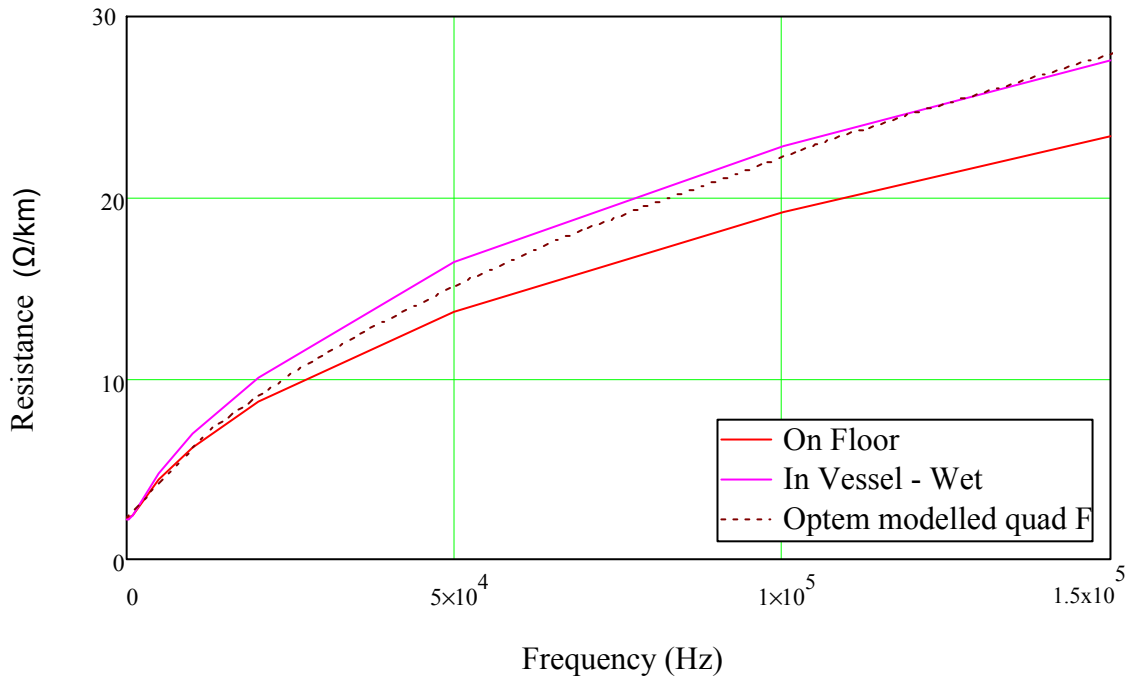

Figure 6-9 EM Modelled and measured resistance for bare16mm^2 quad cable and in the flooded pressure vessel

In Figure 6.9 it is seen, that although core F was modelled with sea water in the adjacent hydraulic hoses, and not with it surrounded by sea water, with results within 10% over the full frequency band measured, it still gives a good prediction of the cable resistance of a deployed quad in proximity of a steel surface. Since resistance can only be affected by the impact of induced eddy currents on the cores then, as might be expected, comparison with Figure 6.5 shows that the addition of water to the pressure vessel does not have a significant impact on the measured resistance as the conductivity of the water is extremely low when compared with that of any local metallic objects. In actual fact, as described at the beginning of Section 5.3.2, due to low conductivity of sea water when compared with copper or steel, a similar result could be reasonably expected, had the tests used sea water.

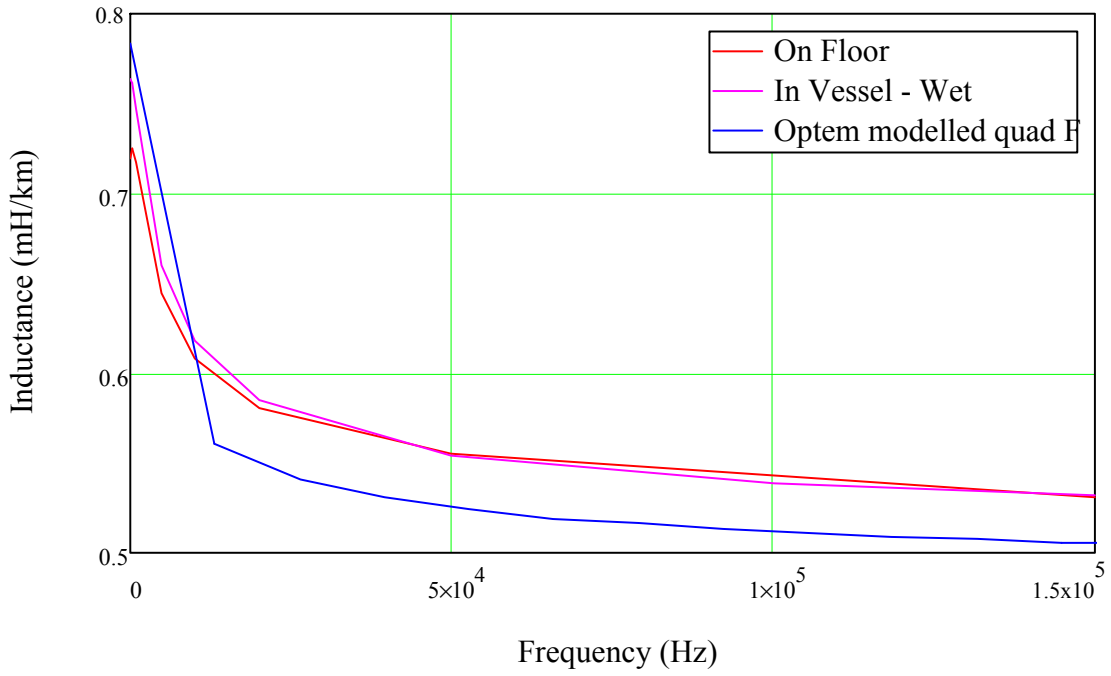

Figure 6-10 EM Modelled and measured inductance for bare16mm^2 quad cable and in the flooded pressure vessel

Core F was again modelled with sea water in adjacent hydraulic hoses but not surrounded by sea water. The modelled results shown in Figure 6.10 seem consistently lower than the measured figures, whether on the floor or in the pressure vessel, but are still within about 5% across the full frequency band measured. Since, like the resistance in figure 6-9, inductance also can only be affected by the impact of induced eddy currents on the cores, then as might be expected, comparison with Figure 6.6 suggests the addition of water to the vessel does not have a great impact on the inductance.

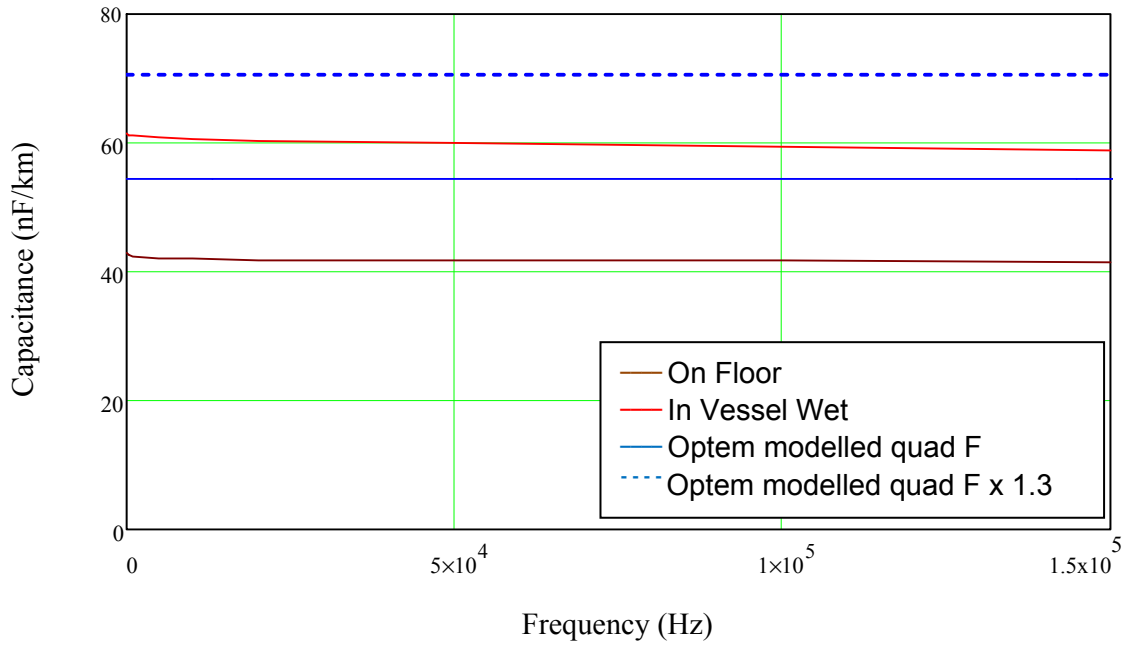

Figure 6-11 EM Modelled and measured capacitance for bare16mm^2 quad cable and in the flooded pressure vessel

Core F was modelled with sea water in hydraulic hoses but not surrounded by sea water. The capacitance was seen to increase by around 30% when the quad cables are modelled as surrounded by sea water and this is shown in Figure 6.11. This is similar to the change in capacitance measured with the quad cable on the floor and in the flooded pressure vessel, also shown in Figure 6.11. As the addition of seawater to the vessel will increase the dielectric constant of the material surrounding the cable, this change is as expected and is in line with known practical scaling factors as outlined in section 3.1.

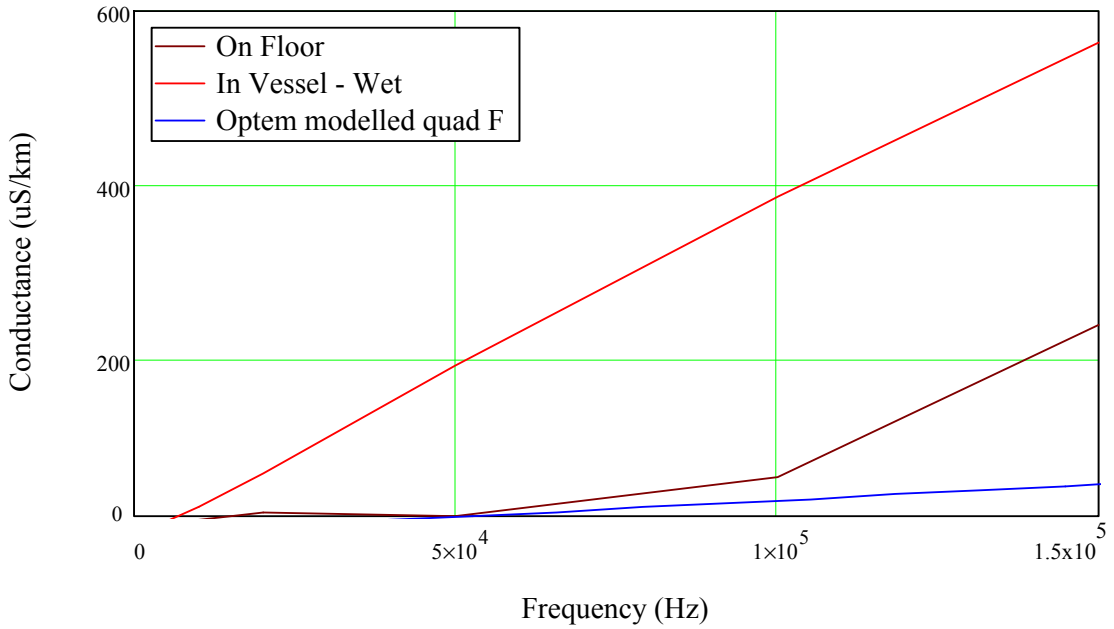

Figure 6-12 EM Modelled and measured conductance for bare 16mm^2 quad cable and in the flooded pressure vessel

When compared with Figure 6.8, the conductance is seen to increase significantly with the addition of the water to the vessel. This would be as anticipated, as the dielectric constant of the material surrounding the cable has now increased substantially. Although, as noted before in section 6.1, there is a major difference between modelled and measured figures, the 'vessel dry' results in Figure 6.8 are clearly lower than the 'vessel wet' data in Figure 6.12.

6.4 Comparison of measured vs. predicted RLGC parameters with pressure chamber flooded and under pressure

This series of measurements and predictions in Figures 6.13 to 6.16 show the effect of the steel housing in proximity to the quad cable, simulating the effect of the steel wire armour of the umbilical and also the effect on the loss when the cable is flooded.

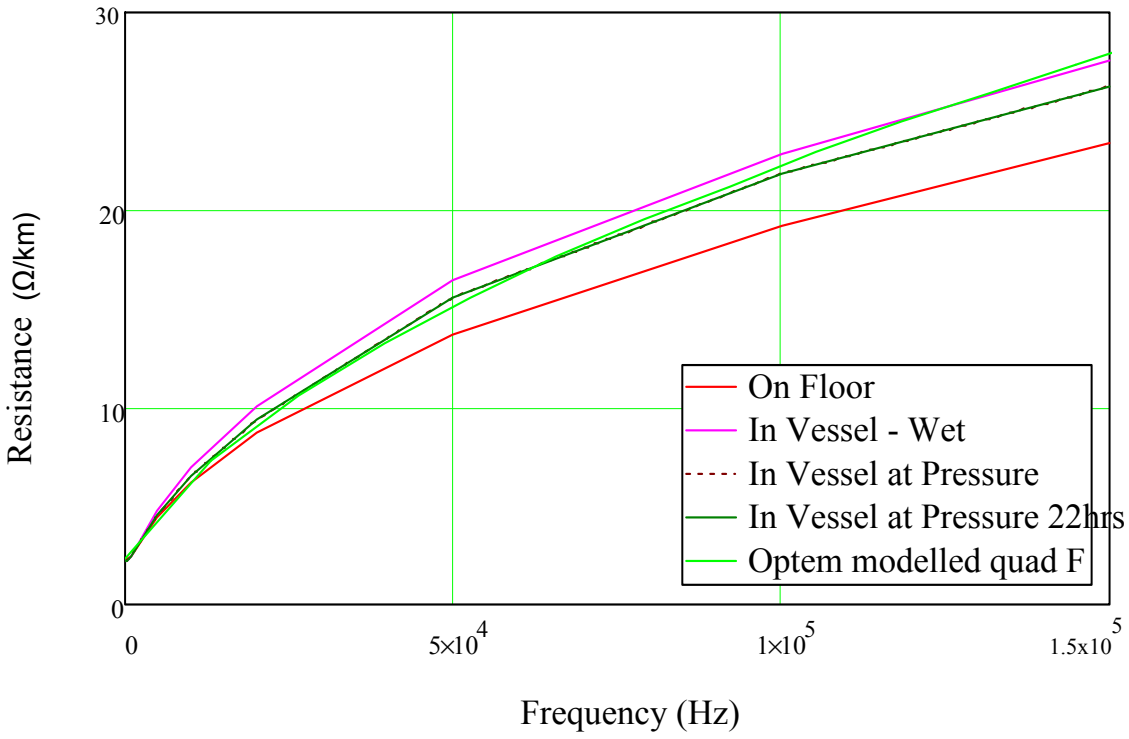

Figure 6-13 EM Modelled and measured resistance for bare16mm^2 quad cable and in the vessel under pressure

From Figure 6.13, it seems that the resistance drops slightly (around 5% at 100kHz) with the addition of pressure but does not seem to vary as pressure is maintained. This would suggest there is an initial deformation of the cable which reaches a compression limit within the first few minutes of pressure being applied.

Although the perceived change is small, and therefore inconclusive, this change would seem to be the converse of what might be expected. It is known from the models in Section 2.2.1 that the resistance increases as conductors are brought closer due to proximity effect and induced eddy currents but it must also be remembered however, that subjecting the quads to pressure will not only reduce the separation of the conductors due to compression of the insulation, but will also affect the conductor cross section (although not the cross sectional area of copper in each conductor) due to compression of the copper strands as well as potentially altering the distance from the conductors to the pressure chamber wall itself.

The implications of measurements taken previously in Section 5.3.1 in the presence of water, and the examination of the effect of water treeing in Section 3.2.5 and the relatively short time scales and low voltages involved, would rule out any effect from water or water treeing on these results. Although there would also be expected a compression of the insulation, thereby changing the dielectric constant, as shown in these sections, this itself should not affect the cable resistance.

More information would be required to fully examine the change in resistance with pressure, however due to the pressures in time brought to bear on the manufacturing process by the project and very high cost involved in delaying umbilical deployment due to the potential of lost revenue in oil recovery, it was not possible to further examine this on the project.

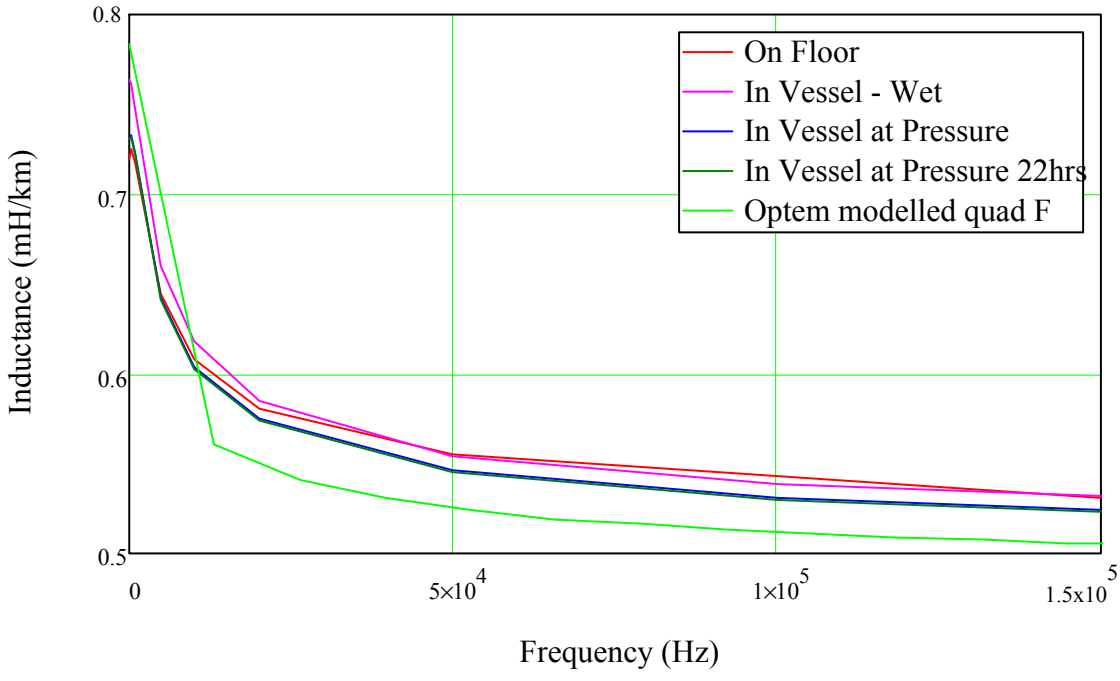

Figure 6-14 EM Modelled and measured inductance for bare16mm^2 quad cable and in the vessel under pressure

Figure 6.14 shows that the inductance drops slightly (around 2% at 100KHz) with the addition of pressure but does not seem to vary significantly as pressure is maintained. This would again suggest there is an initial deformation of the cable which reaches a

compression limit within the first few minutes of pressure being applied. As the mutual inductance is a proportional to the distance between the cores, this reduction in inductance as the cores are forced together would be expected.

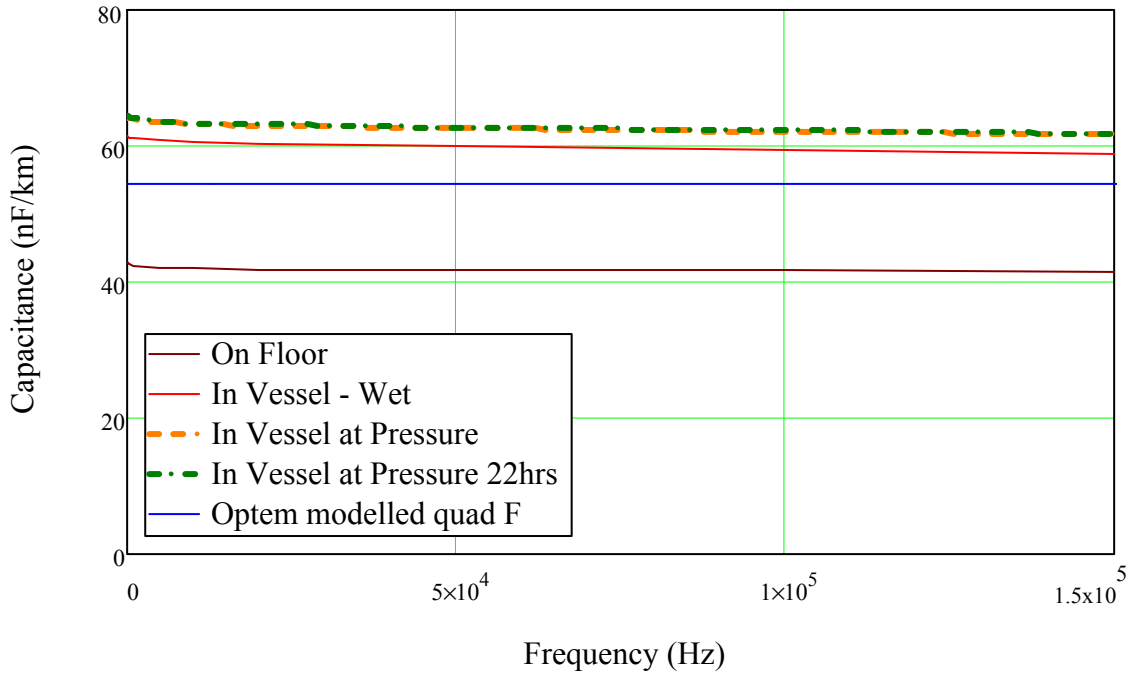

Figure 6-15 EM Modelled and measured capacitance for bare16mm^2 quad cable and in the vessel under pressure

From Figure 6.15 it is seen that the application of pressure increases the measured capacitance by about 5% at 100kHz. This again remains largely unchanged over the next 22 hours suggesting there is no ongoing compression of the cores. It would seem reasonable to expect that, as the pressure causes a compression of the quad and forces the cores closer together, an increase in capacitance would be seen.

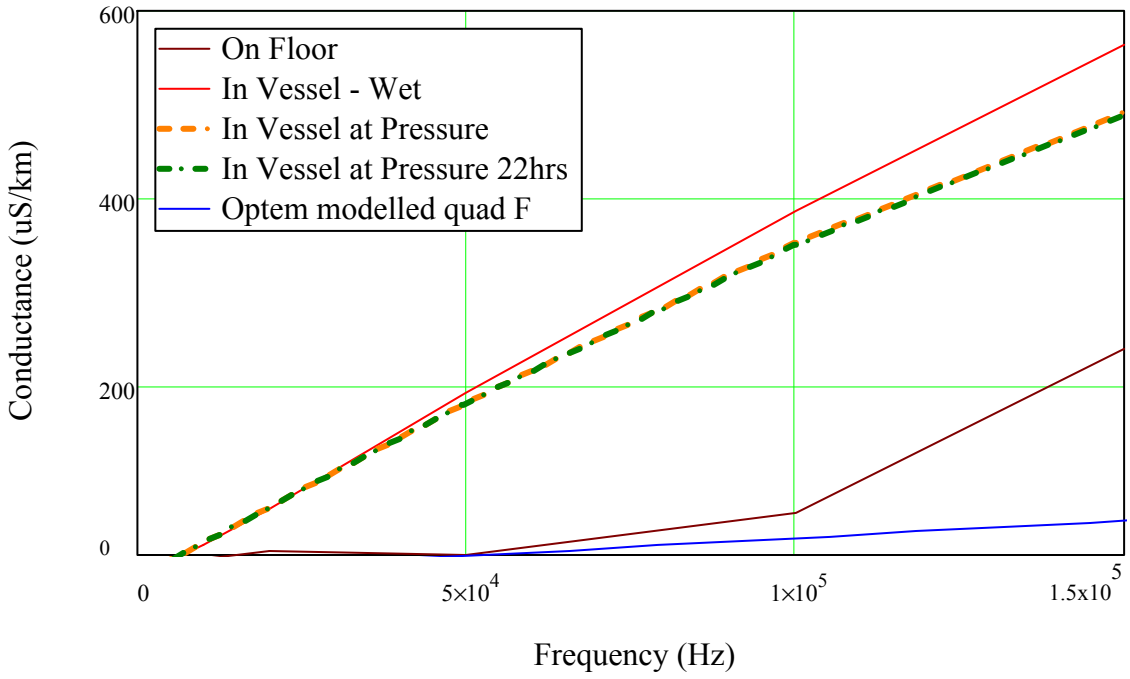

Figure 6-16 EM Modelled and measured conductance for bare16mm^2 quad cable and in the vessel under pressure

The measured conductance drops with the application of pressure and again remains constant over the test interval as shown in Figure 6.16. As with the resistance measurements shown in Figure 6-13, the results here may seem to be contrary to what might be expected, the implications of compression of the dielectric, alteration of the conductor separation, and variation in the distance to the chamber wall will all have an impact on the conductance measured in these tests. Again pressures of manufacturing time due to the high financial penalty in delay in delivery, meant further investigation was not possible on the project.

6.5 Comparison of measured vs modelled attenuation

Given all these data, the loss in the umbilical cores under different conditions can be derived as follows:

As shown in Section 5.1, the theoretical calculations show the effect of bringing the quad cable next to the armouring is to increase the resistance and inductance with very

little impact on the capacitance and conductance. However the increase in conductance and capacitance by the filling of the hoses with sea water is marked, while the effect of the sea water on the resistance and inductance is minimal. These same effects were also seen in the measurements taken at various stages, such as in Section 5.3 with the addition of the sea water to the plastic tank when it was also clear that the addition of sea water had no real effect on the resistance and inductance, but a considerable increase was seen in the capacitance and conductance parameters.

Therefore cores toward the centre of the umbilical and remote from the influence of the armouring, will have their resistance and inductance best reflected by the bare cable measurements and predictions. After deployment, the umbilical will be flooded with sea water and the thermoplastic hoses filled with water based hydraulic fluid. It would seem, therefore, that capacitance and conductance, which are largely unaffected by the vessel will be best reflected by the measurements in the flooded vessel while the resistance and inductance would be best represented by the non-vessel measurements.

However for cores at the outer edge of the umbilical near the steel wire armour, it would be expected that the measurements obtained with the cores in the steel chamber would give the best indication of resistive and inductive properties. Similarly the measurements in the flooded vessel would give best indication of the expected capacitance and conductance once deployed subsea.

Although this gives a prediction of the expected RGLC parameters and allows calculation of the expected attenuation of the cables, there is no way of verifying this unless measurements from the umbilical itself can be compared. In the later stages of the project, after manufacture of the umbilical, opportunity for some final data arose; due to the criticality of the cable performance for the project, the manufacturer was

asked to measure and make available the RGLC parameters for a section of the cable as part of his Factory Acceptance Test (FAT), and access to the full umbilical would be given for a short time during which communications testing would be carried out and umbilical attenuation measurements could be made. As hoses in the full length umbilical had been filled with hydraulic fluid for pressure testing, these were still filled, although depressurised when the full umbilical attenuation measurements were made so it was possible to get attenuation measurements over the full length of the umbilicals with all adjacent hydraulic hoses filled with hydraulic fluid.

As pointed out in section 3.1, due to the high company confidentiality of the equipment produced for the subsea industry, opportunities like this, where cable measurements in a variety of configurations, electromagnetic predictions, umbilical sample measurements and umbilical attenuation measurements are performed and made available for analysis, are extremely rare. FAT results were provided by the manufacturer for comparison however, it was later seen that the short length used for the manufacturer's test was a section from the riser umbilical, the part that connects the subsea static umbilical with the surface equipment and not the main static umbilical used for the other tests. Figure 6.17 shows this riser umbilical cross section which is made up as follows:

- Cores A - M are the 16mm^2 electrical quad cables for power and communications
- Cores N - O are 4mm^2 quads for connection to the Subsea Isolation Valves
- Cores P - U are 12 Fibre Optic Cables
- Cores 14 - 42 are 12.7mm 345 Bar hoses for chemical and hydraulic fluids
- Cores 1 - 3 are 19mm 345 Bar hoses for chemical and hydraulic fluids

- Cores 4 - 13 are 12.7mm 690 Bar hoses for chemical and hydraulic fluids

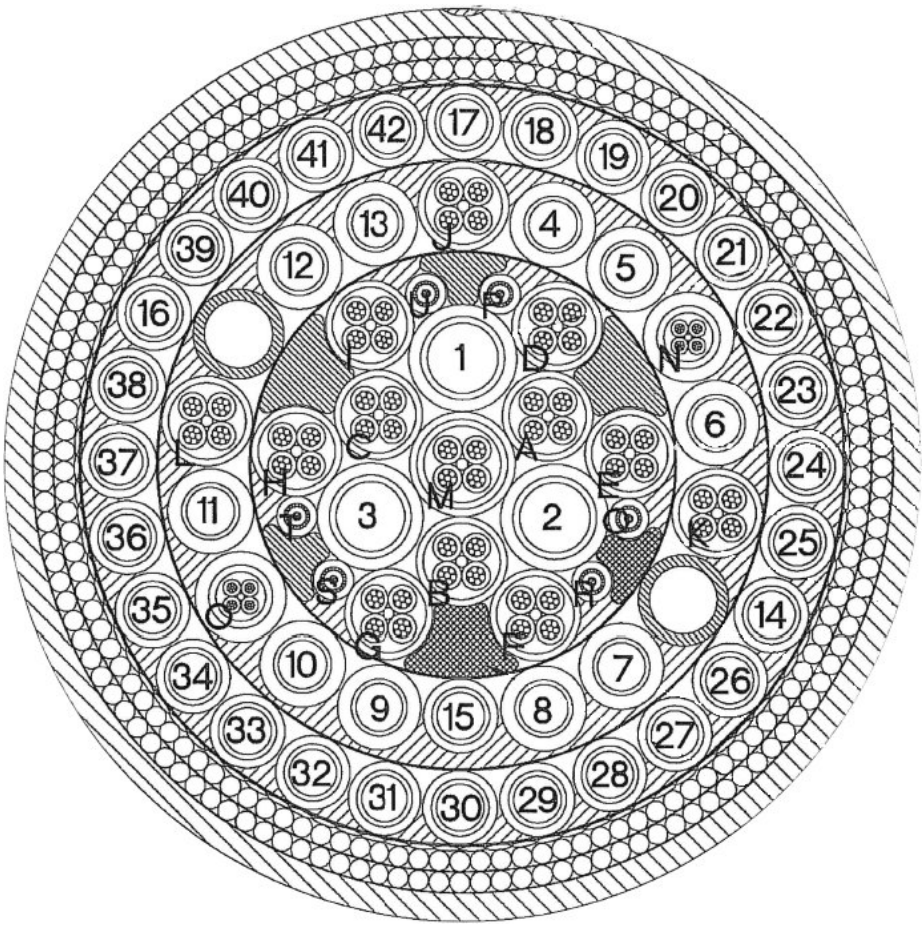

Figure 6-17 Riser 246.9mm Diameter Umbilical Cross section

The cores which connect through to core F in the static umbilical of Figure 5.2 (the core of particular interest next to the armouring) are not next to the armouring in this riser umbilical and so do not allow a good direct comparison, particularly of the R and L values which are affected most significantly by the steel wire. The values from these measurements are not used in the following measurement and prediction comparisons, but some of the results, particularly from the conductance measurement are significant in the understanding of the comparisons. This will be clarified in the following paragraphs.

Attenuation measurements on the full length of static umbilical however were possible and these are used to compare with the vessel data and EM data that best suits the cores being examined.

The following graphs give a comparison of the predictions from the pressure vessel data, the predictions from the EM model and the measurement of the attenuation in the full length of the static umbilical for cores C and F as shown in Figure 6.17.

Similarly core C runs for a distance of 27.6km and controls the wells at this location. Again to facilitate measurement, the attenuation was measured over a double length using cores C and D with a loop back at the far end. Measurement length was 55.2km and this is shown in Figure 6.18.

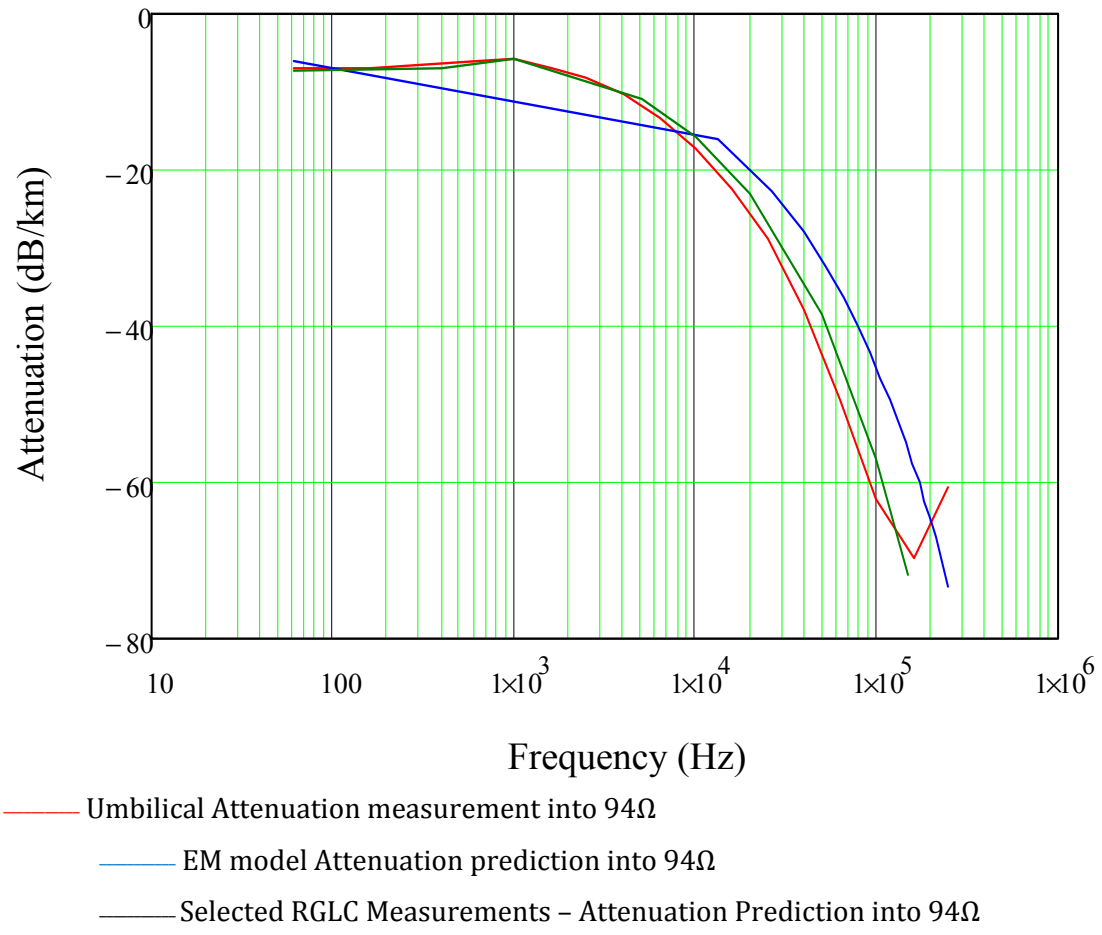

Figure 6-18 Measured and predicted attenuation for core C over 55.2km on static umbilical

Core F runs in the umbilical for a distance of 17.9km at which point it is split out from the umbilical where it controls the wells at this location. In order to facilitate measurement, the attenuation was measured over a double length using cores F and E with a loop back at the 'far' end. Measurement length was therefore 35.8km and this is shown in Figure 6.19.

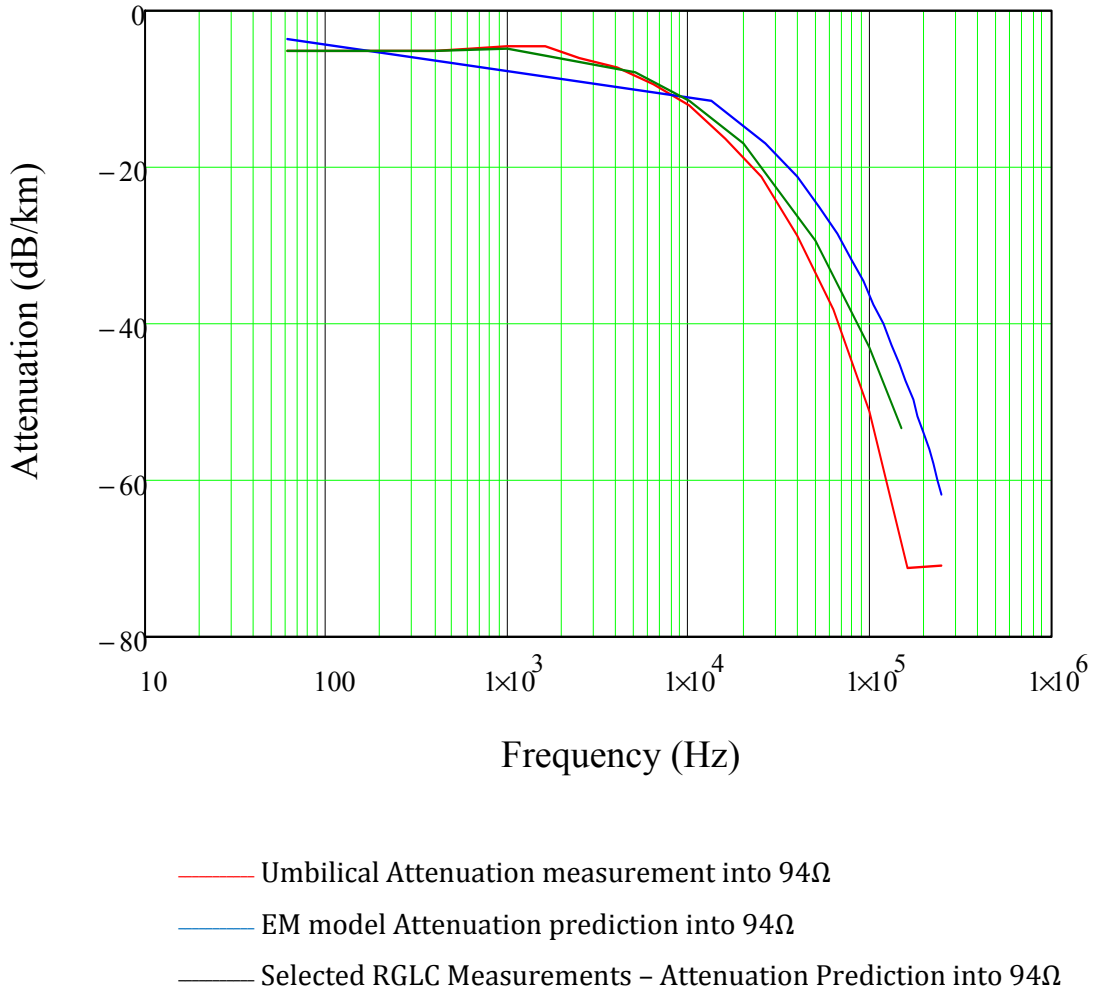

Figure 6-19 Measured and predicted attenuation for core F over 35.8km on static umbilical

Bearing in mind the EM figures were derived in 19 equal steps between 60Hz and 250kHz and so only the first two plotted values are 60Hz and 13.215kHz, attenuation here shows good correlation in both cases over the first 10kHz or so. However after

this graphs diverge quickly such that predictions of loss are definitely optimistic, both from modelled as well as measured data.

6.5.1 Conductance Variation

Observation of previously compared data in Chapter 5 and Chapter 6, section 6.1 to 6.4 show that resistance, inductance and capacitance predictions and measurements generally correlate well, at least when compared to the discrepancy in the measured and calculated Conductance.

Figure 6-20 shows the variation in conductance observed between the FAT sample data, EM prediction and the Pressure Chamber measurements.

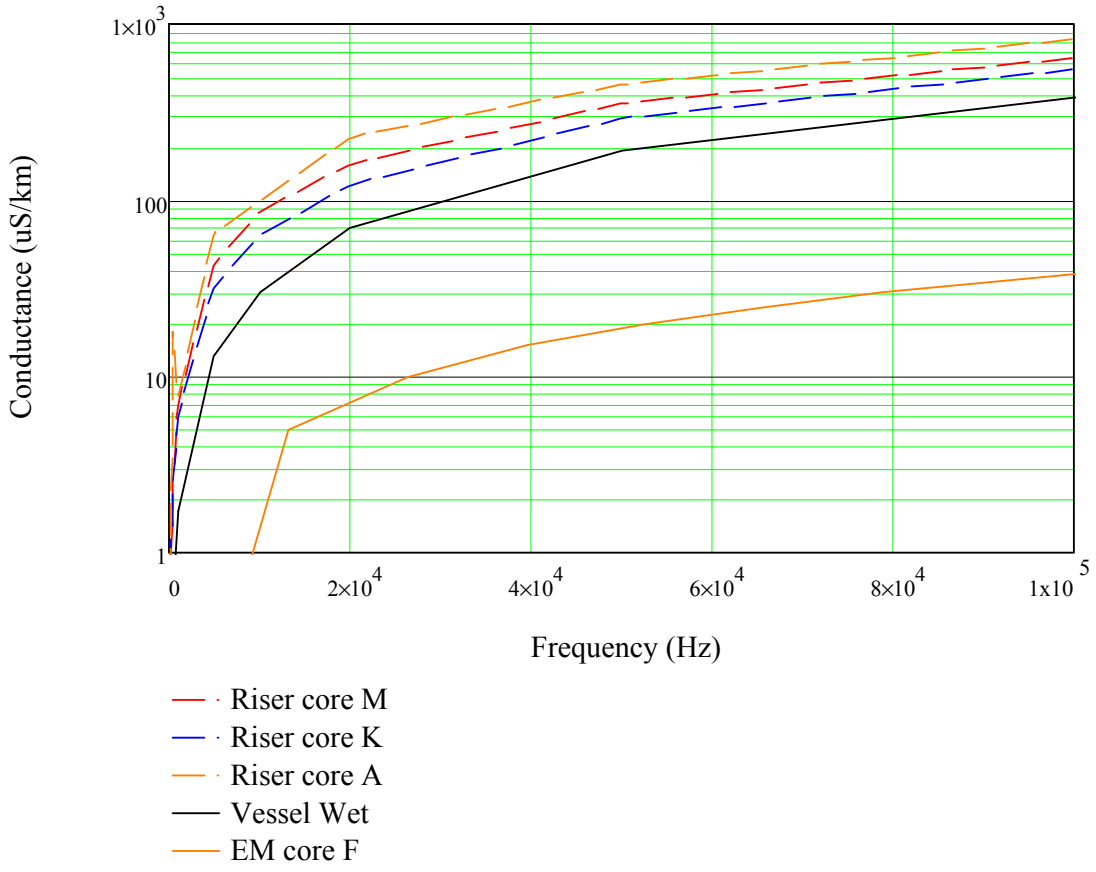

Figure 6-20 Comparison of conductance from FAT, pressure vessel and EM model

It is seen here that the riser umbilical shows a conductance of between 500 and 800μS/km at 100kHz when tested during the FAT, compared with around 400μS/km for the pressure vessel measurements and 40μS/km for the EM calculated figure for core F. As indicated in the previous chapters, in sections 4.2.2, 4.2.3, 5.2.4 and 6.1 to 6.4, measurement of the conductance with equipment such as the Solartron 1260 and Wayne Kerr 6440 requires very small currents and given the non-ideal measurement set up of testing a full umbilical in a production yard where:

- the umbilical is coiled on a carousel;
- umbilical ends are separated by tens of metres, necessitating the need to loop back the cores to get valid measurements;
- supply ends are remote from the test equipment by about 45m,;
- test leads and loop backs are connected with ‘crocodile clips’;

leakage between the test leads is very likely, and is very probably significantly affecting the attenuation measured by way of an increase in the perceived conductance. If, for the sake of comparison it is assumed that the predicted conductance figures are accurate, as has been the case with the other R, L and C data and the conductance figures are now scaled accordingly, around x20 for the EM figure and x2 for the vessel measurement figure to bring them into line with the FAT measured conductance and the attenuation above is recalculated using the adjusted conductance values, the difference between predicted and measured attenuation is now significantly less as shown in Figures 6-21 and 6-22.

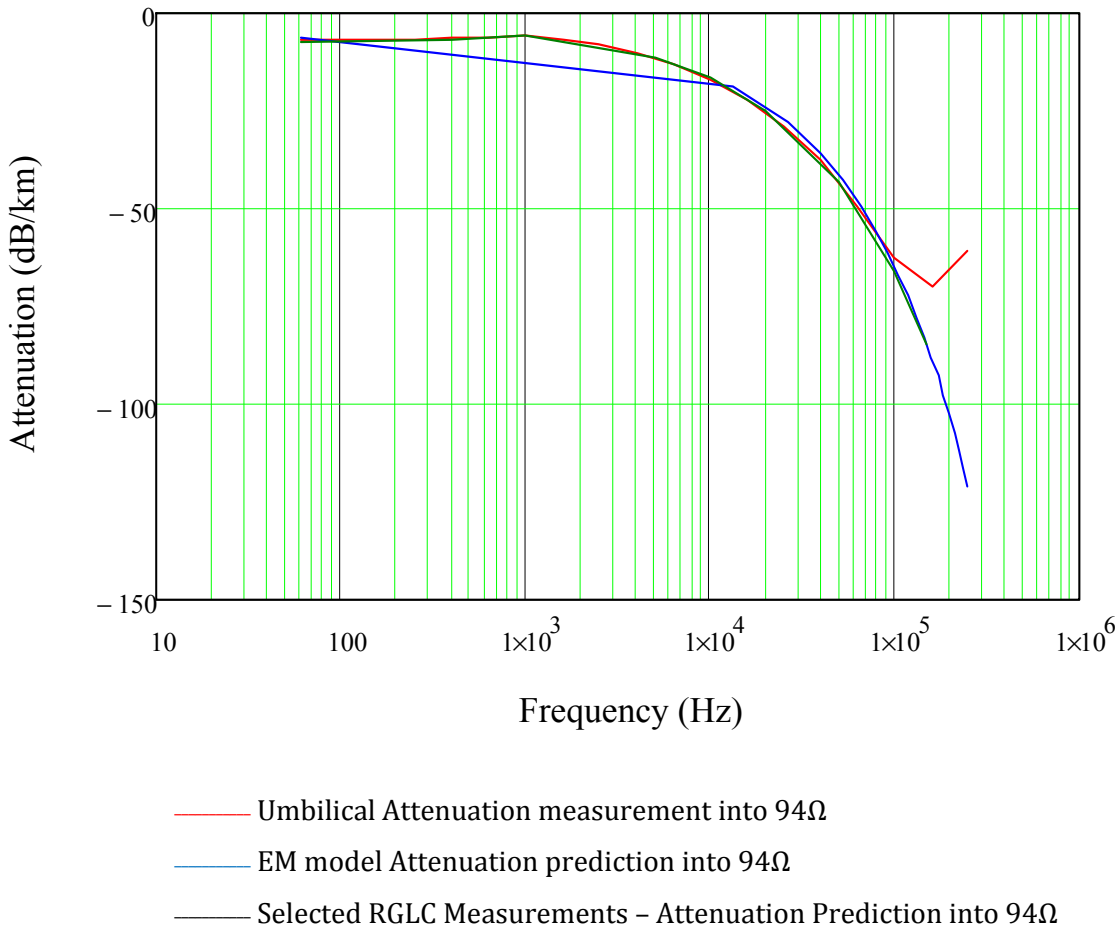

Figure 6-21 Measured and predicted attenuation for core C over 55.2km with adjusted conductance

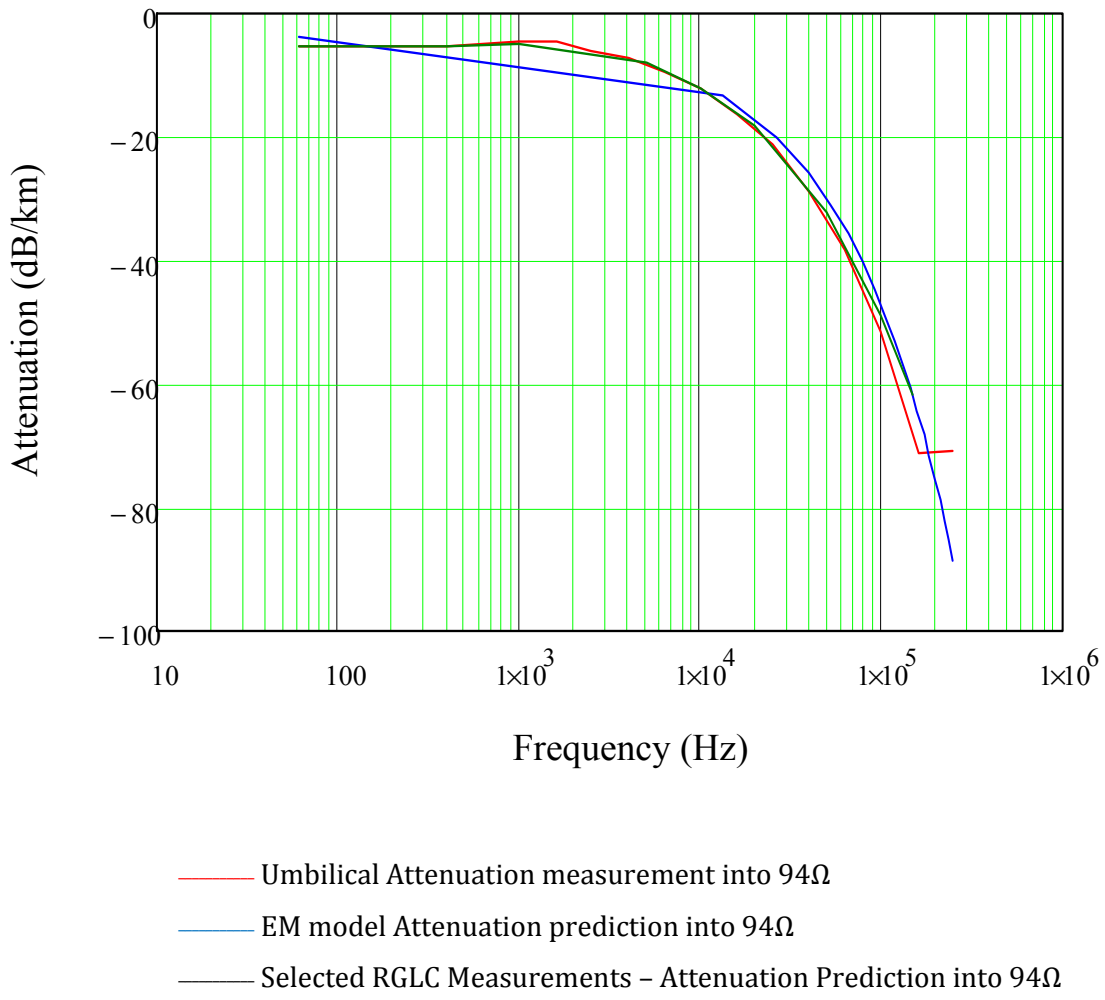

Figure 6-22 Measured and predicted attenuation for core F over 35.8km with adjusted conductance

So it can be seen that on measuring the actual umbilical, due primarily to a poor conductance contribution to the measurements, the attenuation measurements are greater than the theoretical figure. Similarly the pressure vessel measurements are degraded by a poor conductance measurement (albeit closer to the theoretical figures than the full umbilical measurement due to a better test environment) and so again an attenuation prediction greater than the theoretical is seen. When all these are aligned with the FAT conductance measurements on the similar riser umbilical, which has the

highest conductance value of all the measurements (also taken in a poor test environment), the attenuation calculations and measurements now correlate well.

Therefore it can be stated that the measured attenuation is the real figure with the given test equipment in that environment. Better measurement methods and conditions, for example a drier atmosphere, would reduce the measured attenuation and these figures give strong evidence that the predicted RLC figures are good and it is the measurement environment and method and their influence on the measured G that are causing the difference. A perfect test environment and method would give figures much closer to the theoretical, but the adjustment to model the effect of the armouring and the filled hydraulic tubes is verified by these attenuation measurements.

6.6 The effect of screen thickness on cable impedance

In Section 2.5, it was suggested that screen thickness has an impact on cable resistance and it would seem likely that, in the same way that the cable armouring impacts the inductive and resistive parameters of the cable, the material and thickness of the screen could also affect these parameters. Intuitively, it makes sense that the cable capacitance will be modified by the addition of the screen due to the change in the surrounding dielectric material of the conducting cores, however the following measurements from NSW cables in Figure 6-23 shows that the resistance of the cable is also affected by the screen.

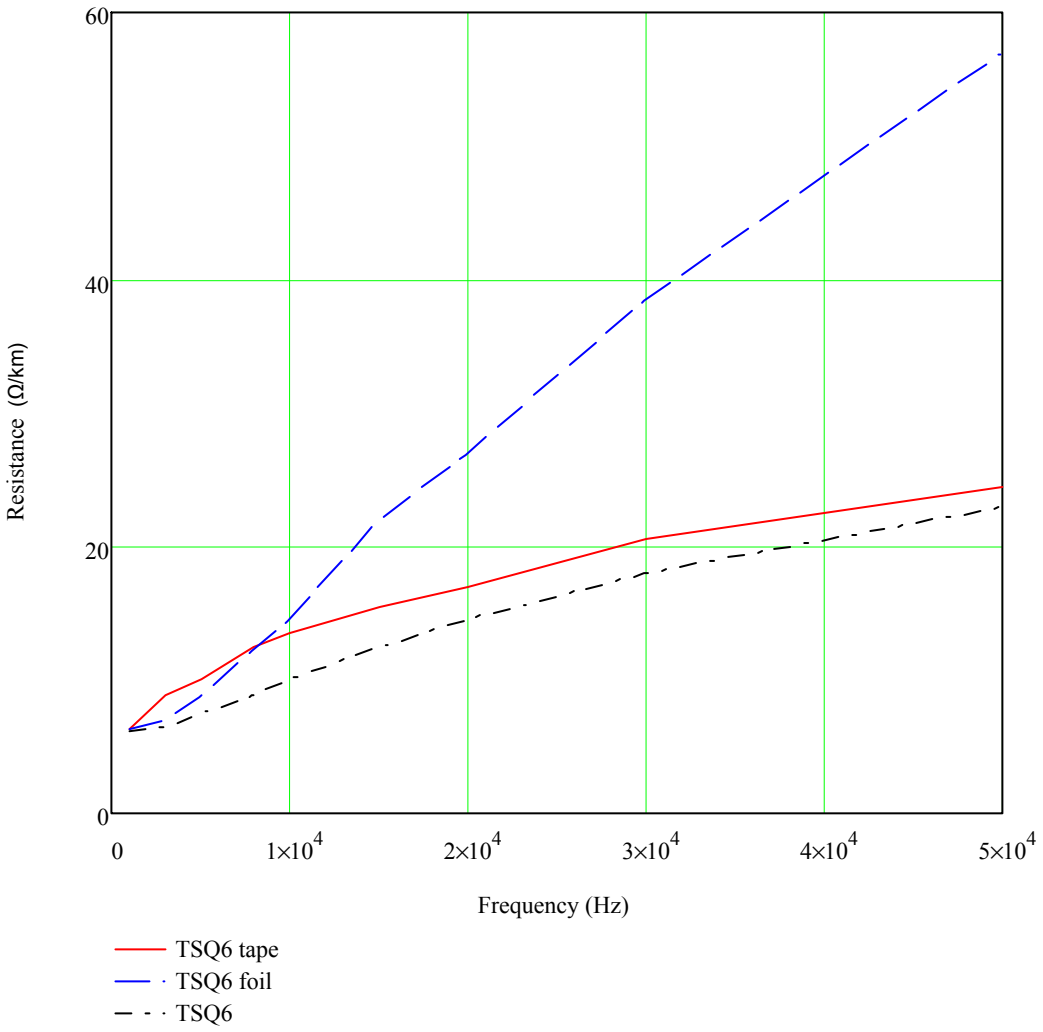

Figure 6-23 Comparison of resistance in various 6mm^2 cables

The effects of power loss in the electrical screen or 'sheath' due to induced currents is well studied with respect to high voltage power cables, as described by Barrett and Anders (2009), Ferkal et al.(1996), Yan Li et al. (2008), but the impact on signal transmission line cables and cables for lower power applications such as used in subsea well control is less well reported.

Figure 6-23 clearly shows the dependency of resistance on screen thickness with the two cable samples' screens being described in the cable specifications as foil and tape, with the foil being the thinner of the two. The graph shows the resistance measured on

a pair of conductors, with the tape screen resistance significantly lower than that on an identical pair with a foil screen. If like materials are being compared, this would appear counter intuitive if this thought is carried through to its conclusion i.e. as the screen decreases towards zero thickness the resistance should be at its highest and from the figures above it is clear that the bare cable resistance is lowest.

As it has now been established that the proximity to steel wire armour has a significant impact on the cable resistance and inductance, it would seem likely that screen material and/or thickness may also impact these parameters.

To see if this effect can be reproduced by modelling, a quad cable with 3.1mm core diameter, polyethylene insulation and copper screen was modelled using Maxwell SV to assess the effect and the data in Table 6-1 was derived.

Frequency	Screen Thickness (mm)	Resistance (Ω)	Inductance (H)	Maximum Magnetic Field Position	Maximum Current Density Position	Max Current Density (A/m^2)
100kHz	0.809	0.024709	3.9384E-7	Outside	Equal	
100kHz	0.409	0.024419	3.938E-7	Outside	Equal	$1.4x10^6$
100kHz	0.2011	0.025366	3.913E-7	Outside	Equal	
100kHz	0.108	0.02931	3.9013E-7	Outside	Equal	
100kHz	0.0495	0.03954	3.9324E-7	Outside	Equal	
100kHz	0.0219	0.058101	4.1118E-7	Equal	Equal	
100kHz	0.0195	0.061271	4.1611E-7	Equal	Equal	$3x10^6$
100kHz	0.013	0.07171	4.4062E-7	Inside	Inside	$3.9x10^6$ screen/core
100kHz	0.008559	0.076996	4.7214E-7	Inside	Inside	
100kHZ	0.00787	0.077206	4.7952E-7	Inside	Inside	
100kHz	0.007	0.077017	4.8731E-7	Inside	Inside	$5.3x10^6$ screen/core
100kHz	0.0045	0.070317	5.229E-7	Inside	Inside	
100kHz	0.0021	0.057473	5.4802E-7	Inside	Inside	$6.6x10^6$ screen/core
100kHz	0.0013	0.042714	5.6255E-7	Inside	Inside	
100kHz	0	0.025483	5.6949E-7	Inside	Inside	

Table 6-1 Series impedance of Quad Screened Cable for a variety of screen thicknesses

It seems that there is a turning point in the calculated resistance; as screen thickness decreases, conductor resistance increases to a maximum at around 0.008mm and then falls off again. Figure 6-24 shows this data.

The graph and Table 6.1 also show where the region of maximum magnetic field strength lies on the quad cable. The hatched area indicates the field maxima are between the core conductors i.e. marked ‘inside’ in the table, while the non-hatched area shows the maxima lie to the ‘outside’ of the quad. At a screen thickness of around 0.02mm, the field lies evenly distributed on both sides of the conductor cores. Similarly the position of the current density maximum is also indicated in Table 6.1

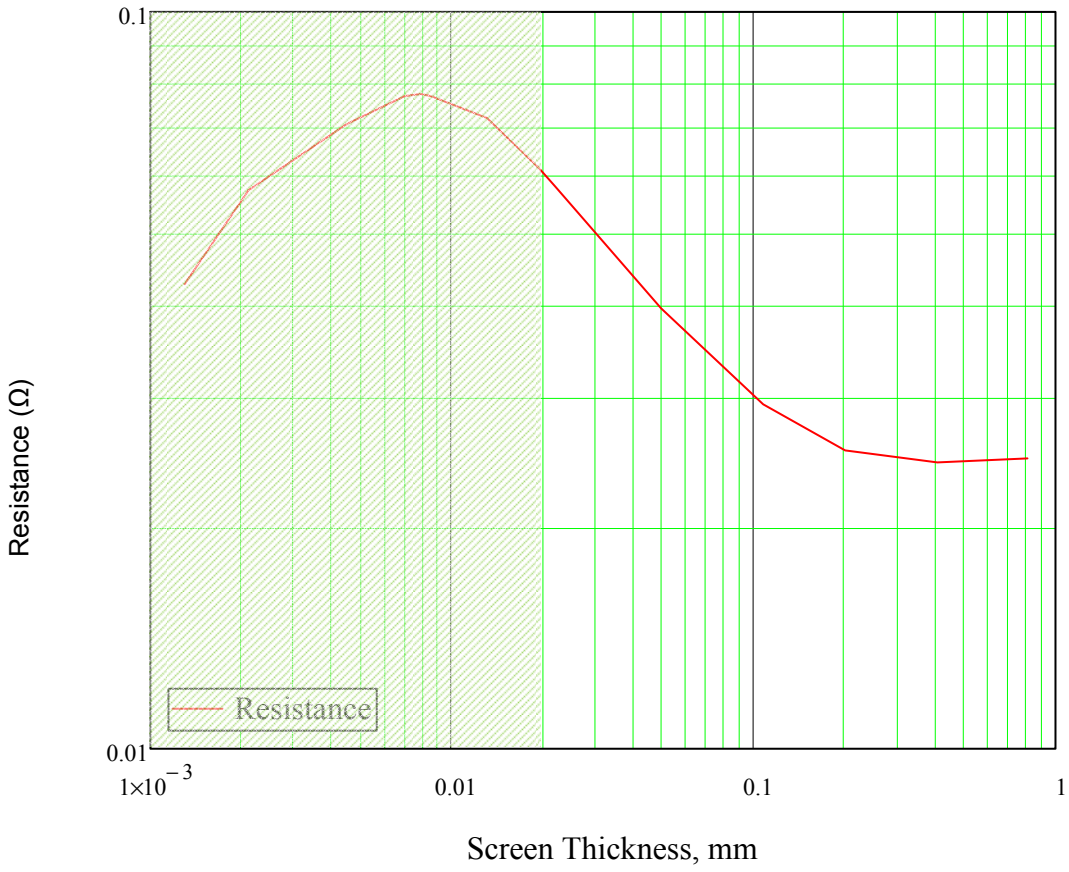

Figure 6-24 Cable resistance and magnetic field position in screened quad cable at 100 kHz

In order to understand this phenomenon, it is helpful to look at the magnetic field plots produced by the model. The plots of Figures 6-21 to 6-38 showing, either the magnitude of the magnetic field strength or current density in a typical quad cable of diameter 14.6mm as indicated, with a variety of screen thicknesses, help to clarify the interaction of several effects. The scale shown on the plots indicates the bands of magnetic field strength in Tesla, or current density in A/m^2 as applicable, with the magnitude indicated by colours of the spectrum, with the highest values in red to lowest in blue.

When the screen is on the 'thinner' side of the resistance turning point, i.e. less than 0.008mm, it can be seen that the magnetic field is skewed to the inner of the conducting cores due to the proximity effect between the conductors, as would be seen

with an unscreened quad. Figures 6-25 and 6-26 show plots of the magnetic field and current density produced by two conductors at 100kHz in a quad with a screen of 0.0021mm.

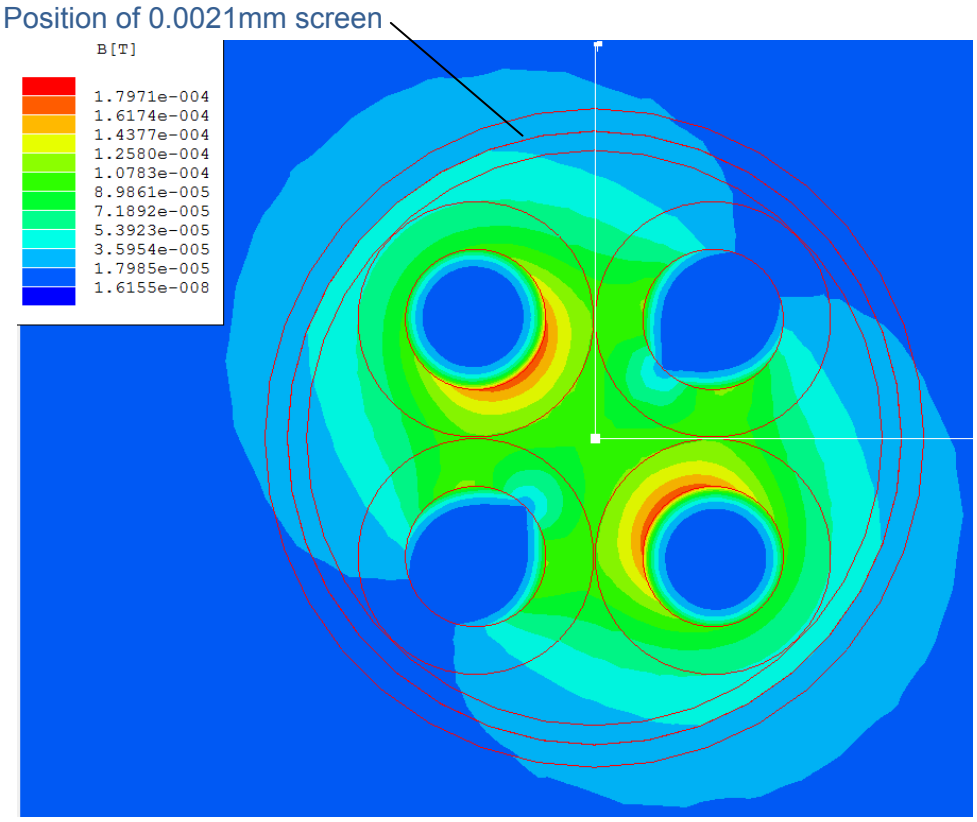

Figure 6-25 Magnetic field distribution in a quad cable with a screen thickness of 0.0021mm

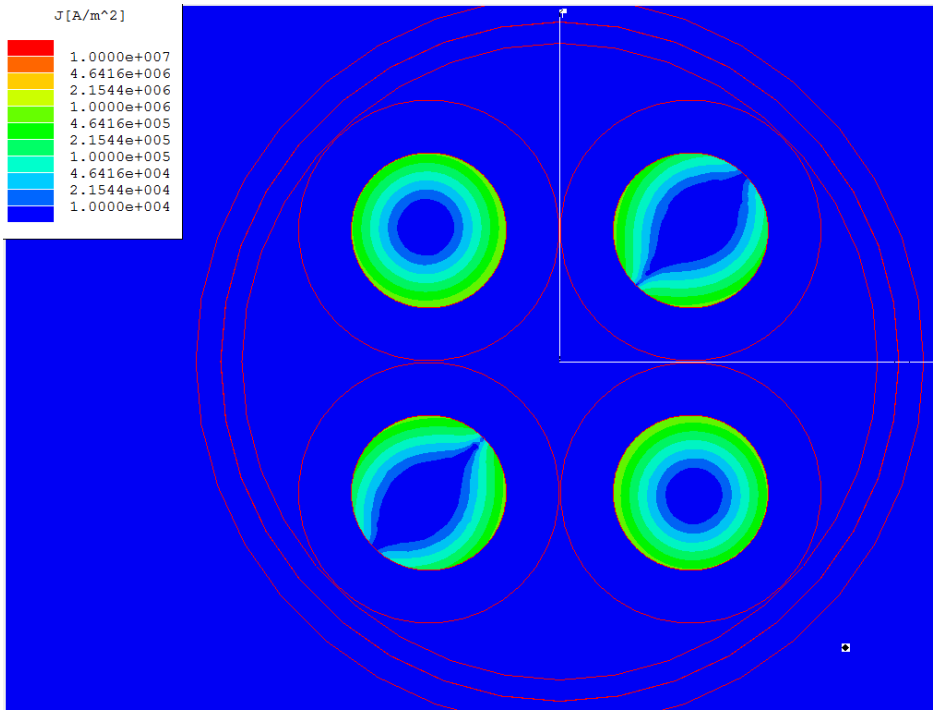

Figure 6-26 Current Density distribution in a quad cable with a screen thickness of 0.0021mm

With the area of screen nearest the conducting cores demonstrating a current density pattern as shown in Figure 6-27:

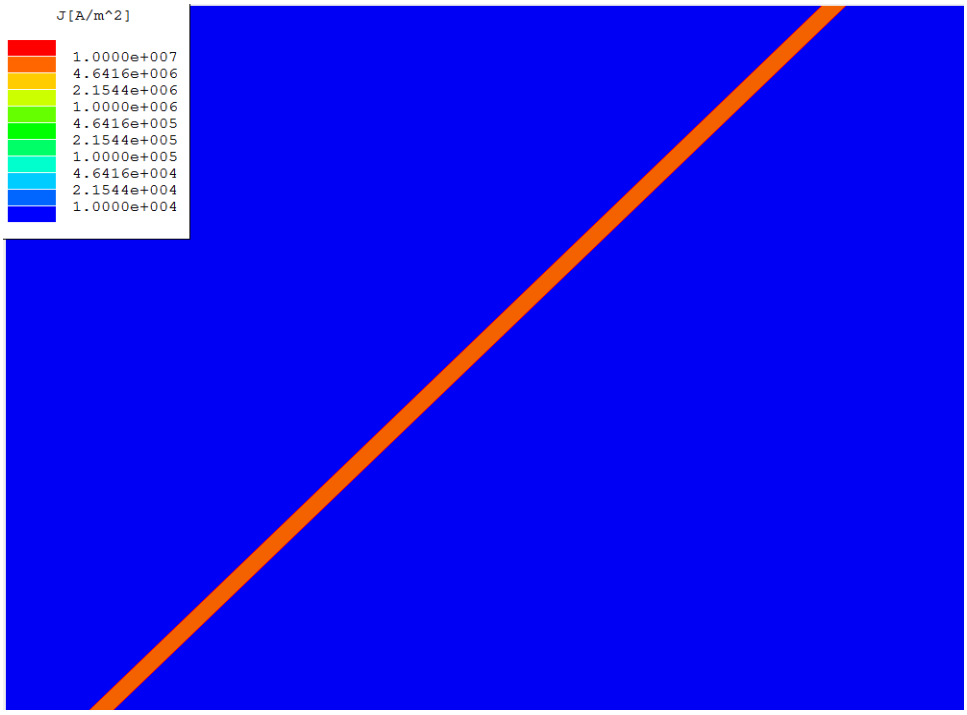

Figure 6-27 Current Density distribution in a 0.0021mm screen adjacent to conducting cores on a quad cable

And nearest the non-conducting cores showing where the current density drops to zero as the induced currents cancel as shown in Figure 6-28

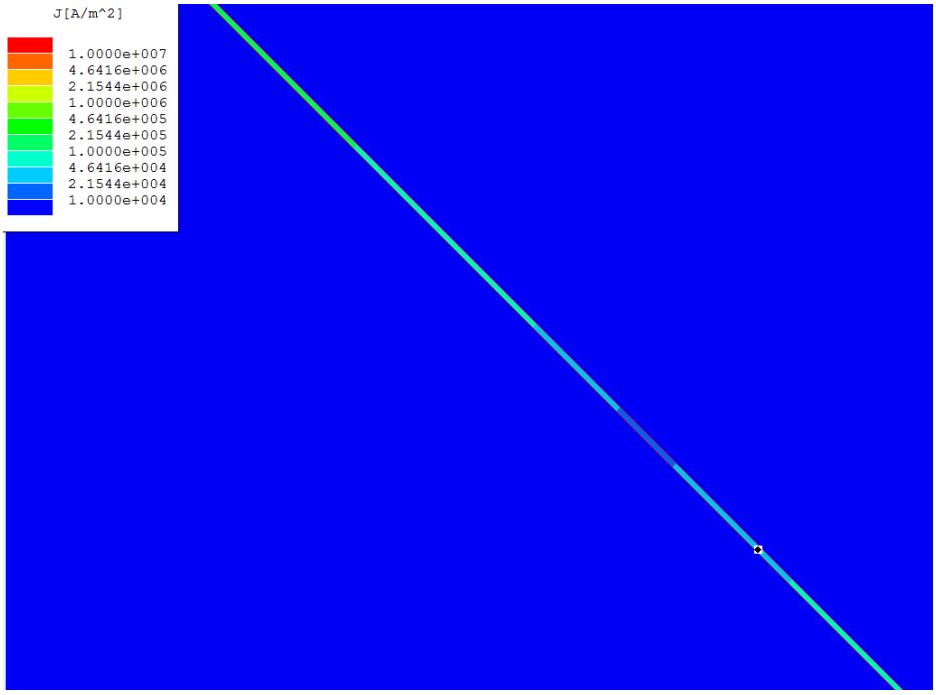

Figure 6-28 Current Density distribution in a 0.0021mm screen adjacent to non-conducting cores on a quad cable

However, when the screen is much thicker than the turning point, say 0.05mm, the magnetic field has now shifted, so that the greater magnitude is to the outside of the cores as shown in Figure 6-29

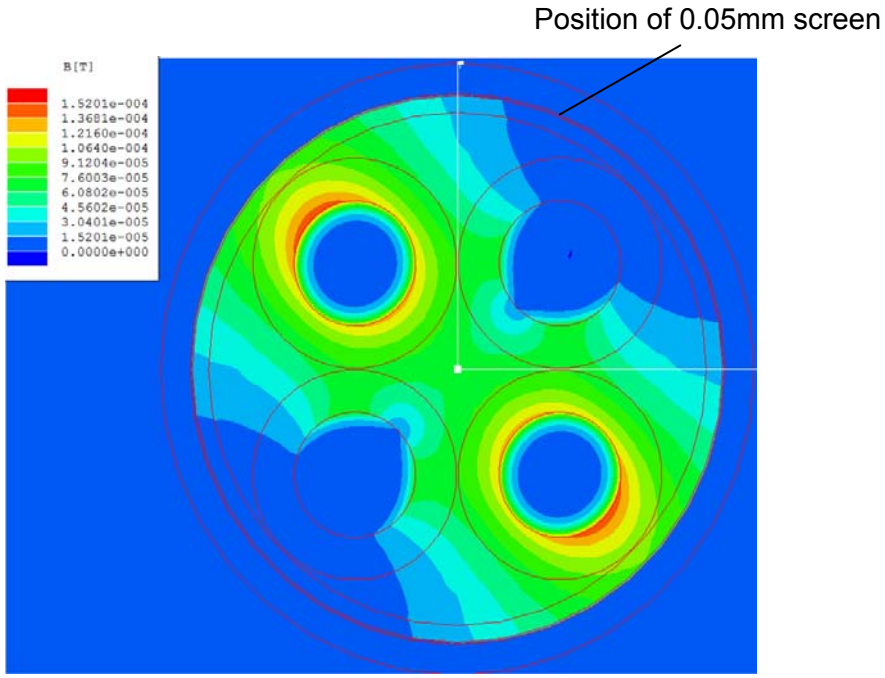

Figure 6-29 Magnetic field distribution in a quad cable with a screen thickness of 0.05mm

With the current density now as shown in Figure 6-30:

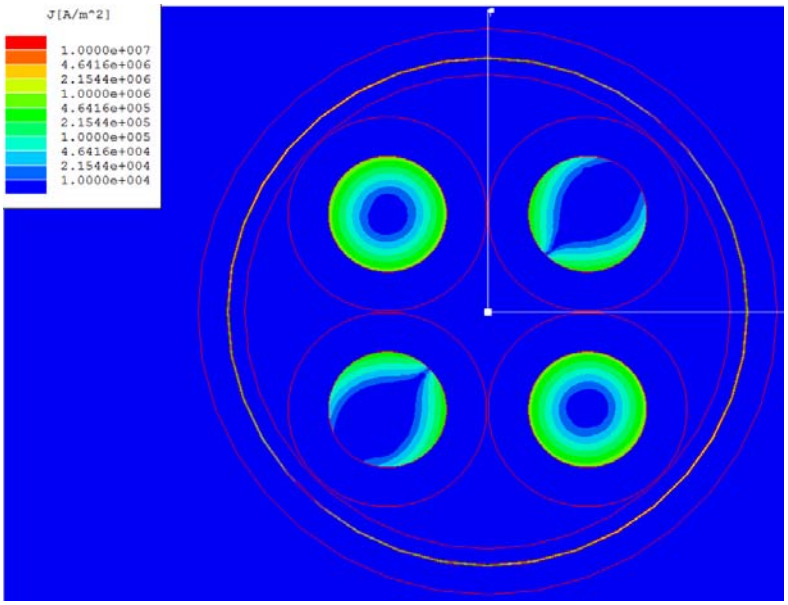

Figure 6-30 Current Density distribution in a quad cable with a screen thickness of 0.05mm

and the current density in the screen shown in Figures 6-31 and 6-32:

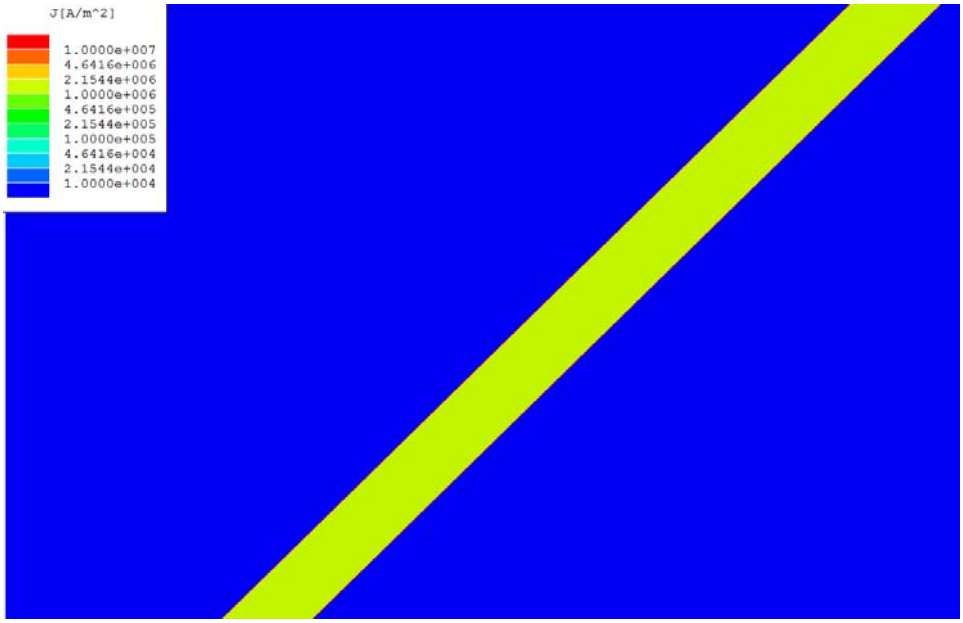

Figure 6-31 Current Density distribution in a 0.05mm screen adjacent to conducting cores on a quad cable

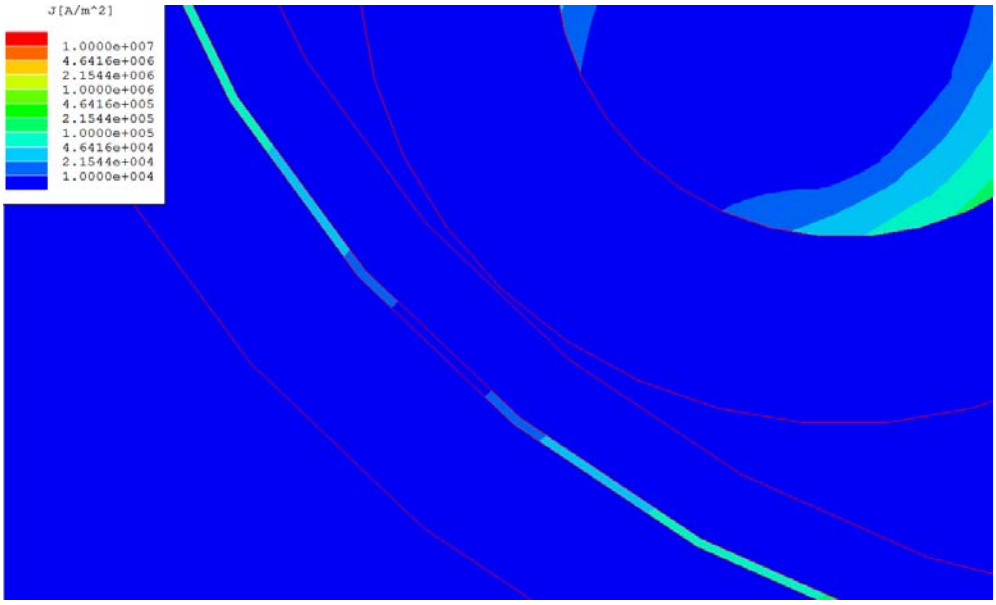

Figure 6-32 Current Density distribution in a 0.05mm screen adjacent to non-conducting cores on a quad cable

The point where the magnetic field appears to be roughly equal on either side of the core is when the screen is around 0.02mm thick as shown in Figure 6-33

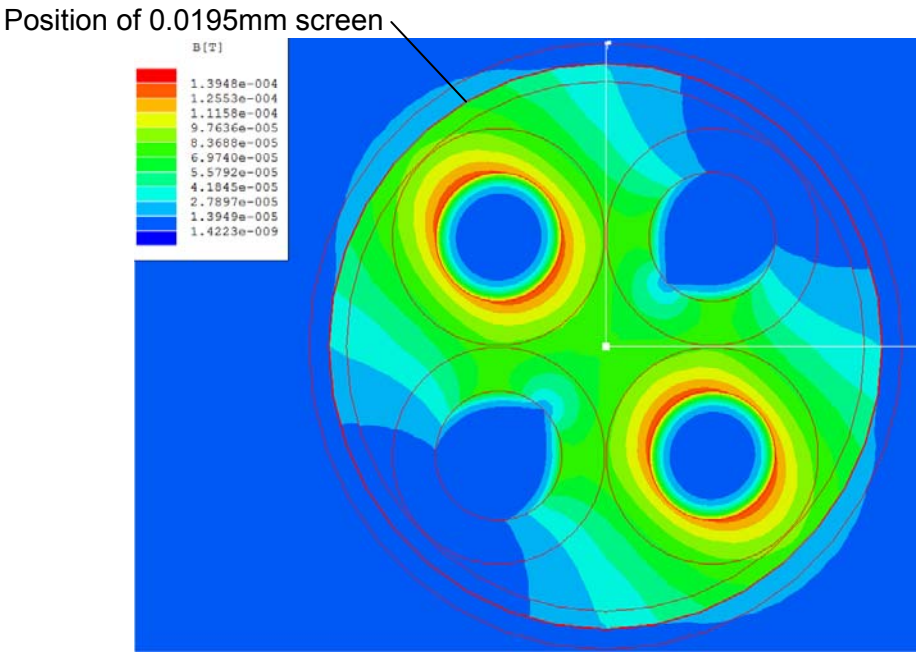

Figure 6-33 Magnetic field distribution in a quad cable with a screen thickness of 0.0195mm

With the current density distribution in the cores shown in Figure 6-34

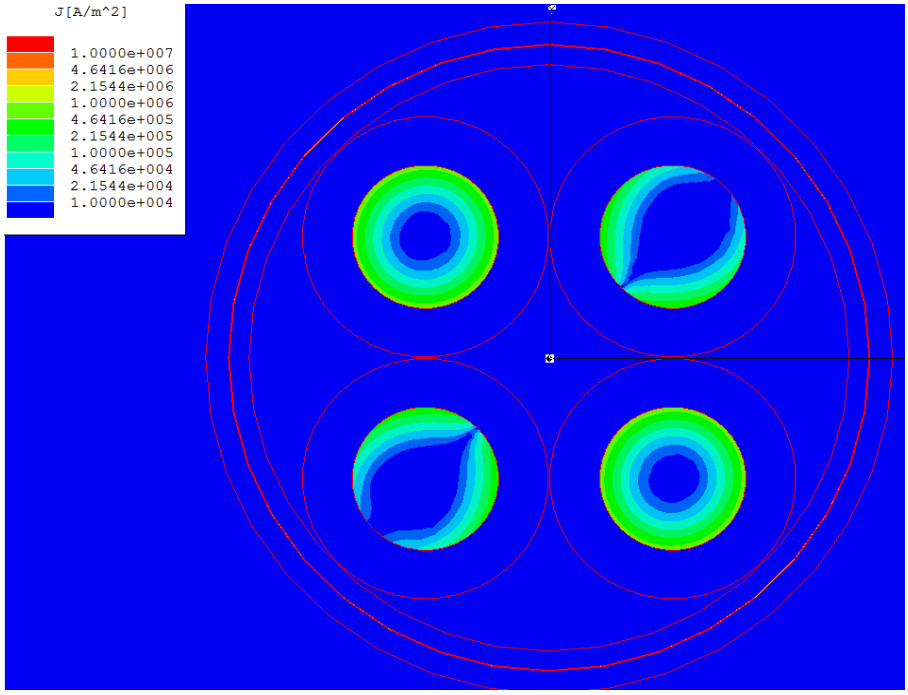

Figure 6-34 Current Density distribution in a quad cable with a screen thickness of 0.0195mm

And in the screen shown in Figures 6-35 and 6-36:

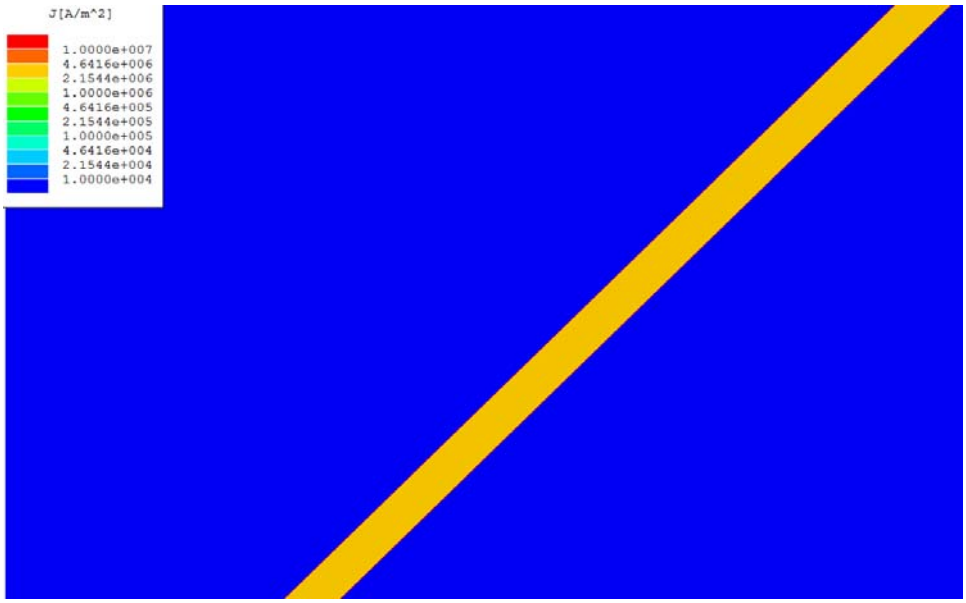

Figure 6-35 Current Density distribution in a 0.0195mm screen adjacent to conducting cores on a quad cable

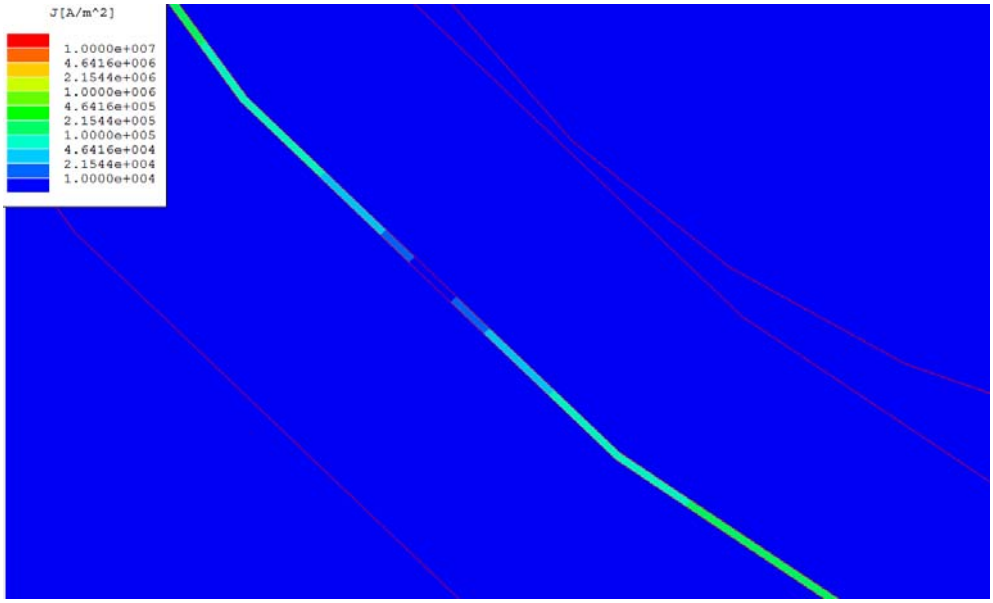

Figure 6-36 Current Density distribution in a 0.0195mm screen adjacent to non-conducting cores on a quad cable

So when the screen thickness is around the 0.02mm point, the field is biased approximately equally between the screen and the adjacent core,

6.6.1 Observations from plots

So it seems there are three operating conditions:

- With the screen between zero thickness up to around 0.008mm, the eddy currents produced in the screen are not sufficient to cause a major magnetic field redistribution although do cause a gradual increase in the conductor resistance due to induced eddy currents. Here the field pattern is similar to that with no screen, when proximity effect between the conductors causes a redistribution of the field and current density in the conductors.

- On the other hand, when the screen is relatively thick, greater than 0.02mm in the example and the eddy currents induced in the screen become more significant, then as these eddy currents modify the conduction properties of the

cores, the proximity effect to the screen becomes the dominant effect (other than skin effect) on the current distribution pattern in the core causing the current to skew towards the screen.

- Somewhere in between these two conditions there is a turning point where, now, as the eddy currents in the screen modify the conduction properties of the cores, the proximity effect to the screen and between the cores is of equivalent strength.

It seems then that the resistance turning point occurs when the copper screening material is around 0.008mm thick but at this thickness as shown in Figures 6-37 and 6-38, the magnetic field and area of maximum current density are still located primarily between the conductor cores. The field crossover point, when the field moves to the outside of the conductors, does not coincide with the point of maximum resistance of the conductors and happens when the screen is considerably thicker, around 0.02mm.

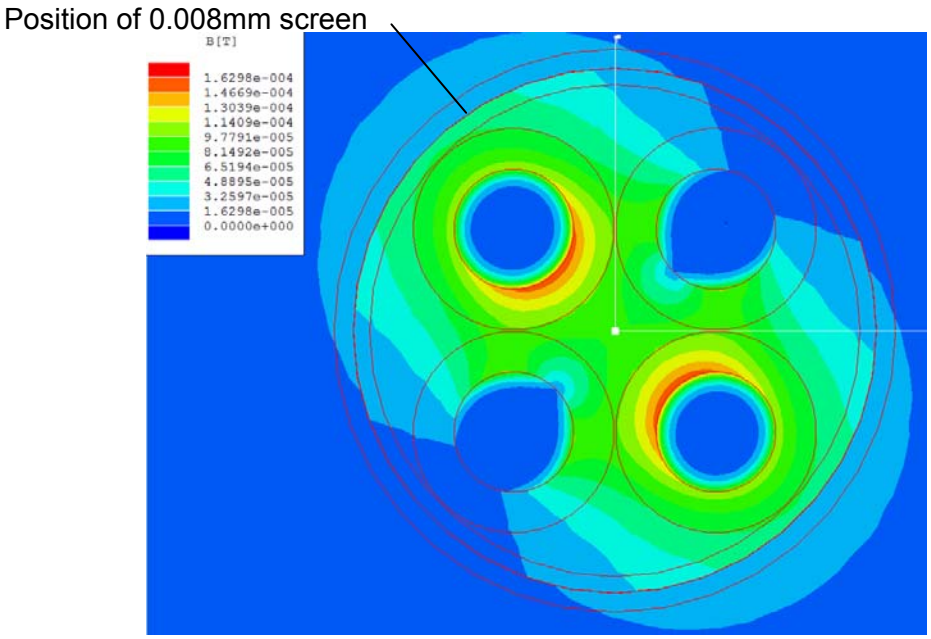

Figure 6-37 Magnetic field distribution in a quad cable with a screen thickness of 0.007mm

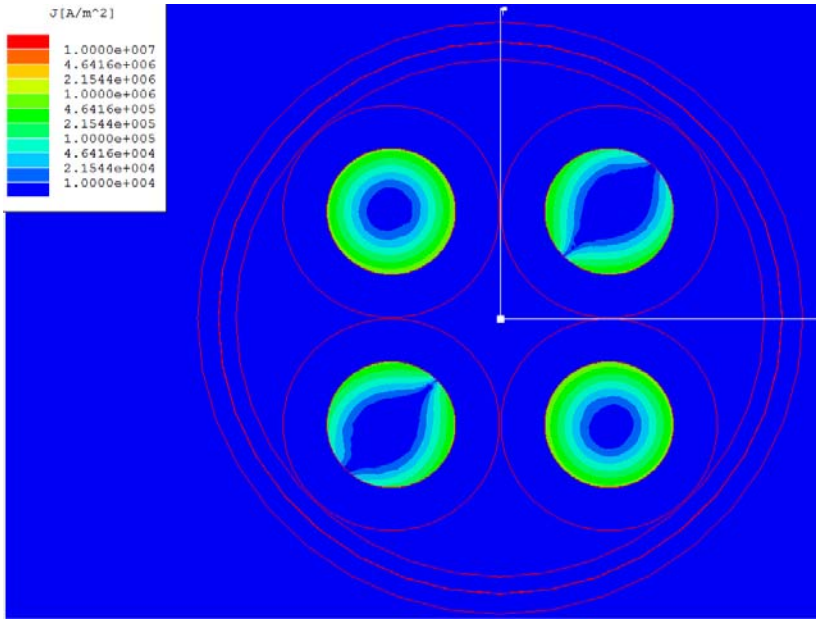

Figure 6-38 Current Density distribution in a quad cable with a screen thickness of 0.008mm

6.6.2 Explanation of Screen effect

It seems there are three effects acting simultaneously and, to some extent, in opposition here.

- Eddy currents induced in the screen in turn produce their own field opposing the flow of current in the core conductors and increasing core resistance
- As the screen thickness increases and its resistance decreases, the induced eddy currents for a given field strength will increase.
- However at the same time as the screen thickness increases and the resistance between any two points decreases, eddy currents produced in the screen at the 'diagonally opposite' current carrying conductors of the quad, are 'short circuited' by the screen in the area of the non-current carrying conductors, this 'shorting' being more effective as screen thickness increases.

To sum up then, it can be seen that the opposing field acting on the conductor cores and increasing the resistance is proportional to the induced eddy current (higher with thicker screen) and inversely proportional to the current flowing round the screen (lower with thicker screen). As the screen thickness increases, the induced eddy currents also increase, increasing the resistance in the core conductors, however this is counteracted by the screen's decreasing resistance and its shorting of the eddy currents round the screen diameter. As such, there is a crossover point in the increase of the core resistance caused by the induced eddy currents.

Similarly with no screen, or very thin screens, the opposite polarity of the signals in the conductors causes the current density to skew such that the adjacent sides of the conductors carry the greater part of the current.

6.7 Chapter Conclusion

In this chapter an analysis of the results from modelled predictions of the impedance parameters of the cable and measurements made on short lengths were shown to give consistent results. Also, these modelled and measured impedance parameters are shown to give excellent predictions of the umbilical attenuation when compared with the figures measured on the 35.8km and 55.2km umbilical lengths examined.

Additional models were used to examine the effects of screen thickness on the cable impedance parameters and an explanation for this unexpected phenomenon is presented. Chapter 7 suggests some areas for future work to further explore some of the subsequent issues that have arisen during this research, while Chapter 8 concludes this thesis by addressing the research goals set out at the beginning of this thesis in Section 1.3.

Chapter 7. Future work

While the effects of umbilical construction, flooding and pressurising have been both modelled and measured and the results show close correlation, there are inevitably some further questions raised which are worthy of further investigation if we are to obtain a more precise understanding of the effects of subsea umbilical deployment in all its potential applications. Because, from what has observed in this research regarding the longevity of the ageing effects on the cables, it is likely that further study into the effects on cable impedance from water, hydraulic and chemical fluids and the physical distortion seen from the application of pressure may require significant study periods, so some of the suggested follow on work could well have to form part of ongoing studies, and research could extend to months or even years of analysis.

7.1 Hydraulic Fluid Properties

Both the electromagnetic model and the final umbilical measurements were carried out with the adjacent hydraulic hoses filled with a water based fluid. While, in the project, being studied, this was correct and appropriate, there are also many other hoses employed within the subsea umbilical carrying fluids such as Scale Inhibitor, Corrosion Inhibitor and Methanol amongst others, which are carried subsea to ensure a good flow of the recovered hydrocarbons and extend the operational life of the components. The effects of these other types of fluids on the electrical properties of the cables was not assessed in this research and the results from such a study would provide valuable input to improving the broader relevance of the models in all subsea applications.

7.2 Cable Construction

The bulk of this research considered the electrical effects of pressure, water and umbilical construction on the quad cable with polyethylene jacket as most commonly used for the oil industry subsea control systems. There are however, other types of cables used subsea: twin cables are used, for example, for dedicated communications cables; triad cables are also used often for carrying three phase power; subsea high voltage cables are constructed with a copper sheath surrounding each core to control emitted fields and some quad cables are themselves surrounded with steel wire armour to improve strength. These different cable constructions would be expected to react differently to the effect of pressure and flooding and a study of these effects would be of use in a great deal of applications and industries outside those studied in this research.

7.3 Further Examination of the Effect of Pressure on Impedance

As shown in Section 6 and highlighted particularly in Figures 6.13 and 6.16, the effect of pressure on the impedance parameters was not always as expected, however due to the costs involved in testing and in the delaying of deployment, additional measurement was not possible as part of this research. A further, more detailed examination of these effects would be extremely valuable to ascertain whether the unexpected results seen were the result of measurement error or whether in fact some other additional effect was at work during these measurements.

7.4 Elastic Overshoot

In some cases, there was observed what appeared like an overshoot when pressure was released from the tested cables. The impression was that, after compression under pressure, when the pressure was released, the cable expanded to an extent beyond the initial dimensions. It is anticipated that the restoration time would depend

on a multitude of factors so in order to gain a more complete understanding of this result, further study into these effects would be required and this would need to cover issues such as:

- cable jacket materials,
- construction i.e. quads, twins, screened, armoured type cables
- core cross section, i.e. 4mm^2, 10mm^2 etc.

In addition, it would be valuable to know whether there also will come a point where the cable is compressed beyond its elastic limit and restoration to original dimensions is no longer possible. What then would be the effect on impedance and the susceptibility to water ingress is crucial information if cables are to be deployed for any length of time in high pressure environments.

7.5 Screen Impact on Cable Design

Results observed during the testing and presented in section 6.6 highlighted a dependency of cable impedance, in particular the resistance and inductance, on the thickness of the cable screen. Results showed that, depending on the cable's physical construction, cable impedance could be significantly increased at a particular frequency, by design of the cable screen. These results suggest the possibility of optimising cable design for particular applications and frequencies, and further work in this area would certainly be worthwhile.

7.6 Water Treeing

Although Water Treeing is an area of ongoing research, particularly within the power industry where, with the ever growing number of offshore wind farms, the deployment subsea of power cables is increasingly common, a study of the specific impact of water trees on oil industry subsea control system umbilicals would still be of significant interest. As mentioned in 7.1, the umbilical cores carry many fluids and as these are

frequently deployed in thermoplastic hoses, the imperviousness of these is not necessarily perfect. An assessment of these chemicals' effects on the electrical properties of adjacent cores' jackets with time, and whether there is any impact on the rate of growth of water trees, would be extremely valuable information as distances and depths increase, as we are already aware that pressure has a major impact on the growth of trees.

Chapter 8. Conclusions

The overarching aim of this research was to model and understand the issues affecting subsea umbilicals in their use for electrical communications and how construction and deployment affect performance. Specifically, the subsidiary goals of the research, to be examined by measurement, modelling and comparison were

- **To model and elucidate the effect on the cable distributed electrical impedance of adjacent conductors, screens and umbilical steel wire armouring;**
- **To understand the effect on the cable distributed electrical impedance when the umbilical is flooded with sea water;**
- **To understand the effect on the cable distributed electrical impedance when the umbilical is deployed subsea and under pressure.**

8.1 The effect on subsea umbilicals in their use for electrical communications of construction and deployment

The answer to the primary research goal is established by tests and models carried out for the secondary questions. These test and calculations provide the following conclusions:

The effect of the surrounding metallic materials in an umbilical can cause a significant increase to the resistance and inductance of the cables. Even the adjacent copper conductors in a quad cable will cause additional losses.

The effect of surrounding fluids, whether sea water from flooding or that carried in thermoplastic hoses or other tubing, is to increase the capacitance and conductance in line with the change in dielectric properties of the water. The pressure chamber measurement results, showed an increase in the capacitance over 20%. The measurements made in the tank showed an even greater increase, of around 40%.

The pressurising of the cable will increase capacitance due to the reduced separation between the conductors, however resistance, inductance and conductance all showed a slight reduction by the application of pressure.

A good electromagnetic model is essential if an accurate prediction of the subsea cable loss is to be derived. This must be based on a good knowledge of all the operating parameters and materials, so as well as the dimensions of the cable being utilised for the subsea power and communications, the following also have a significant impact on the cable loss:

- Flooding of the umbilical with sea water
- Depth of deployment and applied pressure
- Location of conductors relative to steel wire armour and/or hydraulic steel tubes
- Location of conductors relative to hydraulic hoses
- Thickness and material of cable screens

8.1.1 The effect on the cable distributed electrical impedance of adjacent conductors, screens and umbilical steel wire armouring

The umbilical contains hydraulic tubes, steel wire armour, additional cables, copper screening as well as methanol, hydraulic fluid and various other fluids such as scale inhibitor and even crude oil. The tests carried out in this research showed clearly that

the resistance and inductance are both affected significantly by the proximity of metallic materials however in the main, the fluids have little effect on these parameters. On the other hand, fluids in the adjacent pipework do have a significant effect on capacitance and conductance.

The EM models provide us the means to accurately model the cable parameters in the various physical constructions of the umbilicals with armouring and filling of hoses all modelled with good accuracy.

The EM modelling establishes some principles that we generally observe to be true in the measurements:

1. Since the dielectric constant and loss tan are virtually independent of frequency (below 1 GHz), the capacitance will be constant and the conductance proportional to frequency over our frequency range of interest.

2. The armour only has any real impact on inductance at very low frequencies, below about 100Hz. An increase in L of about 12% at 60 Hz was seen for test case F with the quad in proximity to the armour.

3. Inductance has the highest values at the lower frequency range as the skin effect is reducing the inductance value as frequency increases

4. Resistance, representing the losses in all conducting bodies, increases proportionally to the square root of frequency due to skin effect.

There are two important input parameters of the EM modelling that are very difficult to define: conductivity of the water and permeability of the steel. From the results of measurements, it appears that the water used in the pressure vessel experiment had very low conductivity so the addition of water to the vessel has virtually no effect on the resistance and inductance as only through eddy currents can the water influence these.

The other parameter of interest, permeability, has a significant effect on resistance and inductance and since the exact copper and steel properties of the objects modelled were unknown, estimates of the magnetic characteristics using typical values were used. This, and the fact that, for practical reasons, only a section of armouring adjacent to the cores being analysed was modelled, are certainly possible causes for any discrepancy seen with the measured results.

8.1.2 The effect on the cable distributed electrical impedance when the umbilical is flooded with sea water

When the umbilical is deployed and fills with sea water, the change to the cable impedance is marked.

There is an immediate increase in capacitance in the order of 20 to 30% due to the change in the dielectric properties of the surrounding materials. This was shown clearly by both the tests in the pressure vessel and with the sample cable submerged in sea water and was reflected by the results of the EM model which showed a capacitance increase by the introduction of sea water to the adjacent hoses. In a similar way both the pressure chamber measurements and EM model showed an increase in conductance due to the change in surrounding dielectric material of the cables. It is clear that to properly model the cable loss in a subsea environment, this additional loss must be anticipated and an electromagnetic modelling tool, such as the Optem or Ansoft software used for this research, used to derive realistic impedance predictions.

8.1.3 The effect on the cable distributed electrical impedance when the umbilical is deployed subsea and under pressure

The expected physical implications of the application of pressure would be to cause a compression of the cable, thereby bringing the cores closer to each other. If this is the case though, measurements were not always as would have been expected.

1) A decrease in resistance was seen by the application of pressure to the cable in the pressure vessel. This was contrary to the effect anticipated as it was expected that, as the cores were brought closer together by the application of pressure, the greater effect of the core currents on each other would cause an increase in the measured resistance. It was notable, also, that the resistance returned to a value beyond the original, implying some kind of elastic overshoot effect in the cable material. More work would be needed to ensure a full explanation.

2) There was a reduction in inductance due to the reduced separation between the cores and therefore in the overall loop area. It is notable that the inductance also returns to a value beyond the original value again implying some kind of elastic overshoot effect in the cable material. More work would be needed to ensure a full explanation.

3) Measurements showed an increase in capacitance due to the reduced core separation, this time however showing a return to very close to the original value. This would imply the cable has restored to its original dimensions. If this had followed the pattern of the resistance and inductance, a final value below that at the start of the tests, would have been seen, suggesting no form of elastic overshoot is taking place.

However it maybe that the measurements are erroneously high if, for example as the cable had been withdrawn from a water filled pressure vessel, the cable was not entirely dry when the final test was carried out thereby causing a slight increase in the measured capacitance.

4) The effect of pressure on conductance was also not as expected. A decrease in conductance was seen in the pressure measurements, whereas the anticipated effect of a reduction in the core separation due to pressure would be an increase in the conductivity between the cores. On removal from the vessel, measurements slightly above those on the floor at the start of the test were seen. This would be consistent with a small amount of elastic overshoot as the cable returns to a point slightly beyond its original dimensions.

8.2 The effect of cable screen

The incorporation of a screen on a cable has a significant impact on all the impedance parameters of a cable. It was seen that, not only is the capacitance increased by the proximity of the conductive wrapping, but that this additional path of coupling between the cores also has a significant impact on the resistance and inductance of the cable.

References

1. AB Sandvik Materials Technology (2010) Umbilical Tube Product Data, http://www2.sandvik.com/sandvik/0140/internet/se01265.nsf/(DocumentsInternetWeb)/D935FE274C96588D05256793006FE26E, 14/09/2010, first accessed 5th February 2013

2. Aker Solutions (n.d.) Subsea Control Systems Product Data, http://www.akersolutions.com/Documents/Subsea/Brochures/Subsea_controls_systems_low%20res.pdf, first accessed 23rd January 2013

3. Aker Solutions (2013), Vertical Subsea Tree Product Data, http://www.akersolutions.com/en/Global-menu/Products-and-Services/technology-segment/Subsea-technologies-and-services/Subsea-production-systems-and-technologies/Subsea-trees/Vertical-subsea-tree/, first accessed 24th January 2013

4. Angoulevant O. (2010) Transmission, Grid Connection and cabling solutions, (first published 15th March 2010) Presented at conference - Offshore Wind China 2010, Shanghai 7th to 9th of June,

5. Arnold A.H.M. (1941) Proximity effect in solid and hollow round conductors. IEE Journal of Power Engineering vol 88 no 4 part II pp 349-359

6. Barber K W, Marazzato H (2005), Reliable undergrounding of electricity supply in Asia. Asia Pacific Conference on MV Power Cable Technologies. 6-8 September 2005

7. Barret J S, Anders G J (1997), Circulating current and hysteresis losses in screens, sheaths and armour of electric power cables mathematical models and comparison with IEC Standard 287. IEE Proceedings – Science Measurement and Technology; May, 1997; 144; 3; p101-p110

8. Bertmand T.(2003), Ormen Lange Long Distance Subsea Monitoring and Control From Shore The Remote Monitoring Conference, 4.November 2003 http://nugrohoadi.files.wordpress.com/2008/04/ormen-lange.pdf, 4th Nov 2003 p 18), first accessed 23rd January 2013

9. Burns B (2009), History of the Atlantic Cable & Undersea Communications. http://atlantic-cable.com/Cables/1947Anglo-Dutch/index.htm, first accessed 1st Feb 2011.

10. Chai G, Kivisäkk U, Tokaruk J, Eidhagen J, (2009), Stainless Steel World March 2009, http://www.stainless-steel-world.net/pdf/SSW_0903_SANDVIK.pdf first accessed 5th February 2013

11. Ciuprina F, Teissèdrea G, Filippinia J, Notingher P, Campusb A, Zaharescuc T (2004) Water treeing in chemically crosslinked polyethylene, Journal of Optoelectronics and Advanced Materials Vol. 6, No. 3, pp.1077 - 1080

12. Cristina S., Feliziani M. (1989) A finite element method for multiconductor cable parameter calculation. IEEE Transactions on Magnetics Vol 25 no 4, pp 2986-2988

13. Czaszejko T (1998), Statistical Analysis of Water Tree Lengths. Conference Record of the 1998 IEEE International Symposium on Electrical Insulation, Arlington, Virgina, USA, June 7-10, 1998, pp. 89-92

14. Douglas N. (n.d.), Snøhvit development employs subsea-to-beach long-offset control system, http://www.offshore-mag.com/articles/print/volume-66/issue-2/subsea/snoslashhvit-development-employs-subsea-to-beach-long-offset-control-system.html, first accessed 23rd January 2013

15. Dwight H. (1923) Proximity effect in wires and thin tubes. American Institution of Electrical Engineers Journal Vol 42 no 9 pp 961-970

16. Egiziano L., Vitelli M. (2004) Time domain analysis of proximity effect current driven problems. IEEE Transactions on Magnetics Vol. 40 no 2 part 1 pp 379-383

17. Ferkal K, Polouadoff, M, Dorison, E. (1996) Proximity effect and eddy current losses in insulated cables. IEE Transactions on Power Delivery, Vol11, No3, pp 1171-1178

18. GE Vetco (n.d.) Subsea Controls & Informatics Product Data, http://www.ge-energy.com/content/multimedia/_files/downloads/Subsea%20Controls%20%26%20Informatics.pdf, page 5, first accessed 24 Jan 2013.

19. Hai V T, Thank N D (2006), Final Breakdown on Water Tree Degrade Polymer Insulation, Advances in Natural Sciences, Vol. 7, No. 1&2 (2006) (57 – 61)

20. Hvidsten S, Floden R, Olafsen K, Lundegaard L, Melve B, (2005), Long Term Electrical and Mechanical Properties of XLPE Cable Insulation System for Subsea Applications at Very High Temperatures. Annual Report Conference on Electrical Insulation and Dielectric Phenomena; 2005, CONF 2005:265-268

21. IEEE GHN (2012), http://www.ieeeghn.org/wiki/index.php/Oliver_Heaviside, first accessed 8th September 2012

22. ISO 13628-5 (2009) Petroleum and natural gas industries -- Design and operation of subsea production systems - Part 5: Subsea umbilicals

23. Johnson, H.W. Graham M. (2003) High speed signal propagation: advanced black magic. Prentice-Hall ISBN 0-13-084408-X

24. Joseph (2010), http://residualanalysis.blogspot.co.uk/2010/02/temperature-of-ocean-water-at-given.html (13th April 2012) with data derived from http://apdrc.soest.hawaii.edu/projects/Argo/data/gridded/On_standard_levels/Ensemble_mean/1x1/m00/index.html, first accessed 13th April 2012.

25. Kane M., Auriol P.(1994). Analytical modelling of frequency parameters of lines. IEEE 2nd International Conference on Computation in Electromagnetics pp 239-242

26. Kaye and Laby, National Physics Laboratory, Tables of Physical & Chemical Constants, (2012) www.kayelaby.npl.co.uk/general_physics/2_6/2_6_5.html, first accessed 10th April 2012

27. Lago A, Penalver C, Marcos J, Doval-Gandoy J, Melendez A N et al. (2009), Geometric Analysis and Manufacturing Considerations for Optimizing the Characteristics of a Twisted Pair. IEEE Transactions on Electronics Packaging Manufacturing, Vol 32 No1, pp. 22-31

28. Lesurf J (2009) , Skin Effect and cable impedance, http://www.st-andrews.ac.uk/~jcgl/Scots_Guide/audio/skineffect/page1.html, first accessed 12th August 2009

29. Matsushima A, Nakama S, Shiomi K, Ishiguma M (1999), Numerical analysis of ac effective resistance of a set of conducting circular cylinders using integral equations. Electronics and Communications in Japan Part 2 Electronics, Volume: 82 Issue: 7 Pages: 1-8, JUL 1999

30. Miyashita T, Deterioration of Water-immersed Polyethylene Coated Wire by Treeing", Proceedings 1969 IEEE-NEMA Electrical Insulation Conference, Boston, September, pp. 131-135, 1969

31. Murgatroyd P.N. (1989) Calculation of proximity losses in multistranded conductor bunches. Proc. IEE A - Sci. Meas. Technol., vol. 136, no. 3, pp. 115–120

32. Xi Nan., Sullivan C R (2003) An improved calculation of proximity effect loss in high frequency windings of round conductors. IEEE 34th Annual Power Electronics Specialist Conference PESC '03 Vol 2 pp 853-860

33. Xi Nan., Sullivan C R (2005), An equivalent complex permeability model for litz-wire windings. Industry Applications Conference, 2005. Fourtieth IAS Annual Meeting. Conference Record. Volume: 3 pp: 2229 - 2235

34. New England Wire (2012), http://www.newenglandwire.com/catalog/page129-litz-winding_wires-litz_wire_types-type_1-type_2-type_3-type_4-type_5-type_6-type_7-type_8.htm, first accessed 5th September 2012

35. Nilsson S, Hjertberg T, Smedberg A (2010) The Effect of Different Type of Crosslinks on Electrical Properties in Crosslinked Polyethylene. 2010 International Conference on Solid Dielectrics, Potsdam, Germany, July 4-9, 2010

36. NORSOK Standard (1995), Common Requirements Subsea Production Control Umbilical, U-CR-006 Rev. 1, January 1995

37. Ozaki T, Ito N, Sengoku I, Kawai J, Nakamura S (2001) Changes of Capacitance and Dielectric Dissipation Factor of Water-Treed XLPE with Voltage. Proceedings of 2001 International Symposium, pages 451 - 462

38. Paul C. (1994), Analysis of Multiconductor Transmission Lines, 2nd edition, Wiley - IEEE Press, ISBN 978-0470131541

39. Platbrood G, Hennuy B, Tits Y, Sutton S J (2009) Water Trees in Medium Voltage XLPE Cables: Comparison of Different Polyethylene Insulation Using Short Time Accelerated Ageing Tests. 2009 Annual Report Conference on Electrical Insulation and Dielectric Phenomena

40. Proserv (2013), Subsea Product Data, Proserv's Subsea Control Module, http://www.proserv.com/modules/xnews/article.php?storyid=992, first accessed 24 Jan 2013

41. Ramo, S, Whinnery, J.R, Van Duzer, T (1994) Fields and waves in communication electronics. Wiley ISBN 0-471-81103-3

42. Rocha P, Lima A, Carneiro (Jr) S, Propagation Characteristics and Overvoltage Analysis on Unconventional Submarine Cables, International Conference on Power Systems Transients (IPST'07) Lyon, France on June 4-7, 2007

43. Rossmanith H, Doebroenti M, Albach M, Exner D (2011), Measurement and Characterization of High Frequency Losses in Nonideal Litz Wires. IEEE Transactions on Power Electronics Vol 26, No 11, November 2011, pp3386-3394.

44. Sarkar A, Easter M, Temple W, Walcott E, Smith J T (2010) Effect of Ethylene Content on Bowtie Trees and Wet Electrical Performance in Filled EPR Insulation Materials. Conference Record of the 2010 IEEE International Symposium 2010, pages 1 to 6

45. Shackleton D, Abib L, Balena R, (2007), Electrical and Thermal Design of Umbilical Cable, 7th International Conference on Power Insulated Cables – Jicable, 2007, Versailles, France

46. Smith G.S, Nordgard J.D (1980). On the design and optimisation of the shielded pair transmission line. IEEE Transactions on Microwave Theory and Techniques vol MTT-28 (8) pp 887-893

47. Stancu C, Notingher P V, Notingher P, Castellon J, Agnel S, Toureille A (2009) Computation of the Electric Field in Cable Insulation in the Presence of Water Trees and Space Charge. IEEE Transactions on Industry Applications Vol 45 No1, pp30-43

48. Steenis E F, Kreuger F H (1990) Water Treeing in Polyethylene Cables. IEEE Transactions on Electrical Insulation Vol. 25 No. 5, pp 989 to 1028

49. Stewart R H, 2010, Chapter 6 - Temperature, Salinity, and Density, Department of Oceanography, Texas A&M University http://oceanworld.tamu.edu/resources/ocng_textbook/chapter06/chapter06_05.htm , first accessed 12th April 2012

50. Sun Y, Xu Y, Yang W, Jin J, Cao X (2009), A Study of Water Trees in Polymers under Different Conditions. Proceedings of the 9th International Conference on Properties and Applications of Dielectric Materials July 19-23,2009, Harbin, China

51. Tang X, Sullivan, C.R. (2003) Stranded wire with unisulated strands as a low cost alternative to litz wire. IEEE 34th Annual Power Electronics Specialist Conference PESC ’03, Vol 1 pp 289-295.

52. Thomas A J, Saha T K (2005) The analysis of DC and AC conductivity in the detection of water tree degradation in XLPE cables. Power Engineering Society General Meeting, 2005, Pages 87 - 94 Vol. 1

53. Tsai, I-S, Chen, C.H (1990) Perturbed-TEM analysis of transmission lines with imperfect conductors. IEEE Transactions on Microwave Theory and Techniques Vol 38 no 6 pp 754-759

54. Tuncer E., Lee B., Islam M., Neikirk D. (1994). Quasi conductor loss calculations in transmission lines using a new conformal mapping technique, IEEE Transactions on Microwave Theory and Techniques Vol MTT-42,(9) pp 1807-1815

55. U.S. National Oceanographic Data Center: Global Temperature–Salinity Profile Programme. June 2006. U.S. Department of Commerce, National Oceanic and Atmospheric Administration, National Oceanographic Data Center, Silver Spring, Maryland, 20910. http://www.nodc.noaa.gov/GTSPP/. first accessed 13th April 2012

56. Vitelli M (2004) Numerical evaluation of 2-D proximity effect conductor losses. IEEE Transactions on Power Delivery Vol 19 no 3 pp 1291-1298

57. Weatherford (2008) http://www.weatherford.com/weatherford/groups/web/documents/weatherfordcorp/WFT097737.pdf, first accessed 25 Jan 2013

58. Wu R B, Yang J C (1989), Boundary Integral Equation Formulation of Skin Effect Problems in Multiconductor Transmission Lines. IEEE Transactions on Magnetics, Vol 25, No 4, July 1999

59. Yan Li, Peng Fa-dong, Chen Xiao-lin, Cheng Yong-hong, Li Xu (2008), Study on Sheath Circulating Current of Cross-linked Power Cables , 2008 International Conference on High Voltage Engineering and Application, Chongqing, China, November 9-13, 2008, pp645-648

Bibliography

1. Anatory J., Theethayi N.,Kissaka M., Mvungi N. (2007) The effects of load impedance, line length and branches in the PLC-transmission lines analysis for medium voltage channel. IEEE Transactions on Power Delivery Vol 22 no 4 pp 2156-2162

2. Andreou G.T., Labridis D.P. (2007), Experimental evaluation of a low voltage power distribution cable model based on a finite element approach. IEEE Transactions on Power Delivery Vol 22 no 3 pp 1455-1460

3. Barmada S., Musolino A., Raugi M. (2005) Wavelet-based time_domain solution of multiconductor transmission lines with skin and proximity effect. IEEE Transactions on Electromagnetic Compatibility. Nov2005, Vol. 47 Issue 4, pp774-780

4. Barmada S., Musolino A., Raugi M., Tucci M (2007) Analysis of power lines uncertain parameter influence on power line communications. IEEE Transactions on Power Delivery Vol 22 no 4 pp 2163-2171

5. Bianconi G (2002) Shallow seas ecosystems. Encyclopedia of Life Sciences, Wiley InterScience, ISBN 978-0-470-06651-5

6. Bogle A G (1940), The effective Inductance and Resistance of Screened Coils. Wireless Section, Institution of Electrical Engineers - Proceedings of the Wireless Section of the Institution, Volume 15, Issue 45, pp 221-238

7. Canganella F, (2006) Hydrothermal Vent Communities, Encyclopedia of Life Sciences Wiley InterScience, ISBN 978-0-470-06651-5

8. Canganella F., Chiaki Kato (2002), Deep ocean ecosystems, Encyclopedia of Life Sciences Wiley InterScience, ISBN 978-0-470-06651-5

9. Davis W (2012), Radio Frequency Circuit Design , Wiley-IEEE Press. http://ieeexplore.ieee.org.libezproxy.open.ac.uk/xpl/bkabstractplus.jsp?bkn=5628344 , first accessed 1st Aug 2012

10. Emerson and Cumming, Dielectric materials Chart http://www.eccosorb.com.hk/sites/default/files/related_info/Dielectric%20Material%20Chart.pdf, first accessed 10th April 2012

11. Ferreira J. (1994), Improved analytical modeling of conductive losses in magnetic components. IEEE Transactions on Power Electronics Vol. 9 no 1 pp127-131

12. Gilbertson, O.I. (2000) Electric cables for power and signal transmission. Wiley ISBN 978-0471359968

13. Holt J T, James I D (1999), A Simulation of the Southern North Sea in Comparison with Measurements from the North Sea Project. Part 1: Temperature. Continental Shelf Research 19 (1999) 1087-1112

14. Papandreou N., Antonakopoulos T (2007), Resource allocation management for indoor power line communications systems. IEEE Transactions on Power Delivery Vol 22 no 2 pp 893-903

15. Snelgrove P, (2003), Marine communities. Encyclopedia of Life Sciences Wiley InterScience www.els.net

16. Suzuki M, Itoh A, Yoshimura N (2008) Three-dimensional equivalent circuit analysis of water tree. Proceedings of 2008 International Symposium on Electrical Insulating Materials, September 7-11, 2008, Yokkaichi, Mie, Japan

17. Svendsen E, Saetre R, Mork M (1991), Features of the North Sea Circulation. Continental Shelf Research , Vol11 No5 pp493-508

18. True K.M. (1992) Long transmission lines and data signal quality, National Semiconductor application note AN808

19. True K.M. (1992) Data Transmission Lines and Their Characteristics, National Semiconductor application note AN806

20. True K.M. (1992) Reflections: Computations and Waveforms, National Semiconductor application note AN807

21. Umgiesser G, Luyten P J, Camiel S, (2002), Exploring the thermal cycle of the Northern North Sea area using a 3-D circulation model: the example of PROVESS NNS station. Journal of Sea Research 48 (2002) 271– 286

22. Van Haren H, Howart M, Jones K, Ezzi, I (2002), Autumnal reduction of stratification in the northern North Sea and its impact. Continental Shelf Research 23 (2003) 177–191.

23. Wojda R P, Kazimierczuk M K, (2011) Winding resistance of litz-wire and multi-strand inductors. IET Power Electronics, Volume: 5, Issue: 2, Page(s): 257 - 268

24. Yazdani J, Glanville K, Clarke P. Modelling, Developing and Implementing Sub-Sea Power-Line Communications Networks. Power Line Communications and Its Applications, 2005 International Symposium on 6-8 April 2005, Page(s): 310 – 316